JPRS L/8653

11 September 1979

USSR Report

METEOROLOGY AND HYDROLOGY

No. 6, June 1979

FBIS FOREIGN BROADCAST INFORMATION SERVICE

NOTE

JPRS publications contain information primarily from foreign newspapers, periodicals and books, but also from news agency transmissions and broadcasts. Materials from foreign-language sources are translated; those from English-language sources are transcribed or reprinted, with the original phrasing and other characteristics retained.

Headlines, editorial reports, and material enclosed in brackets [] are supplied by JPRS. Processing indicators such as [Text] or [Excerpt] in the first line of each item, or following the last line of a brief, indicate how the original information was processed. Where no processing indicator is given, the information was summarized or extracted.

Unfamiliar names rendered phonetically or transliterated are enclosed in parentheses. Words or names preceded by a question mark and enclosed in parentheses were not clear in the original but have been supplied as appropriate in context. Other unattributed parenthetical notes within the body of an item originate with the source. Times within items are as given by source.

The contents of this publication in no way represent the policies, views or attitudes of the U.S. Government.

For further information on report content call (703) 351-2938 (economic); 3468 (political, sociological, military); 2726 (life sciences); 2725 (physical sciences).

APPROVED FOR RELEASE: 2007/02/08: CIA-RDP82-00850R000100090012-8

JPRS L/8653

11 September 1979

USSR REPORT

METEOROLOGY AND HYDROLOGY

No. 6, June 1979

Selected articles from the Russian-language journal METEOROLOGIYA I GIDROLOGIYA, Moscow.

CONTENTS PAGE

CONTENTS (Continued) Page

CONTENTS (Continued)

PUBLICATION DATA

English title	:	METEOROLOGY AND HYDROLOGY No 6, Jun 79
Russian title	:	METEOROLOGIYA I GIDROLOGIYA
Author (s)	:	V. P. Dymnikov, A. V. Ishimova et al.
Editor (s)	:	Ye. I. Tolstikov
Publishing House	:	GIDROMETEOIZDAT
Place of Publication	:	Moscow
Date of Publication	:	1979
Signed to press	:	25 May 79
Copies	:	3930
COPYRIGHT	:	"Meteorologiya i gidrologiya," 1979

UDC 551.509.313

NONADIABATIC MODEL OF SHORT-RANGE WEATHER FORECASTING

Moscow METEOROLOGIYA I GIDROLOGIYA in Russian No 6, Jun 79 pp 5-14

[Article by Candidate of Physical and Mathematical Sciences V. P. Dymnikov and A. V. Ishimova, Computation Center Siberian Department USSR Academy of Sciences and West Siberian Regional Hydrometeorological Institute, submitted for publication 4 August 1978]

Abstract: The article gives a description of a nonadiabatic weather forecasting model for a broad territory on the basis of the full equations of hydrothermodynamics for a period of 72 hours in advance. For solving the transfer equations use is made of difference schemes of the fourth order of accuracy with a smoothing operator, also of the fourth order. Phase influxes are taken into account in the heat influx equation. The boundary layer and orography are parameterized. The fields of geopotential, temperature, wind, dew point spread and steady precipitation are precomputed. The results of numerical experiments for predicting the fields of geopotential, dew point spread and steady precipitation are given.

[Text] Introduction. The weather forecasting model examined in this study is a natural development of the model described in [6].

Before proceeding to a detailed exposition of the equations for the model and the results of numerical experiments we will briefly discuss those changes and additions which have been introduced in this version of the model. We have introduced a description of the planetary boundary layer and orography, computed the fields of humidity and steady precipitation, taken into account the phase influxes of heat, and also have changed the method for solving the transfer equation. The experience of work with a nonadiabatic short-range weather forecasting model, used in the routine practice of the West Siberian Regional Hydrometeorological Institute,

indicated that the use of schemes with a second order of accuracy for space variables for solving humidity transfer equations introduces large errors (both phase and amplitude errors) as a result of the significant nonmonotonicity of these schemes and the great spatial gradients of humidity fields. The use of a special structure of the humidity transfer equations [3] only partially eliminates this problem. Therefore, in this study we have changed to schemes with a fourth order of accuracy for space variables in the transfer equations with a smoothing operator also of the fourth order [13]. These numerical experiments with model initial conditions indicated that this scheme, although it does not belong to a class of schemes with an even exponent [7], is one of the best for describing generalized discontinuous solutions. Since a fourth-order scheme in smooth solutions in essence has a lesser phase error than a second-order scheme, it is also used in a model for solution of the equations for transfer of heat and moment of momentum. The above-mentioned operational model [5] uses a special structure of the equations [3] for computing the humidity and precipitation fields; this requires direct computations of vertical currents in the atmosphere for computing the phase transitions of moisture. It is known that the problem of computing vertical currents in the atmosphere is very complex and as yet has not been completely solved. Therefore, in this study we carried out parallel comparative computations of the humidity and precipitation fields using the equations proposed in [3] and the generally accepted equations [11].

In conclusion we will discuss the problem of introducing of orographic nonuniformities of the earth's surface into numerical weather forecasting models. If one speaks of the joint description of the planetary boundary layer and orography, this problem has not yet been solved. Moreover, we feel it has not even been clearly formulated. Along these lines the source [2] is rather interesting; we have used these results in our model.

Formulation of Problem

We will examine a baroclinic nonadiabatic model of the atmosphere in a quasistatic approximation in the coordinate system x, y, p in a stereographic projection. The equations of the model, first reduced to a semidivergent form, read as follows

$$\frac{\partial u}{\partial t} + \frac{1}{2} m^2 u \frac{\partial u}{\partial x} + \frac{1}{2} m^2 v \frac{\partial u}{\partial y} + \frac{1}{2} \omega \frac{\partial u}{\partial p} + \frac{1}{2} \frac{\partial m^2 uu}{\partial x} + \\ + \frac{1}{2} \frac{\partial m^2 uv}{\partial y} + \frac{1}{2} \frac{\partial u \omega}{\partial p} + l_1 v = -g \frac{\partial z}{\partial x}, \tag{1}$$

$$\frac{\partial v}{\partial t} + \frac{1}{2} m^2 u \frac{\partial v}{\partial x} + \frac{1}{2} m^2 v \frac{\partial v}{\partial y} + \frac{1}{2} \omega \frac{\partial v}{\partial p} + \frac{1}{2} \frac{\partial m^2 uv}{\partial x} + \\ + \frac{1}{2} \frac{\partial m^2 vv}{\partial y} + \frac{1}{2} \frac{\partial v \omega}{\partial p} - l_1 u = -g \frac{\partial z}{\partial y}, \tag{2}$$

$$\frac{\partial T}{\partial t} + \frac{1}{2} m^2 u \frac{\partial T}{\partial x} + \frac{1}{2} m^2 v \frac{\partial T}{\partial y} + \frac{1}{2} \dot{\sigma} \frac{\partial T}{\partial p} + \frac{1}{2} \frac{\partial m^2 uT}{\partial x} +$$

$$+ \frac{1}{2} \frac{\partial m^2 vT}{\partial y} + \frac{1}{2} \frac{\partial \dot{\sigma} T}{\partial p} - mT \left(u \frac{\partial m}{\partial x} + v \frac{\partial m}{\partial y} \right) -$$

$$- \frac{R\bar{T}}{pg} (\gamma_a - \bar{\gamma}) \dot{\sigma} = \frac{\varepsilon_\Phi}{c_p}, \tag{3}$$

$$m^2 \left(\frac{\partial u}{\partial x} + \frac{\partial v}{\partial y} \right) + \frac{\partial \dot{\sigma}}{\partial p} = 0, \tag{4}$$

$$\frac{\partial z}{\partial p} = -\frac{RT}{pg}, \tag{5}$$

[Φ = ph]

where u, v, $\dot{\sigma}$ are the projections of the velocity vector relative to the axes x, y, p;

$$m = \frac{1 + \sin 60^\circ}{1 + \sin \varphi};$$

φ is the geographic latitude of the particular point of the grid; T, z are the deviations of temperature and altitude of the isobaric surface from their standard values; $\bar{\gamma}$, $\bar{T}$ are the standard values of the temperature gradient ($\bar{\gamma} = -\partial \bar{T} / \partial z$) and temperature; γ_a is the dry adiabatic temperature gradient; ε_{ph} are the heat influxes due to the phase transitions of moisture; c_p is the specific heat capacity at a constant pressure

$$l_1 = l + m \left(u \frac{\partial m}{\partial x} + v \frac{\partial m}{\partial y} \right),$$

where l is the Coriolis parameter.

We note that the origin of coordinates for our grid is situated in the upper left corner.

In describing transfer and evolution of the humidity fields in the model we will use two systems of equations, one of which is formulated in terms of the combination of the deficit of specific humidity and liquid-water content [3]; the second describes the evolution of specific humidity (for example, see [11])

$$\frac{\partial \Phi}{\partial t} + \frac{1}{2} m^2 u \frac{\partial \Phi}{\partial x} + \frac{1}{2} m^2 v \frac{\partial \Phi}{\partial y} + \frac{1}{2} \dot{\sigma} \frac{\partial \Phi}{\partial p} + \frac{1}{2} \frac{\partial m^2 u \Phi}{\partial x} + \tag{6}$$

$$+\frac{1}{2}\frac{\partial m^2 v\Phi}{\partial y}+\frac{1}{2}\frac{\partial \tau\Phi}{\partial p}-m\Phi\left(u\frac{\partial m}{\partial x}+v\frac{\partial m}{\partial y}\right)=-\left(1+\frac{L}{c_p}\frac{\partial q_m}{\partial T}\right)\times$$

[BA = ma]
$$\times\left[\frac{c_p}{L}(\gamma_a-\gamma_{ma})\frac{RT}{pg}\tau-\delta\right], \tag{6}$$

$$\frac{\partial q_1}{\partial t}+\frac{1}{2}m^2u\frac{\partial q_1}{\partial x}+\frac{1}{2}m^2v\frac{\partial q_1}{\partial y}+\frac{1}{2}\tau\frac{\partial q_1}{\partial p}+\frac{1}{2}\frac{\partial m^2 uq}{\partial x}+$$

$$+\frac{1}{2}\frac{\partial m^2 vq_1}{\partial y}+\frac{1}{2}\frac{\partial \tau q_1}{\partial p}-mq_1\left(u\frac{\partial m}{\partial x}+v\frac{\partial m}{\partial y}\right)=-M, \tag{7}$$

where
$$\Phi=q_1-q_m+\left(1+\frac{L}{c_p}\frac{\partial q_m}{\partial T}\right)q_2, \tag{8}$$

q_1 is specific humidity, q_m is maximum specific humidity, q_2 is specific water content, L is the specific heat of condensation, γ_{ma} is the moist adiabatic temperature gradient, δ is a function describing the process of falling of precipitation, M is the condensation rate. In computing the M value it is assumed in equation (7) that the specific humidity in the clouds is equal to the saturating humidity and the condensation process begins under the condition $r = q_1/q_m > 1$.

We will call the first model of computation of the humidity fields model A, and the second model B. The following boundary conditions are set on the lateral boundaries:

$$\frac{\partial T}{\partial t}=\frac{\partial z}{\partial t}=\frac{\partial \Phi}{\partial t}=\frac{\partial q_1}{\partial t}=0.$$

In order to satisfy the integral laws of energy conservation for u, v, τ we will use the condition $u = v = \tau = 0$ on the lateral boundaries of the integration region [7]. At the upper boundary of the atmosphere (in our case -- at the level 200 mb) we set the condition $\partial T/\partial p = 0$. As the boundary condition at the lower boundary of the atmosphere we use $w = w_{tr} + w_{oro}$, where w is the vertical component of the velocity vector in the coordinate system x, y, z. For computing w_{tr} we used a model of the boundary layer taken from [9]. The equation for the model has the form

$$w_{\tau p}=\frac{1}{l}\frac{\partial \tau_y}{\partial x}-\frac{1}{l}\frac{\partial \tau_x}{\partial y}, \tag{9}$$

where
$$\tau_y=u_*^2\sin(\beta_g-\alpha),$$
$$\tau_x=u_*^2\cos(\beta_g-\alpha),$$

u_* is dynamic velocity, β_g is the angle of the geostrophic wind at the altitude of the atmospheric boundary layer, for which an altitude of 850 mb is used in the particular model, α is the angle of wind rotation at the earth's surface.

The solution is obtained in the form of universal dependences on the parameters Ro, δ, μ, where

$$\mathrm{Ro} = \frac{G}{lz_0}, \quad \delta = \sqrt[4]{\frac{\lambda(\gamma_a - \overline{\gamma})}{l^2}},$$

$$\mu = -\frac{\lambda Q_0 \delta^2}{G^2}, \quad G = \sqrt{u_g^2 + v_g^2}.$$

Here z_0 is the roughness parameter, λ is the convection parameter, γ is the temperature gradient at the altitude 850 mb; Q_0 is the value of the turbulent heat flux at the earth's surface.

The orographic component of vertical velocity at the upper boundary of the boundary layer is represented in the form of the sum of the two components

$$w_{oro} = w_{oro1} + w_{oro2}, \tag{10}$$

where

$$w_{op_1} = m^2 u \frac{\partial \xi_0}{\partial x} + m^2 v \frac{\partial \xi_0}{\partial y},$$

[op = oro]

ξ_0 is the elevation of the earth's surface above sea level. The expression for w_{oro1} is widely accepted and reflects the fact of nonpassage of air through the earth's surface. A more complex expression is for w_{oro2}, which arises as a result of nonlinearity of the processes in the boundary layers over an orographically inhomogeneous surface. Adhering to [2], for w_{oro2} we use the expression

$$w_{op_2} = a|u_g|^2 \Delta\xi_0,$$

[op = oro] where $a \sim 10^4$ sec.

In the function $\tilde{z}_0$ used in the model there is filtering out of waves whose length is less than three grid intervals.

Solution Method

The problem (1)-(7) is solved by the splitting method. In the first stage there is solution of a system of equations describing the transfer of the meteorological fields u, v, T, Φ, q_1 along the trajectories:

$$\frac{\partial \varphi}{\partial t} + \frac{1}{2} m^2 u \frac{\partial \varphi}{\partial x} + \frac{1}{2} m^2 v \frac{\partial \varphi}{\partial y} + \frac{1}{2} \frac{\partial m^2 u \varphi}{\partial x} + \frac{1}{2} \frac{\partial m^2 v \varphi}{\partial y} = 0. \tag{11}$$

Here

$$\varphi = \{u, v, T, \Phi, q_1\}.$$

The two-dimensional equation (11) is in turn split into two one-dimensional equations which are approximated using finite-difference schemes with a fourth order of accuracy for space variables and a Crank-Nicholson scheme for time. The semidivergent form of the equations of motion (11) makes it possible to construct finite-difference schemes retaining an obliquely symmetric structure, which ensures an absolute stability of the schemes in spectral norms. The difference scheme for the one-dimensional transfer equation has the form:

$$\frac{\varphi_k^{n+\frac{1}{2}}-\varphi_k^n}{\Delta t}+\left\{\frac{4}{3}D_0(h)-\frac{1}{3}D_0(2h)\right\}\varphi^{n+\frac{1}{4}}=\varepsilon h^3(D_+D_-)^2\varphi^n, \qquad (12)$$

where

$$D_0(h)\varphi=\frac{\varphi_{k+1}-\varphi_{k-1}}{2h},$$

$$D_0(2h)\varphi=\frac{\varphi_{k+2}-\varphi_{k-2}}{4h},$$

$$D_+\varphi=\frac{\varphi_{k+1}-\varphi_k}{h},$$

$$D_-\varphi=\frac{\varphi_k-\varphi_{k-1}}{h},$$

$$\varphi^{n+\frac{1}{4}}=\frac{1}{2}(\varphi^{n+\frac{1}{2}}+\varphi^n).$$

The term present on the right-hand side of (12) is necessary, as was noted in the introduction, in order for the difference scheme to be close to monotonic. The ε parameter is selected not greater than h so that the general order of the scheme will be fourth. The system of finite-difference equations with a five-diagonal matrix relative to the unknowns $\varphi^{n+1/2}$, obtained by solution of the equations (12), is inverted using five-point fitting.

The equations describing the problem in the adaptation stage are approximated by difference schemes with a second order of accuracy for the space and time variables and have the following form:

$$\frac{u^{n+1}-u^{n+\frac{1}{2}}}{\Delta t}+\frac{1}{2}l_1(v^{n+1}+v^{n+\frac{1}{2}})=-\frac{1}{2}g\left(\frac{z_{k+1}^{n+1}-z_{k-1}^{n+1}}{2h}+\right. \qquad (13)$$

$$\left.+\frac{z_{k+1}^{n+\frac{1}{2}}-z_{k-1}^{n+\frac{1}{2}}}{2h}\right),$$

$$\frac{v^{n+1}-v^{n+\frac{1}{2}}}{\Delta t}-\frac{1}{2}l_1(u^{n+1}+u^{n+\frac{1}{2}})= \qquad (14)$$

$$=-\frac{1}{2}g\left(\frac{z_{l+1}^{n+1}-z_{l-1}^{n+1}}{2h}+\frac{z_{l+1}^{n+\frac{1}{2}}-z_{l-1}^{n+\frac{1}{2}}}{2h}\right), \qquad (15)$$

$$k_1T^{n+1}-k_2T^{n+\frac{1}{2}}-\frac{(\gamma_a-\overline{\gamma})R\overline{T}}{pg}\tau^{n+\frac{3}{4}}=\frac{\varepsilon\phi}{c_p},$$

$$m^2\left(\frac{u_{k+1}-u_{k-1}}{2h}+\frac{v_{l+1}-v_{l-1}}{2h}\right)+\frac{\tau_{l+\frac{1}{2}}-\tau_{l-\frac{1}{2}}}{\Delta p_l}=0, \tag{16}$$

$$\frac{z_{l+1}-z_l}{\Delta p_{l+\frac{1}{2}}}=-\frac{RT_{l+\frac{1}{2}}}{p_{l+\frac{1}{2}}g}, \tag{17}$$

where

$$\tau^{n+\frac{3}{4}}=\frac{1}{2}\left(\tau^{n+1}+\tau^{n+\frac{1}{2}}\right),$$

$$k_1=\frac{1}{\Delta t}\left[1-\frac{1}{2}m\Delta t\left(u\frac{\partial m}{\partial x}+v\frac{\partial m}{\partial y}\right)\right],$$

$$k_2=\frac{1}{\Delta t}\left[1+\frac{1}{2}m\Delta t\left(u\frac{\partial m}{\partial x}+v\frac{\partial m}{\partial y}\right)\right].$$

The system of equations (13)-(17), as in [10], is reduced to a system of finite-difference equations of an elliptical type relative to the geopotential trend

$$\delta z^{n+1}=z^{n+1}-z^{n+\frac{1}{2}}$$

and is solved by the biorthogonalization method.

For describing the evolution of the humidity fields in the assimilation stage, for model A we used the scheme

$$\frac{\Phi^{n+1}-\Phi^{n+\frac{1}{2}}}{\Delta t}=-\left(1+\frac{L}{c_p}\frac{\partial q_m^{n+\frac{1}{2}}}{\partial T}\right)\left[\frac{c_p}{L}\left(\gamma_a-\gamma_{sa}\right)^{n+\frac{1}{2}}\times\right. \tag{18}$$

$$\left.\times\frac{\overline{RT}}{pg}\tau^{n+\frac{3}{4}}-\delta^{n+\frac{1}{2}}\right].$$

The vertical currents necessary for computing Φ in equation (18) are computed from the heat influx equation (15). The accuracy in predicting the humidity fields is determined to a substantial degree by the accuracy in computing the systematic vertical currents τ, which constitute one of the principal dynamic factors determining cloud formation processes in the atmosphere. A comparison of the vertical movements, computed from (15), with the currents determined using the continuity equation, indicated that the regions of ascending and descending movements agree rather well with one another; there is a difference only in value. For predicting precipitation, as in [5], we used the following scheme for computing the moisture accumulating in the layer, which, reaching a threshold value $\overline{q}_2$, falls into the lower-lying layer. In the second scheme (B) the computations of precipitation were made under the condition $r = q_1/q_m > 1$. The computation scheme has the form

$$T^{n+1}-T^{n+\frac{1}{2}}=\frac{L}{c_p}\left(q_1^{n+1}-q_1^{n+\frac{1}{2}}\right), \tag{19}$$

$$q_1^{n+1}=q_m\left(T^{n+1}\right).$$

The system of equations (19) is solved by the iteration method.

Numerical Experiments

The numerical experiments were carried out for a five-level model in a rectangular grid measuring 33 x 33 with an interval of 375 km with its center at Novosibirsk. As the initial data we took the geopotential and dew point spread values obtained as a result of objective analysis of meteorological fields under the program developed by the USSR Hydrometeorological Center [1]. The values of the functions u, v, z are determined at the standard levels 1000, 850, 700, 500, 300 mb; the T, τ, Φ, q_1 values are determined at intermediate levels -- 925, 775, 600, 400 mb. Since no systematic measurements are made for the liquid water content in clouds, in computing the initial values of the function Φ it is postulated that the specific liquid water content q_2 at the initial moment in time is equal to zero. The quality of the forecast was evaluated using the results of objective analysis. In order to evaluate the quality of the geopotential forecast use was made of the usual synoptic-statistical characteristics: ε is the mean relative error, k is the correlation coefficient, ρ is the probable success of forecast of trend signs:

$$\varepsilon = \frac{\sum_{i=1}^{n} |(z_{\phi к} - z_0) - (z_{пр} - z_0)|}{\sum_{i=1}^{n} |z_{\phi к} - z_0|},$$

$$k = \frac{\sum_{i=1}^{n} \left\{ \left[(z_{\phi к} - z_0) - \frac{\sum_{i=1}^{n} (z_{\phi к} - z_0)}{n} \right] \left[(z_{пр} - z_0) - \frac{\sum_{i=1}^{n} (z_{пр} - z_0)}{n} \right] \right\}}{\sqrt{\sum_{i=1}^{n} \left[(z_{\phi к} - z_0) - \frac{\sum_{i=1}^{n} (z_{\phi к} - z_0)}{n} \right]^2 \sum_{i=1}^{n} \left[(z_{пр} - z_0) - \frac{\sum_{i=1}^{n} (z_{пр} - z_0)}{n} \right]^2}},$$

$$\rho = \frac{N^+ - N^-}{n},$$

[Φк = act(ual); пр = predicted] where $N^+(N^-)$ is the number of points at which there is a correct (incorrect) prediction of the trend sign; the points at which one of the trends is equal to zero, whereas the other is not equal to zero, are not included in either N^+ or in N^-; z_{act} is the actual height of the isobaric surface at the time for which the forecast is made; z_{pred} is the predicted value; z_0 is the geopotential value at the initial moment in time; n is the number of points of intersection used in evaluating the forecast.

In order to evaluate the dew point spread values we computed the frequency of recurrence of forecasting errors by gradations. The evaluation was made for the territory of the West Siberian region (at 110 points of grid

intersection) in accordance with the program developed in [12]. The results of the evaluations are given in Tables 1-5. N denotes the number of situations used in computing the evaluations.

Table 1

Mean Evaluations of Prediction of Geopotential (for Five Levels) Using the Initial Data for 19 September 1975 for the Time 00(03)

Схема 1	2 Срок прогноза, ч								
	24			48			72		
	ε	k	ρ	ε	k	ρ	ε	k	ρ
а	0,95	0,65	0,46	1,18	0,49	0,30	1,23	0,41	0,37
б	0,86	0,72	0,48	1,07	0,60	0,36	1,08	0,50	0,46
в	0,75	0,70	0,52	1,02	0,51	0,32	1,20	0,43	0,37
г	0,71	0,72	0,51	0,95	0,55	0,36	1,01	0,51	0,45

KEY:
1. Scheme
2. Forecast time, hours

Table 2

Frequency of Recurrence of Errors (%) in Prediction of Dew Point Spread Using Initial Data for 19 September 1975 for the Time 00(03) for 24, 48, 72 hrs

Поверхность, мб 1	Схема 2	3 Срок прогноза, ч								
		24			48			72		
		0—3°	4—6°	>7°	0—3°	4—6°	>7°	0—3°	4—6°	>7°
925	а	87	13	0	76	23	1	62	36	2
	б	86	14	0	77	21	2	60	33	7
775	а	64	34	1	58	36	6	57	33	10
	б	76	24	0	74	25	1	79	20	1
600	а	54	36	11	46	36	18	41	31	28
	б	80	18	2	47	47	6	61	34	5
400	а	66	25	9	44	31	24	52	30	18
	б	74	24	1	38	56	6	72	24	4

KEY:
1. Surface, mb
2. Scheme
3. Time of forecast, hours

Table 1 illustrates the probable success of the forecast of geopotential on the basis of initial data for 19 September for the time 00(03) for 24, 48 and 72 hours in advance using four schemes:

a) an adiabatic forecasting scheme, in which the transfer equations are approximated by finite-difference schemes with a second order of accuracy;

b) an adiabatic scheme in which the transfer equations are approximated by difference schemes with a fourth order of accuracy;
c) a nonadiabatic scheme, the basis for which is scheme (b) with the introduction of a boundary layer and phase heat influxes;
d) scheme (c) is supplemented by taking into account orographic nonuniformities of the earth's surface.

Table 2 gives the frequencies of recurrence of errors in predicting the dew point spread using two schemes:

a) a forecasting scheme in which the equations for the transfer of humidity fields are approximated by finite-difference schemes with a second order of accuracy;

b) the equations for the transfer of humidity fields are approximated by schemes with a fourth order of accuracy with the addition of a dissipative term; the scheme shows that the frequency of recurrence of large errors in predicting the dew point spread in essence is less if one uses a scheme with a fourth order of accuracy.

Table 3

Mean Evaluations of Prediction of Geopotential With Allowance for Orography (a) and Without Allowance for Orography (b)

Поверхность, мб (1)	Схема (3)	Срок прогноза, ч (2)											
		24				48				72			
		N	ε	k	ρ	N	ε	k	ρ	N	ε	k	ρ
1000	а	7	0,80	0,69	0,50	4	0,92	0,62	0,44	3	1,05	0,60	0,33
	б	7	0,88	0,61	0,46	4	1,00	0,54	0,40	3	1,18	0,51	0,28
950	а	7	0,80	0,64	0,49	4	0,88	0,58	0,44	3	0,99	0,54	0,42
	б	7	0,91	0,55	0,46	4	1,00	0,50	0,39	3	1,17	0,46	0,45
700	а	7	0,74	0,68	0,54	4	0,85	0,65	0,49	3	0,90	0,56	0,48
	б	7	0,82	0,63	0,52	4	1,00	0,60	0,43	3	1,11	0,49	0,45
500	а	7	0,70	0,78	0,63	4	0,74	0,75	0,56	3	0,81	0,65	0,56
	б	7	0,75	0,76	0,60	4	0,85	0,74	0,57	3	1,03	0,60	0,47
300	а	7	0,67	0,80	0,58	4	0,76	0,79	0,61	3	0,80	0,69	0,60
	б	7	0,70	0,79	0,58	4	0,86	0,78	0,61	3	0,97	0,66	0,55

KEY:
1. Surface, mb
2. Prediction time, hours
3. Scheme

As indicated by Table 3, the inclusion of orography in the model improves the quality of the forecast at the lower levels by approximately 5-10%.

Table 4 illustrates the quality of predictions of the dew point spread using two schemes for computing the humidity fields, described in the model of prediction of meteorological elements cited above. The frequency of recurrence of errors is approximately identical for both schemes. The same can

be said about the zones of steady precipitation (Fig. 1).

Table 5 gives the mean evaluations of prediction of dew point spread for 24, 48, 72 hours in accordance with scheme A.

Table 4

Mean Frequency of Recurrence of Errors (%) in Predictions of Dew Point Spread for 24 hours Using Schemes A and B

Поверхность, мб 1	2 Схема	N	0--3°	4—6°	>7°C
925	A	3	82	14	4
	B	3	73	25	2
775	A	3	79	20	1
	B	3	76	23	1
600	A	3	67	29	4
	B	3	67	32	1
400	A	3	65	29	6
	B	3	68	29	3

KEY:
1. Surface, mb
2. Scheme

Table 5

Mean Frequency of Recurrence of Errors (%) in Prediction of Dew Point Spread for 24, 48, 72 hours Using Scheme A

Поверхность, мб 1	2 Срок прогноза, ч											
	24				48				72			
	N	0--3°	4--6°	>7°	N	0--3°	4- 6°	>7°	N	0--3°	4—6°	>7°C
925	5	69	24	8	5	60	28	12	5	50	32	18
775	5	70	24	6	5	65	29	6	5	70	27	3
600	5	63	31	6	5	60	31	7	5	57	37	6
400	5	69	25	6	5	63	28	9	5	80	32	8

KEY:
1. Surface, mb
2. Prediction time, hours

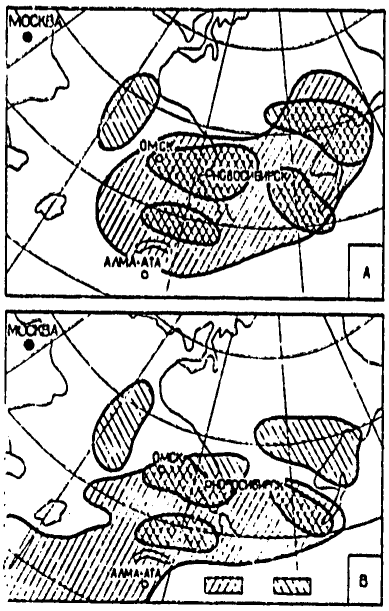

Fig. 1. Prediction of zones of steady precipitation for 24 hours on the basis of initial data for 22 January 1978 for the time 00(03) hours using schemes A and B. 1) zone of predicted precipitation, 2) zone of actual precipitation

Summary

Our numerical experiments make it possible to draw only a preliminary conclusion concerning the quality of the prognostic scheme since the number of experiments is inadequate for a statistically reliable evaluation of the result. Nevertheless, some conclusions can be drawn. It can be said with assurance that the use of special difference schemes with a high order of accuracy and close to monotonic in essence reduces the number of large errors in the prediction of the dew point spread. A comparison of two models of prediction of the humidity fields did not indicate significant advantages of either one. The fact is that in the present version of the model no optimization of computation of vertical currents was carried out. As was already mentioned above, the zones of vertical currents, computed from the heat influx equation and from the continuity equation, and also from the quasigeostrophic ω-equation [4], coincide quite well, but their values differ extremely substantially. Since it is impossible to say what vertical currents are closer to the true currents, it is necessary to adjust their amplitude relative to a particular prognostic model. If it is taken into account that the liquid water content of clouds is also predicted in model A (necessary, for example, for computing cloud albedo), preference must be given to this model. The approach to allowance for orographic nonuniformities of the earth's surface used in the model requires

a more careful analysis, particularly from the point of view of evaluating the success of a prediction of atmospheric cyclonic activity. A separate paper will be devoted to this problem.

BIBLIOGRAPHY

1. Artanova, A. L., "New Variant of a Program for Routine Objective Analysis of Objective Analysis of Geopotential of Isobaric Surfaces," METEOROLOGIYA I GIDROLOGIYA (Meteorology and Hydrology), No 9, 1974.

2. Godev, N., "Influence of Orography and Surface Friction on Changes in Atmospheric Pressure," BULGARIAN GEOPHYSICAL J., Vol 1, No 2, Sofia, 1975.

3. Dymnikov, V. P., "One Formulation of the Problem of Predicting Humidity Fields in the Atmosphere," IZV. AN SSSR, FIZIKA ATMOSFERY (News of the USSR Academy of Sciences, Physics of the Atmosphere and Ocean), Vol 7, No 12, 1971.

4. Dymnikov, V. P., Guseva, N. V., "Some Methods for Computing Vertical Movements in the Free Atmosphere," TRUDY ZAP.-SIB. RNIGMI (Transactions of the West Siberian Regional Scientific Research Hydrometeorological Institute), No 14, 1975.

5. Dymnikov, V. P., et al., "Prediction of Meteorological Elements in a Restricted Territory Using Full Equations," METEOROLOGIYA I GIDROLOGIYA, No 9, 1975.

6. Dymnikov, V. P., Ishimova, A. V., "Adiabatic Model of Weather Forecasting Using Full Equations for a Grid in a Stereographic Projection Over an Extensive Territory," TRUDY ZAP.-SIB. RNIGMI, No 25, 1976.

7. Zhukov, A. I., "Limiting Theorem for Difference Operators," USPEKHI MATEMATICHESKIKH NAUK (Advances in the Mathematical Sciences), 14, No 3, 1959.

8. Ishimova, A. V., "Adiabatic Model for Prediction of Meteorological Elements Using Full Equations Over an Extensive Territory," SBORNIK DOKLADOV VTOROY VSESOYUZNOY KONFERENTSII MOLODYKH UCHENYKH GIDROMETSLUZHBY SSSR (Collection of Reports of the Second All-Union Conference of Young Scientists of the USSR Hydrometeorological Service), Moscow, Gidrometeoizdat, 1977.

9. Lykosov, V. N., Shemetova, G. V., "Allowance for the Atmospheric Boundary Layer in the Short-Range Weather Forecasting Problem," TRUDY ZAP.-SIB. RNIGMI, No 25, 1976.

10. Marchuk, G. I., Kontarev, G. R., Rivin, G. S., "Short-Range Weather Forecasting Using Full Equations for a Limited Territory," IZV. AN SSSR, FIZIKA ATMOSFERY I OKEANA, Vol 3, No 11, 1967.

11. Marchuk, G. I., et al., GIDRODINAMICHESKAYA MODEL' OBSHCHEY TSIRKULYATSII ATMOSFERY (Hydrodynamic Model of General Circulation of the Atmosphere), Preprint, VTs SO AN SSSR, No 66, 1977.

12. Okinshevich, R. I., Rivin, G. S., Urazalina, Z. K., "Evaluation of Results of Numerical Experiments," TRUDY ZAP.-SIB. RNIGMI, No 29, 1978.

13. Kreis, Heinz-Otto, Oliger, Joseph, "Comparison of Accurate Methods for the Integration of Hyperbolic Equations," TELLUS, Vol 24, No 3, 1972.

UDC 551.(509.313:465.7)

COMPUTATION OF THE INDEX OF FORECASTING ACCURACY IN AN "OCEAN-ATMOSPHERE" SYSTEM MODEL WITH A GREAT NUMBER OF DEGREES OF FREEDOM

Moscow METEOROLOGIYA I GIDROLOGIYA in Russian No 6, Jun 79 pp 15-20

[Article by Candidate of Physical and Mathematical Sciences V. A. Ryasin, USSR Hydrometeorological Scientific Research Center, submitted for publication 11 October 1978]

Abstract: In order to ascertain the limiting possibilities of a model in predicting reality it is necessary to be able to compute the index of forecasting accuracy within the framework of the model. This paper presents a method for computing this index and the dependence of the accuracy index on the measuring system is considered.

[Text] The results in this study are a logical continuation of the results in [3, 4]. The authors of [4] presented a strategy for ascertaining the limiting accuracy of a forecast of the state of the real "atmosphere-ocean" system in a class of determined models of this system. An important component of the strategy is computation of the forecasting accuracy index within the limits of the selected model. In [3] the author presented a method for computing the accuracy index of a forecast which is applicable completely to the "atmosphere-ocean" system models with few parameters having the number of degrees of freedom $n \approx 10^2$-10^3. For finite-difference models with the number of degrees of freedom 10^4-10^6 the method [3] cannot be realized using existing electronic computers. Therefore, for models with a great number of degrees of freedom the need arises for developing another method for computing the index of forecasting accuracy. Such a method is set forth in this study.

Assume that a determined model of the "atmosphere-ocean" system with a great number of degrees of freedom is stipulated. "Determinism" of the model means that its initial state ϑ_0 unambiguously determines the state of the model ϑ_t at future moments in time $t > 0$. Assume that it is necessary to compute the index of forecasting accuracy within the framework of the model in the presence of a definite observation network and a stipulated time regime

of operation of its stations. By the measurements $\xi = (\xi_1, \ldots, \xi_N)$ within the framework of this model we will understand the set of values characterizing the model parameters, for example, temperature, height of the isobaric surface, surface pressure, flow velocities, etc., on a trajectory unknown to the observer [4] ϑ, beginning from the point ϑ_0. Each measurement has a temporal and spatial tie-in. The assumption of a determined nature of the model makes it possible to relate the ξ measurements to ϑ_0 by the expression

$$\xi_i = \alpha_i(\vartheta_0) + \Delta_i,$$

where $\alpha_i(\vartheta_0)$ is the parameter to be measured, Δ_i is the measurement error.

In the model it is postulated that ϑ_0 and Δ_i, $i = \overline{1, N}$ represent a random vector and random values stipulated in some stochastic space.

On the basis of the evaluation $\hat{\vartheta}_0$, being a function of ξ, the observer makes a decision about the initial state, from which, in his opinion, emerged the trajectory of the model, giving the set of measurements ξ. This trajectory is prognostic and differs from the actual trajectory ϑ.

Assume that $\|\cdot\|$ is a norm characterizing the energy of the state of the model, p is a confidence coefficient close to unity. The accuracy of the forecast within the limits of the model, on the basis of ξ information, is called the value γ_ξ, satisfying the equation

$$P\{\|\vartheta_T - \hat{\vartheta}_T\| < \gamma_\xi | \xi\} = p,$$

where ϑ_T and $\hat{\vartheta}_T$ are the vectors of state of the model at the forecasting time T on the actual and predicted trajectories. On the left-hand side of the expression we have the conditional probability of the event

$$\{\|\vartheta_T - \hat{\vartheta}_T\| < \gamma_\xi\}.$$

The Γ_ξ value, determined from the condition

$$P\{\|\vartheta_0 - \hat{\vartheta}_0\| < \Gamma_\xi | \xi\} = p,$$

is the accuracy in determining the initial state of the model on the basis of the ξ information.

First we will examine the problem of the dependence of Γ_ξ on the system of measurements. As an evaluation we will consider

$$\hat{\vartheta}_0 = \lim_{s \to \infty} \vartheta_0(s). \tag{1}$$

In (1) $\vartheta_0(s)$ is a solution of the equation

$$\dot{\vartheta}_0(s) = -\operatorname{grad}_{\vartheta_0(s)} J. \tag{2}$$

with the initial condition $\vartheta_0(0) = \vartheta_0^1$. Here ϑ_0^1 is some value of the initial state of the model, selected at the observer's discretion. The functional J in (2) has the form

$$J = \frac{1}{N} \sum_{i=1}^{N} \frac{[\xi_i - \alpha_i(\vartheta_{t_i}(\vartheta_0))]^2}{2\sigma_i^2}, \tag{3}$$

where $0 < \sigma_i^2$ is the dispersion of the measurement error Δ_i, t_i is the time for carrying out the measurement ξ_i.

The solution of equation (2) assumes that in the model we have developed a method for computing the gradient of a functional stipulated in the trajectory space $\{\vartheta\}$.

Source [2] described a method for computing the gradient of the functional and obtaining the evaluation (1) for finite-difference models of an "atmosphere-ocean" system with a dry atmosphere, but still open is the question of computing the accuracy of this evaluation and the relationship between accuracy and the measuring system.

The problem of the relationship between Γ_ξ and the measurement system will be considered on the assumption that the states of the model $\vartheta_0(s)$, ϑ_0^1 entering into (2), (3) fall in the neighborhood of some reference state $\bar{\vartheta}_0$ and that the dependence of the functional (3) on ϑ_0 in this neighborhood can be considered as quadratic relative to $\Delta\vartheta_0 = \vartheta_0 - \bar{\vartheta}_0$:

$$J = \frac{1}{N} \sum_{i=1}^{N} \frac{[\xi_i' - l_i^* \Delta\vartheta_0]^2}{2\sigma_i^2}, \tag{4}$$

where $\xi'_i = \xi_i - \alpha_i(\bar{\vartheta}_0)$ is the difference between the measured value and the value to be measured, computed on the reference trajectory,

$$l_i = \operatorname{grad}_{\Delta\vartheta_0} \alpha_i(\vartheta_0).$$

The asterisk in (4) denotes transposing.

The measurements $\xi' = (\xi'_1, \ldots, \xi'_N)$ are related to $\Delta\vartheta_0$ by the expression

$$\xi' = L\,\Delta\vartheta_0 + \Delta,$$

where L is a matrix of the dimensionality N x n, whose rows are l_i^*, $\Delta = (\Delta_1, \ldots, \Delta_N)$.

Equation (2) under the condition (4) is written in the form

$$\Delta\dot{\vartheta}_0(s) = \frac{1}{N} L^* B \xi' - \frac{1}{N} L^* B L\, \Delta\vartheta_0(s), \tag{5}$$

$$\Delta\vartheta_0(0) = \Delta\vartheta_0^1,$$

where B is a diagonal matrix with the elements σ_i^{-2}, $i = \overline{1, N}$.

Now we will examine the symmetric matrix

$$Q = \frac{1}{N} L^* BL = \frac{1}{N} L^* (B^{1/2})^* B^{1/2} L,$$

where $B^{1/2}$ is a diagonal matrix with the elements σ_i^{-1}, $i = \overline{1,N}$. The eigenvalues $\lambda_1, \ldots, \lambda_n$ of the Q matrix are real; the eigenvectors $h_1, \ldots, h_n$ form an orthogonal base in the space $\{\Delta\vartheta_0\}$ [1]. Moreover, the Q matrix is nonnegatively determined and its eigenvalues are nonnegative. We will consider the set $h_1, \ldots, h_n$ to be orthonormalized and ordered in such a way that $0 \leqslant \lambda_1 \leqslant \lambda_2 \leqslant \ldots \leqslant \lambda_n$.

We will use the term "well-determined measuring system" for a system for which $\lambda_i > 0$, $i = \overline{1, n}$; a "poorly determined measuring system" is a system for which Q has zero eigenvalues. Now we will examine the problem of the behavior of solution of equation (5). Assume that H is a matrix whose columns are the eigenvectors $h_1, \ldots, h_n$, Λ is a diagonal matrix with the elements $\lambda_1, \ldots, \lambda_n$. We note that $H^{-1} = H^*$. In (5) we will replace the variables:

$$z = H^{-1}\Delta\vartheta_0(s).$$

We will write a differential equation for z:

$$\dot{z} = \frac{1}{N} H^{-1} L^* B\xi' - \Lambda z, \qquad z(0) = H^{-1}\Delta\vartheta_0. \tag{6}$$

In the case of a well-determined measuring system Λ^{-1} exists, and the solution (6) has the form

$$z(s) = \Lambda^{-1}\frac{1}{N} H^{-1} L^* B\xi' + e^{-\Lambda s}\left[H^{-1}\Delta\vartheta_0 - \Lambda^{-1}\frac{1}{N} HL^* B\xi'\right].$$

Hence

$$\lim_{s\to\infty} z(s) = \Lambda^{-1}\frac{1}{N} H^{-1} L^* B\xi'$$

and

$$\Delta\hat{\vartheta}_0 = H\Lambda^{-1}\frac{1}{N} H^{-1} L^* B\xi'.$$

Now we will examine the relationship between the evaluation vector $\Delta\hat{\vartheta}_0$ and the actual vector of the initial state of the model $\Delta\vartheta_0$ unknown to the observer. We recall that the ξ information was obtained on a trajectory beginning from $\vartheta_0 = \bar{\vartheta}_0 + \Delta\vartheta_0$; therefore $\xi' = L\Delta\vartheta + \Delta$, where Δ is a specific set of measurement errors prevailing in the modeling of ξ. This means that

$$\Delta\hat{\vartheta}_0 = \Delta\vartheta_0 + H\Lambda^{-1}\frac{1}{N} H^{-1} L^* B\Delta. \tag{7}$$

It follows from (7) that the evaluation $\hat{\hat{\vartheta}}_0$ is unbiased if the mathematical expectation Δ is equal to zero.

The error in determining the initial state of the trajectory ϑ, from which the ξ measurements are read, is written in the form

$$\|\vartheta_0 - \vartheta_0\| = \|\Delta\vartheta_0 - \Delta\vartheta_0\| = \left\| H\Lambda^{-1}\frac{1}{N}H^{-1}L^*B\Delta \right\|. \tag{8}$$

Now we will examine the dependence $\|\vartheta_0 - \hat{\hat{\vartheta}}_0\|$ on the accuracy of individual measurements at stations. We will assume that at all stations the accuracy is increased by a factor of m. This means that the new dispersion of the measurement error $\tilde{\sigma}_i^2$ is related to the old σ_i^2 by the expression $\sigma_i^2 = \tilde{\sigma}_i^2 m^2$. In (8), with a change in the measurement accuracy σ_i^2, there is a change in the matrices Λ^{-1}, B and the vector Δ; we have

$$\Lambda^{-1} = \tilde{\Lambda}^{-1}m^2, \qquad \tilde{B} = Bm^2, \qquad m\tilde{\Delta} = \Delta.$$

Accordingly,

$$\left\| H\tilde{\Lambda}^{-1}\frac{1}{N}H^{-1}L^*\tilde{B}\tilde{\Delta} \right\| = \frac{1}{m}\left\| H\Lambda^{-1}\frac{1}{N}H^{-1}L^*B\Delta \right\| \underset{m\to\infty}{\longrightarrow} 0$$

Thus, in the case of a well-determined measuring system by an increase in the accuracy of measurements at stations it is possible to attain the desired accuracy in determining the initial state of the model $\Delta\vartheta_0$, making the Γ_ξ and γ_ξ values of the necessary smallness.

We note that in the case of a well-determined measuring system the observer's choice of the state $\Delta\vartheta_0^1$ necessary for obtaining the evaluation $\Delta\hat{\vartheta}_0$ exerts no influence on the value of the error $\|\vartheta_0 - \hat{\vartheta}_0\|$.

The situation is different in the case of a poorly determined measuring system. Assume that r eigenvalues of the Q matrix are equal to zero. We note that

$$\Lambda = H^{-1}QH = H^*QH = \frac{1}{N}H^*L^*(B^{1/2})^*B^{1/2}LH.$$

Since the first r diagonal elements of the Λ matrix are equal to zero, the first r rows of the matrix $H^*L^*(B^{1/2})^*$ are filled with zeroes. In (6)

$$\frac{1}{N}H^{-1}L^*B\xi' = \frac{1}{N}H^*L^*\cdot B^{1/2})^*(B^{1/2}\xi'),$$

accordingly, in the case of a poorly determined measuring system the first r equations of system (6) have the form

$$\dot{z}_i = 0, \quad i = \overline{1, r},$$

and the equations for z_i, $i = \overline{r+1, n}$ have the form as in the case of a well-determined measuring system.

We will denote by E_r the diagonal matrix for which the first r elements are equal to unity and the others are equal to zero; we use Λ_{n-r}^{-1} to denote a diagonal matrix for which the first r elements are equal to zero and

the others are equal to λ_i^{-1}, $i = \overline{r+1, n}$. Then in the case of a poorly determined measuring system

$$\lim_{s\to\infty} z(s) = E_r H^{-1}\Delta\vartheta_0^1 + \Lambda_{n-r}^{-1}\frac{1}{N} H^{-1}L^* B\xi'$$

and

$$\Delta\hat{\vartheta}_0 = H\lim_{s\to\infty} z(s).$$

The difference between the value of the evaluation $\Delta\hat{\hat{\vartheta}}_0$ and the actual value of the initial state is expressed by the formula

$$\|\Delta\vartheta_0 - \Delta\hat{\vartheta}_0\| = \left\| HE_r H^{-1}(\Delta\vartheta_0 - \Delta\vartheta_0^1) - H\Lambda_{n-r}^{-1}\frac{1}{N} H^{-1} L^* B\Delta \right\|. \qquad (9)$$

In (9) the vector $HE_rH^{-1}(\Delta\vartheta_0 - \Delta\vartheta_0^1)$ is the projection of $\Delta\vartheta_0 - \Delta\vartheta_0^1$ onto the subspace formed by the vectors $h_1,\ldots,h_r$. The norm of the projection is the fundamental, indestructible part of the error $\|\vartheta_0 - \hat{\vartheta}_0\|$. The second part of the error, stipulated by the term $H\Lambda_{n-r}^{-1}\frac{1}{N}H^{-1}L^*B\Delta$, in principle can be made negligible in magnitude by an increase in measurement accuracy at the stations, but such an accuracy increase is economically in no way justified: the error $\|HE_rH^{-1}(\Delta\vartheta_0 - \Delta\vartheta_0^1)\|$ always remains. It is important to take this circumstance into account in developing a modern system of observations of the atmosphere and ocean. Efforts must be directed to creation of a configuration of a well-determined measuring network, not to the creation of observation facilities giving a high measurement accuracy at stations but having poor determinacy.

If it is assumed that in finding the evaluation $\Delta\hat{\hat{\vartheta}}_0$ the observer always selects $\Delta\vartheta_0^1 = 0$, the error in determining the state $\Delta\vartheta_0$ is random, equal to the projection of the state $\Delta\vartheta_0$ onto the subspace of the vectors $h_1,\ldots, h_r$ and falls with the confidence coefficient p in the interval $[0, \Gamma_\xi(\vartheta_0)]$, which is found from the condition

$$P\{\|HE_rH^{-1}\Delta\vartheta_0\| < \Gamma_\xi(\bar{\vartheta}_0)\,|\,\xi\} = p.$$

Now we will discuss the problem of the practical finding of the accuracy indices Γ_ξ, γ_ξ in models of an "atmosphere-ocean" system of great dimensionality. In the author's opinion, for such models the method for computing Γ_ξ and γ_ξ on the basis of constructing the Q matrix and solution of the spectral problem for it is comparable in difficulty to the method for computing the accuracy of the optimum (in the mean square sense) evaluation of state [1] and cannot be realized using existing computers. For determining Γ_ξ and γ_ξ it is reasonable to use the Monte Carlo method, the method of experimental construction of the distribution of probabilities of errors $\|\vartheta_0 - \hat{\vartheta}_0\|$ and $\|\vartheta_T - \hat{\vartheta}_T\|$. Now we will describe this process. We will select the nonrandom initial state of the model $\tilde{\vartheta}_0$. In the forecasting interval [0, T] we compute the trajectory $\tilde{\vartheta}$, from which we take the information $\xi = (\xi_i = \alpha_i(\tilde{\vartheta}_0) + \Delta_i,\ i = \overline{1, N})$, modeling the measurements of the planned observation system. In accordance with the distribution of

probabilities $p(\vartheta_0)$ we obtain the state ϑ_0^1, from which are integrated the equations (2) for obtaining the evaluation $\hat{\vartheta}_0$. The predicted trajectory $\hat{\vartheta}$ is computed by obtaining the evaluation $\hat{\vartheta}_0$ in the interval [0, T]. The two values $\|\hat{\vartheta}_0 - \tilde{\vartheta}_0\|$ and $\|\hat{\vartheta}_T - \tilde{\vartheta}_T\|$ are computed. After this we obtain the new value ϑ_0^1 and the entire cycle is repeated, beginning with integration of equations (2). When obtaining a quite large sample of the values $\|\hat{\vartheta}_0 - \tilde{\vartheta}_0\|$ and $\|\hat{\vartheta}_T - \tilde{\vartheta}_T\|$ it is possible to construct the distribution functions of these values and the $\Gamma_\xi(\tilde{\vartheta}_0)$ and $\gamma_\xi(\tilde{\vartheta}_0)$ values are determined. We emphasize that the problem of determining the accuracies of $\Gamma_\xi(\tilde{\vartheta}_0)$ and $\gamma_\xi(\tilde{\vartheta}_0)$ imposes requirements on the methods for integrating equations (2) and the equations of the model. These methods must be precise so that the error in integration at the norm will be a value of a lesser order than the accuracy to be determined.

The Γ_ξ and γ_ξ values are found as

$$\Gamma_\xi = \max_{\tilde{\vartheta}_0 \in \Omega} \Gamma_\xi(\tilde{\vartheta}_0), \quad \gamma_\xi = \max_{\tilde{\vartheta}_0 \in \Omega} \gamma_\xi(\tilde{\vartheta}_0),$$

where Ω is the region in which with a probability close to unity the states of the model $\tilde{\vartheta}_0$ can be situated.

In applying the described method it is necessary to solve the problem (2) jointly with the problem of integrating the fundamental and conjugate equations of the model. The general dimensionality of the problem is 3n, where n is the number of degrees of freedom of the model. Therefore, the described method for computing the accuracy of a forecast can be applied using existing electronic computers for finite-difference models of the "atmosphere-ocean" system. In comparison with the method for computing the accuracy of a forecast from [1], the described method requires a lesser memory (3n instead of n^2), but a substantially greater operating time for the electronic computer.

BIBLIOGRAPHY

1. Gantmakher, F. R., TEORIYA MATRITS (Matrix Theory), Moscow, Nauka, 1967.

2. Penenko, V. V., Obraztsov, N. N., "Variation Method for Assimilation of the Fields of Meteorological Elements," METEOROLOGIYA I GIDROLOGIYA (Meteorology and Hydrology), No 11, 1976.

3. Ryasin, V. A., "Method for Computing the Accuracy Possibilities of a Measuring Network Consisting of Modern Means for Monitoring the State of the 'Atmosphere-Ocean' System," METEOROLOGIYA I GIDROLOGIYA, No 6, 1978.

4. Ryasin, V. A., Sal'nik, V. A., "Maximum Admissible Accuracy of a Forecast in a Class of Models of the 'Atmosphere-Ocean' System," METEOROLOGIYA I GIDROLOGIYA, No 9, 1978.

UDC 551.513

HYDRODYNAMIC THREE-LEVEL MODEL OF GENERAL CIRCULATION OF THE ATMOSPHERE

Moscow METEOROLOGIYA I GIDROLOGIYA in Russian No 6, Jun 79 pp 21-32

[Article by Candidates of Physical and Mathematical Sciences V. P. Meleshko, B. Ye. Shneyerov and L. R. Dmitriyeva-Arrago, and Professor M. Ye. Shvets, Main Geophysical Observatory, submitted for publication 5 September 1978]

Abstract: The article describes a hydrodynamic model of general circulation of the atmosphere based on solution of a full system of equations of atmospheric dynamics in a σ-system of coordinates. A finite-difference approximation of the equations, written applicable to the map plane in a stereographic projection, ensures conservation of mass and total energy in an adiabatic approximation without the dissipation of energy taken into account. The model takes into account the principal physical processes of heat and moisture exchange. Numerical experiments were carried out for the modeling of atmospheric circulation, atmospheric heat regime and the moisture cycle for January conditions. The computed characteristics of circulation, heat and water balance are compared with actual data.

[Text] Introduction. Hydrodynamic models of the atmosphere are now being developed in the USSR, United States and in a number of other countries [15]. These models differ both with respect to the degree of complexity of the schemes for the parameterization of physical processes and the mathematical approach employed. The mechanisms of general circulation of the atmosphere have been studied using such models. Data from numerical experiments have been used in computing the mean distributions of the principal meteorological elements, and also the energy characteristics and components of the heat and water balances. The results of comparison with real data indicated that in general hydrodynamic models reproduce

well the large-scale characteristics of general circulation and the thermal regime of the atmosphere, but less successfully reproduce such characteristics whose formation is greatly influenced by processes associated with baroclinic instability, and also mesoscale processes. As a rule, in the models there is an exaggeration of the intensity of mean zonal flow in the middle latitude troposphere, whereas the eddy component of kinetic and available potential energy is underestimated.

In this article we will describe a three-level hydrodynamic model of general circulation of the atmosphere for a hemisphere, developed at the Main Geophysical Observatory imeni A. I. Voyeykov. This model is a compromise variant between the technical possibilities of existing electronic computers and the aspiration to construct a model more meaningful from the physical point of view. Using this model we carried out numerical experiments for the modeling of general circulation and the thermal regime of the atmosphere for January conditions. Some of the results of these experiments are discussed below.

1. Description of Model

1.1. Fundamental Equations and Boundary Conditions

In the model we used the full equations of atmospheric dynamics, written in a σ-system of coordinates applicable to the plane of a stereographic projection.

a) Equations of horizontal motion

$$\frac{\partial U}{\partial t} + m\left[\frac{\partial Uu}{\partial x} + \frac{\partial Vu}{\partial y}\right] + \frac{\partial \dot{\sigma} U}{\partial \sigma} - V(f^{(1)} + f^{(2)}) = \\ = -p_s\left(\frac{\partial \Phi}{\partial x} + RT\frac{\partial \ln p_s}{\partial x}\right) - \frac{g}{m}\frac{\partial \tau_x}{\partial \sigma} + F_{su}, \tag{1}$$

$$\frac{\partial V}{\partial t} + m\left[\frac{\partial Uv}{\partial x} + \frac{\partial Vv}{\partial y}\right] + \frac{\partial \dot{\sigma} V}{\partial \sigma} + U(f^{(1)} + f^{(2)}) = \\ = -p_s\left(\frac{\partial \Phi}{\partial y} + RT\frac{\partial \ln p_s}{\partial y}\right) - \frac{g}{m}\frac{\partial \tau_y}{\partial \sigma} + F_{sv}. \tag{2}$$

b) Heat influx equation

$$\frac{\partial \tilde{T}}{\partial t} - m\left[\frac{\partial U\tilde{T}}{\partial x} + \frac{\partial V\tilde{T}}{\partial y}\right] + \frac{\partial \dot{\sigma}\tilde{T}}{\partial \sigma} - \frac{AR}{c_p}\frac{T}{m}\frac{\omega}{\sigma} = \\ = \frac{g}{c_p m}\frac{\partial H}{\partial \sigma} + \frac{\varepsilon}{m} + \frac{Lp_s}{c_p m}r + F_{s\tilde{T}}. \tag{3}$$

c) Heat transfer equation

$$\frac{\partial \tilde{q}}{\partial t} + m\left[\frac{\partial U q}{\partial x} + \frac{\partial V q}{\partial y}\right] + \frac{\partial \dot{\sigma} \tilde{q}}{\partial \sigma} = \frac{g}{m}\frac{\partial E}{\partial \sigma} - \frac{p_s r}{m} + F_{sq}. \tag{4}$$

d) Continuity equation

$$\frac{\partial p_s}{\partial t} = -m^2\left(\frac{\partial U}{\partial x} + \frac{\partial V}{\partial y}\right) - p_s\frac{\partial \dot{\sigma}}{\partial \sigma}. \tag{5}$$

e) Equation of hydrostatics

$$\frac{\partial \Phi}{\partial \sigma} = -\frac{RT}{\sigma}. \tag{6}$$

In addition, we use an expression for vertical velocity in a σ-system of coordinates, obtained from the continuity equation

$$p_s\dot{\sigma} = m^2\left[\sigma\int_0^1\left(\frac{\partial U}{\partial x} + \frac{\partial V}{\partial y}\right)d\xi - \int_0^\sigma\left(\frac{\partial U}{\partial x} + \frac{\partial V}{\partial y}\right)d\xi\right]. \tag{7}$$

Here u and v are the horizontal components of velocity in the direction of the x- and y- axes respectively, T is temperature, q is specific humidity, p_s is pressure at the earth's surface, Φ is geopotential, ω is vertical velocity in an isobaric coordinate system, $\dot{\sigma}$ is vertical velocity in a σ - coordinate system, $\sigma = p/p_s$, p is pressure, $f^{(1)}$ is the Coriolis parameter, $f^{(2)}$ is the metric term of the equations of motion, τ_x and τ_y are the components of turbulent frictional stress in projection onto the x-, y-axes, $\mathcal{E}$ is the radiative heat influx, r is the quantity of condensed moisture, H and E are the vertical turbulent fluxes of heat and moisture respectively, F_{su}, F_{sv}, F_{st} and F_{sq} are terms describing the horizontal diffusion of momentum, heat and moisture,

$$|U, V, \tilde{T}, \tilde{q}| = \left\{\frac{up_s}{m}, \frac{vp_s}{m}, \frac{Tp_s}{m}, \frac{qp_s}{m}\right\},$$

m is the scale factor for a map in a stereographic projection, L is the specific heat of condensation, c_p is the specific heat capacity of dry air at a constant pressure, R is the specific gas constant for dry air, g is the acceleration of free falling, A is the thermal equivalent of a work unit.

The following boundary conditions are used in the model: at the upper and lower boundaries of the atmosphere $\dot{\sigma} = 0$. The vertical turbulent fluxes of momentum, heat and moisture at the lower boundary of the atmosphere are determined from the equations for the atmospheric boundary layer. At the lateral boundaries, which approximately coincide with the equator, we have the condition that the normal component of horizontal velocity and also the derivatives (along the normal) of temperature, humidity and the tangential component of wind velocity are equal to zero.

1.2. Spatial Structure of Model

In the model we use a square grid for a stereographic projection with the principal scale at latitude 60°. The total number of points of intersection at each level in a hemisphere is 1481; the mean grid interval is 425 km.

The vertical structure of the model includes three layers with a uniform σ interval. The principal variables u, v, T, q and ω are determined at the levels σ = 0.167, 0.5, 0.833.

1.3. Numerical Solution of System of Equations

For solution of the system of equations (1)-(7) we use the finite-difference scheme proposed by Lilly [8], having a second order of approximation with respect to space variables. For the adopted boundary conditions and in the absence of energy losses and gains this scheme ensures conservation of mass and total energy. In computing the force of the pressure gradient in the equations of motion (1)-(2) we will use the difference approximation proposed in [12]. As demonstrated in [6], this approximation ensures an accuracy of computations in a σ-system which is the same as in an isobaric coordinate system.

Equations (1)-(5) are integrated in time by the central differences method with an interval of 10 minutes. In order to exclude the fictitious solution which arises, after each 48 intervals in three successive intervals we employ the three-point filter

$$\bar{A}^{\tau} = A^{\tau} + 0{,}5\,(A^{\tau-1} + A^{\tau+1} - 2\,A^{\tau}). \qquad (8)$$

Then the equations are integrated again in one interval by the Matsuno scheme [4], after which the calculations are continued using the central differences scheme. For the equations of motion the adopted scheme is partially implicit, since the force of turbulent friction is taken in the succeeding time interval.

In order to construct matched initial fields of the principal meteorological elements for a hemisphere a complex of computer programs was developed and applied. The initial fields are constructed in two stages. In the first stage, in an isobaric coordinate system, for seven uniformly situated levels we constructed the relative humidity fields, and also the temperature fields, matched vertically using the equation of statics and the fields of horizontal components of velocity, matched horizontally in a quasisolenoidal approximation, by solution of the balance equation. In the second stage there is transformation from an isobaric coordinate system to a σ- system taking into account the relief of the continents and the vertical structure of the particular model of the atmosphere.

1.4. Parameterization of Nonadiabatic Processes

The model takes into account the principal energy gains and losses operative in the real atmosphere.

a) Radiation. In computing the radiation heat influxes and the radiation balance at the underlying surface an allowance is made for the absorption of radiation by water vapor and carbon dioxide, scattering on molecules of air and aerosol, and also absorption and scattering of radiation by clouds. In computations of long-wave radiation use is made of the integral transmission function proposed by F. N. Shekhter [10], by means of which an allowance is made for the absorption of radiation by water vapor and CO_2. In computing short-wave radiation we use the sub-ozone solar constant, integral transmission function for the spectral section 0.7-5 μm [3] and the scattering function proposed by V. V. Sobolev [9].

The model takes into account two-layer cloud cover with fixed boundaries: the lower level is situated in the layer (0.667-0.833), the upper level -- in the layer (0.333-0.667). It is assumed that the cloud emits as an ideally black body at the temperature of its upper and lower boundaries. The albedo of clouds of the upper and lower levels was assumed equal to 0.25 and 0.50 respectively. The radiation fluxes under conditions of variable cloud cover are computed on the assumption that the fractions of the celestial sphere simultaneously covered by clouds at the two levels is equal to the product of the tenths of cloud cover at these levels.

b) Large-scale condensation and convection. Allowance for the heat influxes associated with phase transitions of water in the atmosphere is made by the parameterization of two processes: water vapor condensation, caused for the most part by large-scale movements and the release of latent heat during convection, arising in the moist-unstable layers of the atmosphere. Large-scale condensation takes place if the moist air reaches the critical relative humidity $h_k = 0.8$.

In order to compute the heat influxes caused by mesoscale convective processes, we will use the so-called "convective adaptation scheme" [5], in which the equilibrium gradient is assumed to be dependent on relative humidity and the moist-adiabatic gradient [11].

The total quantity of precipitation, both large scale and convective, is determined as the sum of precipitation forming at the individual computation levels.

c) Turbulent influxes of momentum, heat and moisture. The model makes use of a relatively simple and tested scheme for computing the turbulent fluxes and influxes of momentum, heat and moisture, based on the empirical expressions derived by Deardorf [13].

According to [13], the coefficient of vertical exchange in the atmospheric boundary layer is dependent on temperature stratification in the lower layer with a thickness of 1.5 km and the Richardson number.

In the model it is possible to differentiate four types of underlying surfaces:
-- surface of the continents, free of ice and snow. The air temperature T_g at the surface is computed from the heat balance equation

$$\sigma_* T_g^4 + H + LE + \Pi = \tilde{S}_g + R_g^{\downarrow}, \tag{9}$$

where Π is the heat flux into the soil; $\tilde{S}_g$ is the balance of short-wave radiation at the underlying surface, $R_g^{\downarrow}$ is the descending flux of long-wave radiation at the earth, σ_* is the Stefan-Boltzmann constant.

Here use is made of the relationship between the heat flux into the soil Π and the radiation balance for the underlying surface [7];
-- surface of the continents, covered with snow or ice. The temperature is also computed from the heat balance equation; the fluxes of heat into the soil and evaporation are neglected;
-- ice-covered ocean surface. The surface temperature is computed from the heat balance equation. The heat flux through the ice with a stipulated water temperature beneath the ice is taken into account, whereas evaporation is neglected;
-- surface of the oceans and seas free of ice. The temperature at the surface is considered known and the air is considered saturated.
d) Horizontal diffusion. The model uses a nonlinear scheme for computing diffusion which is based on the ideas of three-dimensional isotropic turbulence [8]. In this scheme the eddy viscosity coefficient is proportional to the total deformation of large-scale horizontal flow

$$k = 2\left(\frac{\alpha \Delta s}{m}\right)^2 (D_T^2 + D_S^2)^{1/2}, \tag{10}$$

where D_S is relative shear and D_T is the relative change in linear dimensions with conservation of area. The value $\alpha = 0.25$ was selected for the horizontal resolution Δs used in the model. This diffusion scheme is used widely in a number of models of general circulation of the atmosphere, although, as indicated by recent investigations, it is inadequately selective in suppressing perturbations with a small wavelength.

e) Computation of cloud-cover tenths. As is well known, a number of empirical formulas have been proposed for computing cloud cover tenths in which this characteristic is expressed through relative humidity. A preliminary checking of a number of such formulas has indicated that not one of them makes it possible to obtain satisfactory zonal distributions of cloud cover simultaneously in the low and high latitudes.

In the model the cloud coverage at each level (n_2 and n_3) was computed using the expressions

$$\begin{aligned} n_2 &= -0{,}27 + 1{,}07\, h_2 + 0{,}05\, q_2, \\ n_3 &= -0{,}4 + h_3 + 0{,}01\, q_3, \end{aligned} \tag{11}$$

in which two parameters were used: relative humidity h and specific humidity q in g/kg.

2. Modeling of Atmospheric Circulation for January Conditions

For the purpose of studying the properties of the model and evaluating its possibilities in describing a real climate we carried out a numerical experiment with modeling of circulation, the thermal regime and moisture cycle in the atmosphere for January.

As the a priori stipulated fields we used data taken from different climatic sources on temperature of the ocean surface and boundaries of the ice and snow covers, albedo of the continents and oceans. Solar angle was assumed to be equal to its value for mid-January. As was indicated above, in a number of investigations it has been demonstrated that in the integration of the equations of atmospheric dynamics with a fixed solar angle and a stipulated temperature of the ocean surface the atmosphere attains a quasi-steady regime after approximately 40 days, if at the initial moment the atmosphere was in a state of rest. When using real initial data this point sets in after 10-16 days.

For the particular model the system of equations was integrated for 60 days from the real initial state, for which we used the specific synoptic situation for 5 January 1971. The characteristics of the mean state of the atmosphere were obtained by averaging of the values computed in the model for 31 days (from the 25th through the 55th days of the forecast).

As a result of our numerical experiment we obtained a great number of characteristics of general circulation and heat exchange in the atmosphere. Due to the limited length of the article we will give only some of them.

Figure 1 gives the altitudinal-latitudinal distribution of mean temperature. It can be seen that in the troposphere the computed temperature values coincide well with the actual values. The temperature in the upper layers of the atmosphere is close to the actual temperature in the tropical zone, but to the north it decreases considerably more rapidly than is observed under real conditions. Evidently, the reason is that the upper computation level in the northern latitudes is situated in the stratosphere, which is characterized by processes not taken into account in this model.

With respect to the altitudinal-latitudinal distribution of specific humidity, also represented in Fig. 1, as in the real atmosphere, the specific humidity maximum is observed in the lower layer of the atmosphere at the equator and averages about 14 g/kg. The computed vertical gradient of specific humidity in the lower half of the troposphere in the zone from the equator to 50°N approximately coincides with the actual value. In the polar regions the computed moisture content was less than the actual value.

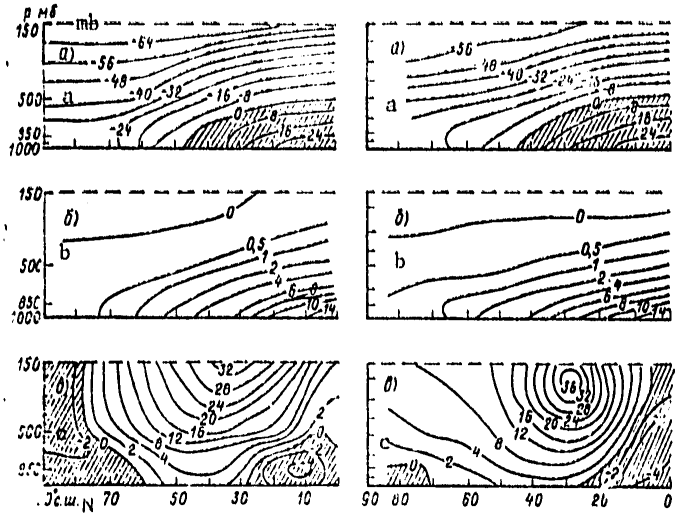

Fig. 1. Altitudinal-latitudinal temperature distribution T°C (a), specific humidity q g/kg (b) and zonal velocity v m/sec (c). Al left -- computed, at right -- actual for January [21].

This same figure shows the computed and actual altitudinal-latitudinal distribution of the zonal component of wind velocity. As in the real atmosphere, there are two regions of easterly flows (in the tropical zone and in the polar latitudes) and an extensive region with west-east transfer, occupying the greater part of the northern hemisphere. The positions of the high-altitude jet stream and its mean velocity are correctly computed. However, in the middle troposphere the velocity of the zonal flow in the model is greater than in the real atmosphere as a result of the exaggerated meridional temperature gradient, computed in the model.

It should be noted that the model correctly reflects the principal characteristics of circulation, and specifically, its tricellular structure. As in the real atmosphere, for January it is the so-called direct Hadley cell, situated in the tropical zone, which is strongest. In January the ICZ is usually situated in the southern hemisphere, but since in the model the boundary is a "wall" at the equator, the Hadley cell, naturally, is displaced somewhat to the north. Nevertheless, its position in the latitude zone to 30°N corresponds to the actual data [14]. The same can also be said with respect to the second circulation cell (Ferrel cell), which, as in the real atmosphere, is situated in the zone from 30 to 70°N. Finally, there is a very weak direct cell in the polar latitudes, as is also observed in actuality.

Now we will cite a number of characteristics of heat and moisture exchange in the atmosphere obtained as a result of the numerical experiment. Figures 2a,b show the latitudinal distributions of the radiation balance at the

underlying surface and at the upper boundary of the atmosphere respectively, which can be considered quite close to the actual distribution of these parameters [1, 15]. The computed mean planetary albedo of the "earth-atmosphere" system is about 35%. The latitudinal variation of the turbulent flux of heat to the atmosphere is represented in Fig. 2c. The computed curve, in general, reflects the distribution of this characteristic obtained on the basis of actual data. A detailed analysis of the experimental results shows that possibly as a result of the scheme for computing the boundary layer adopted in the model the fluxes over the oceans in the high latitudes are somewhat exaggerated, whereas in the low latitudes they are understated in comparison with the actual data.

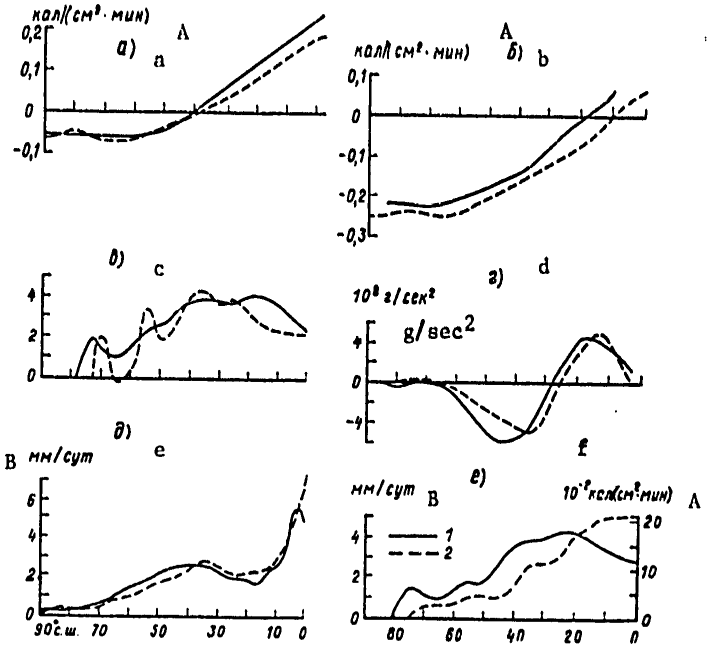

Fig. 2. Latitudinal distribution of characteristics of heat and moisture exchange. 1) actual for January, 2) computed.

KEY:
A) cal/(cm^2·min)
B) mm/day

Figure 2d shows the latitudinal distribution of the moment of surface friction forces. The actual data were taken from a study by Hellerman [14]. In the low latitudes, in accordance with these data, there is an influx of the relative moment of momentum in the atmosphere. In the middle latitudes the loss of momentum was understated by approximately 30%. However, as indicated in a number of studies, Hellerman's data must be considered exaggerated by approximately one-third, since the moment of frictional forces was computed in [14] only for the oceans (without the land being taken into account). Taking this into account, it can be concluded that the values of the moment of frictional forces computed in the model agree well with the actual data.

The latitudinal distribution of precipitation obtained in the model is illustrated in Fig. 2e. Most of the computed precipitation is accounted for by large-scale precipitation, whereas convective precipitation for the most part occurs in the tropical and equatorial zones. The graph clearly shows two maxima, one of which is caused by the intensive falling of precipitation in a zone of baroclinic instability, whereas the other is associated with convection in the tropics. Figure 2f shows the latitudinal distribution of evaporation. The figure shows that at almost all latitudes the quantity of moisture entering into the atmosphere as a result of evaporation is understated in comparison with empirical data. We note that other existing models of atmospheric circulation give lesser values for evaporation in comparison with [1], at least for the temperate latitudes. For the tropical zone our model gives evaporation values closest to the data published by M. I. Budyko [1] in comparison with other existing models.

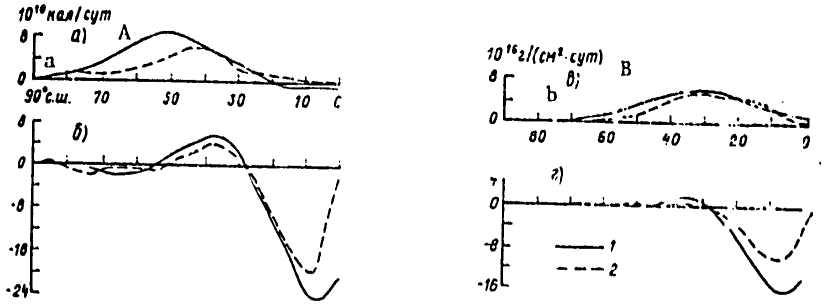

Fig. 3. Meridional transfer of heat and moisture to the north. 1) actual for January [21], 2) computed

KEY:
A) cal/day
B) g(cm^2·day)

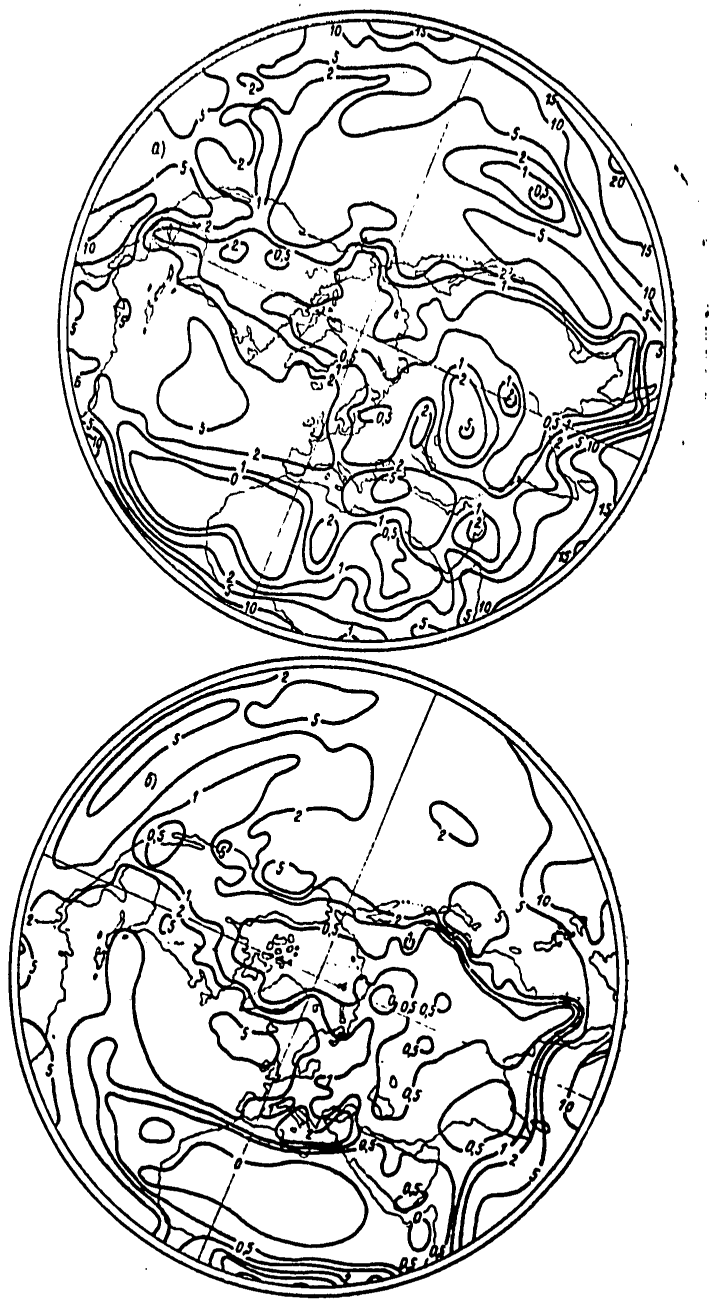

Fig. 4. Precipitation field (mm/day). a) computed; b) actual, January

Figure 3 shows the meridional transfer of heat and moisture. The computed transfer of heat to the north by large-scale eddies (Fig. 3a) agrees satisfactorily with the actual data published by Oort [17]. The computed heat transfer values, associated with mean meridional circulation (Fig. 3b), were less than the actual values, which is attributable in part to absence in the model of heat exchange with the southern hemisphere. The meridional transfer of moisture (Fig. 3c, d) has similar characteristics.

Figure 4 shows the computed and actual precipitation fields. Comparison of these maps shows that both moist and dry regions are modeled rather well.

We give Table 1, characterizing the balance of heat influxes to the atmosphere in the northern hemisphere for January. In computing the actual heat influxes we used data from different authors [1, 17-19].

In the last column of the mentioned table the heat flow across the equator is equal to zero, since in the model this flow is not taken into account as a result of the presence of a "wall" at the equator.

In general, the integral heat influxes agree well with the actual data. The positive balance of heat influxes, obtained using data from independent investigations, is evidently a result of errors in computations of individual components of the balance. With respect to the balance computed in the model, its small value indicates that from the 25th through the 55th days on the average there was a balanced influx of heat with a very weak tendency to cooling.

Table 1

Heat Influx Balance in the Atmosphere for a Hemisphere in January, °C/day

Types of influxes	Actual data	Computed values
Radiation influx	-0.91	-0.88
Turbulent influx	0.22	0.16
Influx as a result of water vapor condensation	0.64	0.73
Influx as a result of heat transfer across equator	0.16	0
Influx as a result of transformation of potential energy into kinetic energy	-0.03	-0.02
Balance of heat influxes	0.08	-0.01

In conclusion we note that S. V. Bogachenko, I. P. Guseva, L. N. Magazenkov, G. V. Parshina, V. I. Ponomarev, D. A. Sheynin and Ye. P. Yushina participated in the numerical experiments and analysis of the results.

BIBLIOGRAPHY

1. ATLAS TEPLOVOGO BALANSA ZEMNOGO SHARA (Atlas of the Earth's Heat Balance), edited by M. I. Budyko, Moscow, Gidrometeoizdat, 1963.

2. Berlyand, T. G., Strokina, L. A., "Cloud Cover Regime on the Earth," TRUDY GGO (Transactions of the Main Geophysical Observatory), No 338, 1975.

3. Yevseyeva, M. G., Podol'skaya, E. L., "Integral Transmission Function in the Near-IR Spectral Region," TRUDY LGMI (Transactions of the Leningrad Hydrometeorological Institute), No 49, 1974.

4. Lilly, D. K., "Computation Stability of Numerical Solutions of Nonstationary Nonlinear Geophysical Problems of Fluid Dynamics," CHISLENNYYE METODY RESHENIYA ZADACH DINAMIKI ATMOSFERY I OKEANA (Numerical Methods for Solving Problems in Dynamics of the Atmosphere and Ocean), edited by L. R. Dmitriyeva-Arrago, L. V. Rukhovets and B. Ye. Shneyerov, Leningrad, Gidrometeoizdat, 1968.

5. Manabe, S., Smagorinsky, J., Strickler, R. F., "Numerical Modeling of the Mean Pattern of General Circulation With Allowance for Moisture Exchange Processes," TEORIYA KLIMATA (Climatic Theory), edited by L. S. Gandin, A. S. Dubov and M. Ye. Shvets, Leningrad, Gidrometeoizdat, 1967.

6. Meleshko, V. P., Sheynin, D. A., "Approximation Errors in Computing the Pressure Gradient in a σ- Coordinate System," TRUDY GGO, No 394, 1967.

7. Ogneva, T. A., "The Necessary Density of a Network of Heat Balance Stations," TRUDY GGO, No 230, 1968.

8. Smagorinsky, J., Manabe, S., Holloway, J., "Results of Numerical Experiments With a Nine-Level Model of General Circulation of the Atmosphere," TEORIYA KLIMATA, edited by L. S. Gandin, A. S. Dubov and M. Ye. Shvets, Leningrad, Gidrometeoizdat, 1967.

9. Sobolev, V. V., RASSEYANIYE SVETA V ATMOSFERAKH PLANET (Light Scattering in Planetary Atmospheres), Moscow, Nauka, 1972.

10. Shekhter, F. N., "On Radiation Diagrams," TRUDY GGO (Transactions of the Main Geophysical Observatory), No 150, 1964.

11. Benwell, G. R. R., et al., "The Bushby-Timpson 10-Level Model on a Fine Mesh," SCIENTIFIC PAPER, No 32, London, 1971.

12. Corby, G. A., Gilschrist, A., Newson, R. L., "General Circulation Model of the Atmosphere Suitable for Long-Period Integrations," QUART. J. ROY. METEOROL. SOC., Vol 93, 1972.

13. Deardorf, T. W., "Empirical Dependence of the Eddy Coefficient for Heat Upon Stability Above the Lowest 50 m," J. APPL. METEOROL., Vol 6(4), 1967.

14. Hellerman, S., "An Updated Estimate of the Wind Stress on the World Ocean," MON. WEATHER REV., Vol 95, 1967.

15. "Modelling for the First GARP Global Experiment," GARP PUBLICATIONS SERIES, No 14, 1974.

16. Newell, R. E., Kidson, T. W., Vincent, D. G., Boer, G. T., THE GENERAL CIRCULATION OF THE TROPICAL ATMOSPHERE AND INTERACTIONS WITH EXTRATROPICAL LATITUDES, MIT, Dept. Meteorol., Vol 1, 1972.

17. Newell, R. E., Vincent, D. G., Dopplick, T. G., Ferruzad and Kidson, T. W., THE ENERGY BALANCE OF THE GLOBAL ATMOSPHERE, American Meteorological Society, Boston, Mass., 1969.

18. Oort, A. H., "The Observed Annual Cycle in the Meridional Transport of Atmospheric Energy," J. ATMOS. SCI., Vol 28, 1971.

19. Oort, A. H., Peixoto, T. P., "The Annual Cycle of the Energetics of the Atmosphere on a Planetary Scale," JGR, Vol 79, No 18, 1974.

20. Oort, A. H., Rassmusson, E. M., ATMOSPHERIC CIRCULATION STATISTICS, Professional Paper No 5, NOAA, 1971.

UDC 551.511

ENERGY CHARACTERISTICS OF THE WINTER WARMING OF 1976/1977

Moscow METEOROLOGIYA I GIDROLOGIYA in Russian No 6, Jun 79 pp 33-40

[Article by Candidates of Geographical Sciences I. V. Bugayeva, L. A. Ryazanova, and D. A. Tarasenko, and Candidate of Physical and Mathematical Sciences G. R. Zakharov, Central Aerological Observatory, submitted for publication 13 July 1978]

Abstract: On the basis of rocket and satellite data obtained during recent years the authors examine the characteristics of synoptic processes during the winter period in the stratosphere and mesosphere. The computations of the energy characteristics indicated that during a period of warmings there is a restructuring of the vertical profiles of kinetic and available potential energy.

[Text] The month February 1977 marked the 25th anniversary of Scherhag's discovery of the so-called "Berlin phenomenon" [4]. This phenomenon was the marked increase in temperature in the winter stratosphere — by more than 40°C. During recent years satellite data, making it possible to determine the temperature and geopotential values on a global scale at different levels in the stratosphere and mesosphere, make possible a detailed study of stratospheric warmings.

In this study, for an analysis of synoptic processes and computation of the energy characteristics, we have used pressure pattern charts for the 10-mb surface, high-altitude charts of constant levels up to 60 km published by the Central Aerological Observatory [1], pressure pattern charts for 5, 2 and 0.4 mb, constructed using satellite and rocket data, and also time sections for the atmosphere based on data from rocket stations in the western and eastern hemispheres.

All the enumerated materials, and also some associated computations, made it possible to ascertain several large waves of a sharp temperature increase in the stratosphere and mesosphere in the winters of 1976/1977 and 1977/1978 in the high and middle latitudes of the northern hemisphere. The

distinguishing characteristics of the mentioned winters were: first, the presence of three temperature increase waves with a final warming in March, second, January and March warmings characterized by a great intensity, occurring with a pressure restructuring in the polar regions and classified as "strong," third, the transpiring processes were greatly influenced by both the Pacific Ocean and Atlantic anticyclones, which frequently extended from tropospheric levels into the mesosphere. The observed characteristics of winter processes played a definite role in the bringing about of early spring stratospheric restructurings.

The first wave of stratospheric warming for the winter of 1976/1977 was observed in the second half of November 1976. Satellite data for this period show a broad region of heat from the Caspian Sea to the Bering Sea with temperatures at the center equal to -20°C at the isobaric surface 5 mb. At the same time, at the cold focus, displaced toward Greenland, the temperature was reduced to -70°C. The maximum temperatures were observed in the region of the stratopause and over Kheys Island attained 12°C, whereas over Volgograd it attained 9°C. This warming was noted only over the eastern hemisphere. During this period there was an intensification of the Pacific Ocean and Indochinese anticyclones, which joined into a single zone of high pressure extending from the Arabian Sea to Chukotka and Alaska. A similar early winter warming was also observed in November 1968.

A second warming wave began about 15 December. During this period there was an intensification of the Pacific Ocean anticyclone. The anticyclone attained maximum development during the period 21-25 December; by this time its center was situated at 65°N near Alaska. Such a marked displacement of the anticyclone to the north caused the development of a high-altitude frontal zone over the pole: over Kheys Island the easterly and southeasterly winds in the layer 45-50 km attained velocities of 130 m/sec and the temperature at an altitude of 45 km was 0°C. The cyclone shifted to the northern sector of the European USSR; the region of cold associated with it was situated over Greenland and then moved to 45°N and was situated over North America.

The Atlantic anticyclone began to develop almost simultaneously with the Pacific Ocean anticyclone and beginning on 27 December there was a marked intensification of the Indochinese anticyclone, which began to move northward rapidly: thus, on 27 December its center was situated at 37°N, whereas by 1 January it had attained 52°C. The regions of heat associated with it at the 10-mb level had a temperature of -15°N. By the end of December there was a joining of the Atlantic and Indochinese anticyclones; the high-level charts show that this combined anticyclone penetrated into the mesosphere. During the period 25-31 December it could be seen well not only at AT_5 and AT_2, but also at $AT_{0.4}$.

At the end of December the temperature field in the stratosphere over the entire northern hemisphere was characterized by relatively high values both over Eurasia and over the western hemisphere. Even in regions of

cold, associated with the cyclonic center, did the temperature increase by 20°C and attain -55°C instead of the usual -70 - - 75°C (at the 10-mb level).

In January the maximum temperature change over Kheys Island was not observed in the neighborhood of the stratopause, as was the case during the first warming, but at an altitude of 35 km. There was a gradual lowering of the region of heat into the middle stratosphere.

At a number of American stations located in the northern regions there was also a marked temperature increase. For example, at Fort Churchill on 3 January its value at the level 42-46 km was more than 20°C.

At the beginning of January the structure of the pressure field differed by layers: in the stratosphere there was a tricellular structure with a cyclone, displaced onto the European USSR, and two anticyclones in the direction of the Pacific and Atlantic Oceans. In the lower mesosphere (50-55 km) a four-celled field was formed: two cyclonic centers and two anticyclones, whereas above 60 km there was a structure with two cells: cyclone and anticyclone. Despite these differences in structure, a pressure restructuring over the pole was observed in all layers.

In mid-January the warming process in the stratosphere continued, but passed into the middle and lower layers. At an altitude of 50 km over Kheys Island the temperature had decreased to -48°C by 19 January. In the mesosphere an ordinary winter circulation began to be restored with a cyclonic eddy in the region of the pole and relatively low temperatures near the mesopause. During the period from 10 through 21 January an anticyclone in the form of a large unified center was established over the pole in the layer 30-40 km, whereas a cyclonic field, represented by several individual regions, surrounded it along 50°N. Such a structure of the pressure field is characteristic for spring restructurings. By the time of forming of anticyclones in the region of the pole at the 10-mb level the temperature had increased to -45°C. The main region of heat was situated in the lower layers of the stratosphere.

After 21 January there was restoration of normal winter circulation.

For the warming, which was accompanied by a restructuring of circulation, we computed the mean geopotential values along different circles of latitude and as a whole for the hemisphere. These values were compared with the mean geopotential values before and after the warming. Interesting results were obtained.

Satellite data were used for computing geopotential. The mean geopotential was computed for 75, 55 and 35°N with an interval of 30° in longitude at the three isobaric surfaces: AT_5, AT_2 and $AT_{0.4}$. In order to evaluate the geopotential values before the warming period we used data for 9 December 1977. As the time of warming we selected the geopotential values for 6

January 1977 and for the end of warming -- for 14 January 1977.

The results of the computations (Table 1) indicated that the heights of the geopotential surfaces increased during the period of warming as a whole for the hemisphere (the height of the $AT_{0.4}$ surface increased by 168 dam). However, in the low latitudes they decrease somewhat ($AT_{0.4}$ -- by 16 dam), but considerably less than they increase in the high latitudes ($AT_{0.4}$ -- by 321 dam). Thus, only a redistribution of energy by latitude cannot explain the warming process. The energy evidently also arrives from the lower- and above-lying layers of the atmosphere.

Table 1

Mean Geopotential Values ($\overline{H}$ dam) Obtained Using Radiometer Data from the Isobaric Surfaces

p мб 1	2 Северная широта, *град*											
	75	55	35	полушарие 3	75	55	35	полушарие	75	55	35	полушарие
	4 9 декабря 1976 г.				5 6 января 1977 г.				5 14 января 1977 г.			
5	3322	3466	3545	3444	3511	3530	3541	3527	3543	3515	3534	3531
2	3890	4044	4205	4047	4175	4175	4195	4179	4128	4138	4190	4152
0,4	5019	5149	5404	5190	5340	5349	5387	5359	5249	5306	5390	5315

KEY:

1. mb
2. North latitude, degrees
3. hemisphere
4. December
5. January

The third, final warming wave began in the third ten-day period in February. The warming process attained its maximum development on 6-9 March, when a temperature of 22°C was noted over Kheys Island at 45 km and the southerly wind had a velocity greater than 60 m/sec.

In the lower mesosphere the anticyclone, extending from the direction of the Pacific Ocean, occupied the pole, changing the circulation over the western hemisphere. The rocket stations Thule, Poker Flat and Primrose Lake during this period noted stable easterly winds. In the mesosphere an anticyclone was observed over the pole about two weeks. In the stratosphere there was no pressure restructuring in the high latitudes. By 20 March the warming process had ended.

In order to characterize the intensity of circulation in the first two warming waves we computed the index of meridional circulation I_M by the Kats method [2] using the daily values of geopotential height at the 10-mb

level along the circles of latitude 70° and 40°N for November and December 1976 and January 1977.

Table 2

Temperature at Stratopause (t°C) and Index of Meridional Circulation (I_M dam/degree meridian) at 10-mb Level During First and Second Warming Waves 1976/1977

	До потепления 1	В период I потепления 2	После потепления 3	В период II потепления 4	После потепления 5
$t_{о. Хейса}$ 6	−36	+12	−24	+2	−48
$I_{м\ 70°\ с.\ ш.}$ 7	0,63	1,66	1,20	2,60	1,0
$t_{Волгоград}$ 8	−15	+9	−30	−8	−23
$I_{м\ 40°\ с.\ ш.}$ 9	1,08	2,2	1,32	3,26	1,88

KEY:

1) Before warming
2) During period of first warming
3) After warming
4) During period of second warming
5) After warming
6) Kheys Island
7) 70°N
8) Volgograd
9) 40°N

The index of meridional circulation during this period in the high and middle latitudes has two clearly expressed main maxima corresponding to the moment of onset of warmings. The maximum value I_M in the high latitudes in the first warming was observed on 17-19 November and exceeded by a factor of 2.5 the I_M value before the warming, whereas in the middle latitudes it was by a factor of two.

The second I_M maximum is noted in the third ten-day period of December; it is greater than the November maximum and in the middle latitudes the I_M value attains 3.26 dam/degree meridian, whereas in the high latitudes it has a value which is somewhat less and equal to 2.6 dam/degree meridian.

A comparison of the index of meridional circulation with the temperature values in the neighborhood of the stratopause according to data for the stations at Kheys Island and Volgograd indicated that near the moments of the I_M maximum it is possible to observe the maximum temperature values (Table 2).

A distinguishing characteristic of the winter of 1977/1978 was an intensive development of the subtropical zone of high pressure in the Atlantic Ocean region. The anticyclones developing in the troposphere were frequently high and attained the 50-mb surface, and sometimes also the 10- and 5-mb surfaces. The warm regions associated with the Atlantic anticyclones moved

into the polar latitudes and caused stratospheric warmings.

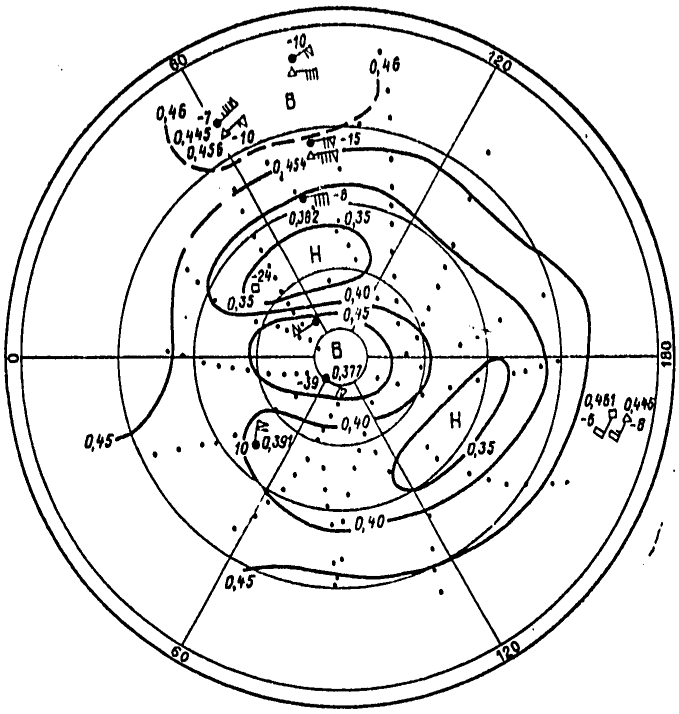

Fig. 1. Pressure map at an altitude of 55 km on 14 March 1978. The dots represent satellite orbits.

The first warming was observed in mid-December-early January; it was local and was noted only in the neighborhood of the stratopause. The temperature in this case increased by 30-40°C. Temperature maps for the levels 35 and 40 km for 3 January 1978, constructed using data from an American satellite, show a displacement of the warm region into the polar region. The temperature at the center of the region became higher than those values which are observed in the subtropical zone. This gives basis for assuming that in addition to advection, other factors also participate in the warming process. During the time of this warming there was no pressure restructuring at the 10-mb level.

The second warming wave began on 25 January. At the end of January, at all levels from 30 to 60 km, a pressure restructuring of the field was observed. The temperature maps, compiled on the basis of satellite data

for 31 January 1978, at 35 and 40 km show a summer temperature distribution in the polar region. At an altitude of 40 km over the pole there is an isotherm for 0°C. In contrast to the preceding warming, this was more extensive, characterized by a pressure restructuring of the field and the lowering of the heat region into the lower stratosphere (to 20 km). According to data for Kheys Island, the greatest amplitude of temperature change, equal to 65°C, was noted in the region of altitudes 28-30 km. Simultaneously with warming in the stratosphere, at mesospheric altitudes there was formation of a region of cold. Over Kheys Island at an altitude of 70 km the temperature decreased by approximately 40°C. The warming was brief, and by 6 February the process for the most part had ended. According to the high-altitude maps, constructed for 8 February 1978, in the layer 35-60 km in the extratropical latitudes of the northern hemisphere a cyclonic circulation had been restored. In the first half of March there is a third warming wave which is accompanied by the advance of the high-pressure region and the heat zone in a poleward direction.

It can be seen from the high-altitude maps for constant levels for 14 March that the anticyclone occupies the polar region at altitudes 35-55 km from the direction of the Pacific Ocean and Canada (Fig. 1).

In the third ten-day period of March the process of final warming ends; the anticyclone was displaced from the pole into the Chukotka region and its altitude decreased to 42 km.

It is of definite interest to examine the change in some energy characteristics during the warming period. As an example we give computations of the following energy characteristics for the second warming wave in the winter of 1976/1977: kinetic energy (KE) per unit volume, meridional advection of kinetic energy (MAKE), generation of kinetic energy of zonal motion (GKEZM), zonal available potential energy (ZAPE), meridional advection of heat and mass [3].

In the computations we used meridional sections of the zonal meridional wind and temperature for two meridians: 65°E and 75°W from the equator to the pole for the layer 20-60 km.

The energy characteristics were computed for 8 December 1976 before the onset of the warming and 22 December 1976 during the warming.

Figure 2 represents meridional sections of kinetic energy for 8 and 22 December. The KE distribution on 8 December is characterized by three clearly expressed maxima associated with the maxima of zonal velocity: in the eastern hemisphere in the middle latitudes at an altitude of 35-38 km (10^1 J/m^3) and in the equatorial region at an altitude 25-27 km (10^1 J/m^3); in the western hemisphere in the high latitudes at an altitude 25-28 km ($2 \cdot 10^1$ J/m^3) (Fig. 2a). The KE reserves in the layer 20-60 km in the eastern and western hemispheres are close and are $0.13 \cdot 10^{20}$ J (these and

similar evaluations were made on the assumption of a zonal distribution of temperature and velocities in the eastern and western hemispheres). Most of the KE is determined by the zonal velocity. Its contribution is $0.12 \cdot 10^{20}$ J in both the eastern and western hemispheres.

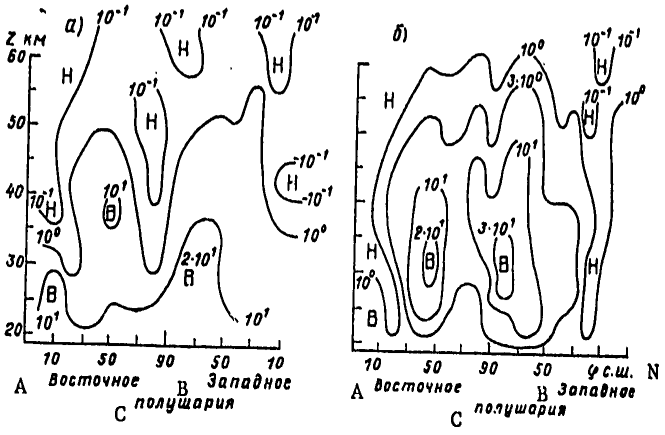

Fig. 2. Meridional section of distribution of kinetic energy. B) regions of maximum values, H) regions of minimum kinetic energy values, J/m^3. a) 8 December 1976; c) 22 December 1976.

KEY:

A. Eastern
B. Western
C. Hemisphere

By 22 December the KE reserves in the eastern hemisphere had increased to $0.26 \cdot 10^{20}$ J and in the western hemisphere -- to $0.22 \cdot 10^{20}$ J. The KE maximum in the eastern hemisphere attained values $2 \cdot 10^1$ J/m^3. The KE maximum attained still greater values in the western hemisphere -- $3 \cdot 10^1$ J/m^3 (Fig. 2b). The greatest KE increase in the eastern hemisphere is observed in the latitude zone 70-90°N from $0.29 \cdot 10^{18}$ J to $0.20 \cdot 10^{19}$ J.

In the western hemisphere in this same latitude zone there is also the maximum KE increase: from $0.19 \cdot 10^{19}$ to $0.52 \cdot 10^{19}$ J.

The development of the Pacific Ocean anticyclone and its northward displacement led to a marked intensification of meridionality in the high latitudes. For example, in the latitude zone 70-90°N in the eastern hemisphere the contribution of zonal velocity to KE was $0.65 \cdot 10^{18}$ J, whereas the contribution of meridional velocity was $0.13 \cdot 10^{19}$ J. In the western hemisphere

the predominance of the contribution of meridional velocity is still greater -- $0.55 \cdot 10^{18}$ and $0.47 \cdot 10^{19}$ J respectively.

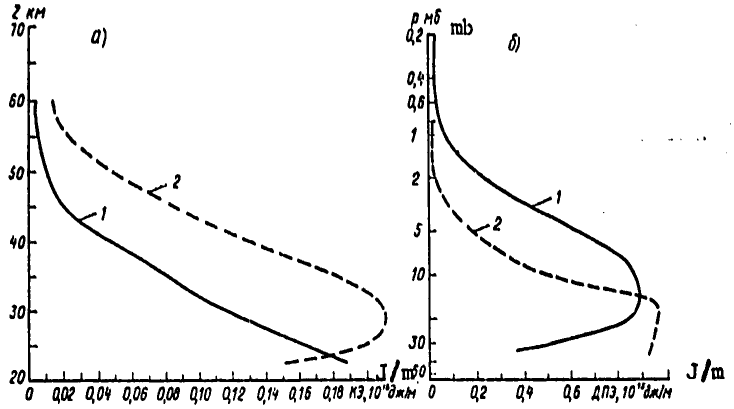

Fig. 3. Vertical profile of kinetic energy (a) and available potential energy of local motion (b). 1) 8 December; 2) 22 December

During the period from 8 through 22 December there was a substantial restructuring and vertical redistribution of KE. Figure 3a shows the vertical profiles of KE for 8 December (curve 1) and 22 December (curve 2), constructed for the northern hemisphere. Whereas for 8 December (before the onset of warming) there was characteristically a monotonic decrease in KE with altitude, the vertical KE profile for 22 December reveals a well-expressed maximum in the region 30 km. In the lower part of the atmospheric region which we considered (approximately to 23 km) there is a decrease in KE during the period from 8 to 22 December; aloft -- up to 60 km -- there is a considerable KE increase. A similar picture is observed in both the western and eastern hemispheres.

The mean rate of KE change from 8 through 22 December (during a period of considerable KE growth) as an average for the hemisphere was $0.20 \cdot 10^{\circ}$ J/(day$\cdot$m^3). The maximum KE increase was observed in the zone 70-90°: $0.44 \cdot 10^{\circ}$ J/(day$\cdot$m^3) in the hemisphere, $0.32 \cdot 10^{\circ}$ J/(day$\cdot$m^3) in the eastern hemisphere and $0.55 \cdot 10^{\circ}$ J/(day$\cdot$m^3) in the western hemisphere. It is interesting to compare these values with the estimates for the generation of kinetic energy of zonal motion (GKEZM). On 8 December the mean absolute GKEZM values were $0.20 \cdot 10^2$ J/(day$\cdot$m^3), on 22 December -- $0.23 \cdot 10^2$ J/(day$\cdot$m^3).

These estimates show that exchange between zonal potential and kinetic energies can introduce a substantial local contribution to the evolution of KE in the atmospheric region which we considered.

The reserves of available potential energy of zonal motion (ZAPE) in the entire layer from 20 to 60 km during the considered period changed insignificantly: from $0.13 \cdot 10^{20}$ J on 8 December to $0.12 \cdot 10^{20}$ J on 22 December. But we note a substantial redistribution of ZAPE with altitude. Figure 3b shows vertical profiles of ZAPE constructed for the northern hemisphere for 8 December (curve 1) and 22 December (curve 2). Approximately above the 16 mb surface there is an appreciable decrease in ZAPE on 22 December in comparison with 8 December; below this surface, on the other hand, there is an increase in ZAPE (at the lower boundary of the region to $0.6 \cdot 10^{15}$ J/m). Thus, the change in KE and ZAPE with altitude is in antiphase.

Table 3

Mean Absolute Values of KE Influxes, Influx of Heat ($J/day \cdot m^3$)) and Influx of Mass ($g/(day \cdot m^3)$) as Result of Meridional Circulation, 1976

	8 December	22 December
KE influx	$0.12 \cdot 10^1$	$0.92 \cdot 10^1$
Heat influx	$0.35 \cdot 10^3$	$0.72 \cdot 10^3$
Mass influx	$0.23 \cdot 10^1$	$0.45 \cdot 10^1$

In conclusion we will discuss the estimates of the influx of KE, heat and mass as a result of meridional circulation. Table 3 gives estimates of these parameters for the northern hemisphere for 8 and 22 December.

The contribution of the meridional circulation to change in KE (in comparison with the mean rate of KE change) is extremely significant and can exert an influence on the KE change. During a period of warming the KE influx as a result of meridional circulation increases by almost an order of magnitude. The influxes of heat and mass as a result of meridional circulation also increased during a period of warming (by a factor of approximately two).

Our computations make it possible to draw the following conclusions:

1. The period before the onset of a warming (8 December) was characterized by a monotonic decrease in KE with altitude; during a warming period there is a well-expressed KE maximum in the region 30 km.

2. During the period of the warming process there is a KE decrease in the lower stratosphere (below 23 km) and an increase in the above-lying layer; in general, in the layer 20-60 km the KE almost doubled.

3. The ZAPE vertical profile (both before the onset of warming and during the warming period) is characterized by the presence of a maximum at approximately the level of the 16-mb surface; above this maximum, during the period of warming there was a decrease, and below — an increase in ZAPE; on the whole the ZAPE reserves in the entire layer 20-60 km changed insignificantly.

The results are evidently characteristic for most warmings occurring with a pressure restructuring.

BIBLIOGRAPHY

1. ATLAS VYSOTNYKH KART SLOYA 35-60 km/TsAO (Atlas of High-Level Charts for the Layer 35-60 km/Central Aerological Observatory), Moscow, Nos 10, 11, 1978.

2. Kats, A. L., TSIRKULYATSIYA V STRATOSFERE I MESOSFERE (Circulation in the Stratosphere and Mesosphere), Leningrad, Gidrometeoizdat, 1968.

3. Lorents, E. N., PRIRODA I TEORIYA OBSHCHEY TSIRKULYATSII ATMOSFERY (Nature and Theory of General Circulation of the Atmosphere), Leningrad, Gidrometeoizdat, 1970.

4. Scherhag, R., "Die explosionsartigen Stratospharen erwarmungen des Spatwinters 1951-1952," BER. DEUTSCH. WETTERDIENST, Bd 6, No 38, 1952.

UDC 543.426:547.6:614.71

INVESTIGATION OF THE BACKGROUND CONTENT OF POLYCYCLIC AROMATIC HYDROCARBONS PRESENT IN AIR

Moscow METEOROLOGIYA I GIDROLOGIYA in Russian No 6, Jun 79 pp 41-45

[Article by Doctor of Chemical Sciences F. Ya. Rovinskiy, T. A. Alekseyeva, Candidate of Physical and Mathematical Sciences T. A. Teplitskaya, Institute of Applied Geophysics, Moscow State University, submitted for publication 23 October 1978]

Abstract: The article describes an investigation of the background content of polycyclic aromatic hydrocarbons (PAH) in atmospheric air by means of extraction at room temperature and narrow-band luminescent spectroscopy (Shpol'skiy effect), including the spectra of fluorescence, phosphorescence and excited luminescence. In the organic matter of aerosols, without use of chromatography, it was possible to determine 11 PAH, a number of pyrene alkyl derivatives, homologues of naphthalene, phenanthrene and chrysene. The quantitative content is given for the seven prevailing compounds. The content of 3,4-benzopyrene varies from 0.001 to 0.04 μg/100 m^3.

[Text] Polycyclic aromatic hydrocarbons (PAH), frequently having toxic and carcinogenic properties, are substances occurring quite widely in the environment.

For the purpose of effective monitoring of the level of concentration of PAH in the environment, especially in atmospheric air, it is necessary to have rapid and reliable methods for the precise identification and quantitative determination of PAH.

In many studies for the determination of carcinogenic polycyclic hydrocarbons in atmospheric air researchers have limited themselves to the search for only the one strong carcinogen 3,4-benzopyrene, regarding it as an indicator of the entire PAH group [10]. But the organic matter of air samples contains tens of aromatic hydrocarbons, some of which have a weak or questionable carcinogenic activity, whereas others are relatively highly active [2]. A significant contribution to the total carcinogenic effect

of PAH is from substituted aromatic structures, since in contrast to the holonuclear structures related to them, in the substituted homologues of PAH there is frequently an intensification of the carcinogenic properties and the biological effect can vary greatly in dependence on insignificant structural variations.

The hydrocarbons accompanying 3,4-benzopyrene most frequently are carcinogens or cocarcinogens, enhancing the overall carcinogenic effect. In some cases some of them can play the role of inhibitors of the carcinogenic effect, and then they lead to a decrease in the degree of the carcinogenic effect. Accordingly, the speedy determination not only of 3,4-benzopyrene, as an indicator of the carcinogenic effect, but also the entire range of PAH, including substituted aromatic structures, is of great importance.

There are a number of physicochemical methods for determining PAH in environmental objects: ultraviolet absorption and molecular mass spectrometry, gas-fluid chromatography, and sometimes use is made of the luminescence spectra obtained under ordinary conditions at room temperature [5]. In the USSR, since the time of discovery of the Shpol'skiy effect in 1952, the development of methods for determining PAH in environmental objects has rested on narrow-band luminescent spectroscopy. Up to the present time this method has been used in various media for determining up to 15 different holonuclear PAH; the particular ones detected has differed greatly among different researchers. The methods of hot extraction of PAH and subsequent chromatographic separation have been generally employed [3, 9].

Modern data on the occurrence of PAH in different natural objects make it possible to postulate that the most usual way in which these molecules arise in nature may be either a thermal effect on organic matter or synthesis, most frequently at high temperatures. The possibilities of chemical transformations in the temperature effect process are also indicated by some principles and experiments in classical chemistry and biochemistry [4, 8]. Therefore, when there is reference to determining the background concentrations of PAH, the methods for preparing the samples for analysis and the techniques for the analysis itself must exclude all types of temperature or any other hard effect, and determination of only some holonuclear structures is inadequate for determining the degree of the overall carcinogenic danger.

In this connection it was important to develop a method for the speedy determination of PAH, including substituted aromatic structures, without using hot extraction and chemical chromatography.

Such a method was developed on the basis of application of the Shpol'skiy effect and has been described in [1, 6, 7]. In order to broaden the range of determined PAH it was necessary to use all types of emission spectra, including not only the fluorescence and phosphorescence spectra, but also the spectra of excitation of luminescence in a wide range of wavelengths

from the ultraviolet to the red. Such an approach made it possible to develop and use a complex of luminescent-spectral methods employing modern types of spectrofluorimeters, which makes it possible not only to determine hydrocarbons having standard analogues, but also to diagnose the type of molecular structure with possible side substitutions of any luminescent molecule, giving structural spectra under the conditions of the Shpol'skiy effect [1]. Identification using standard analogues is carried out on the basis of use of the atlas of quasilinear luminescence spectra [7].

The method was applied to investigation of PAH in the organic matter of air aerosols at the background station Borovoy. The air was passed through an FPA filter for 24 hours at a constant rate; the total volume was 1920 m^3. Extraction was carried out with n-hexane at room temperature.

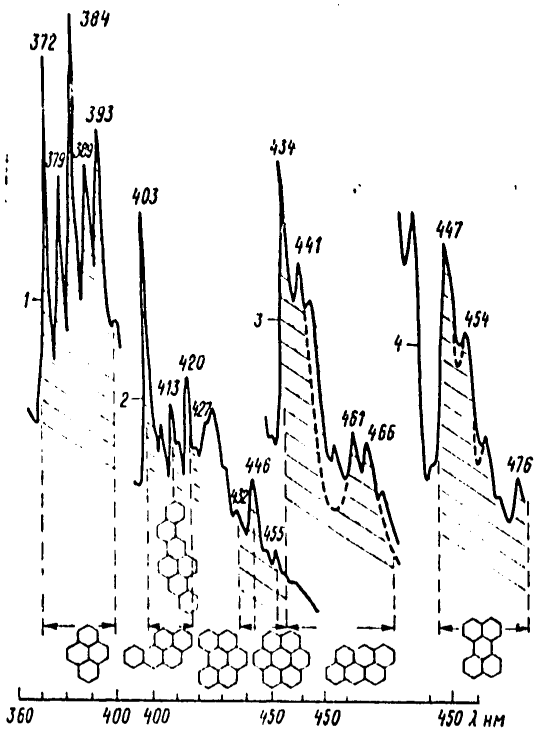

Fig. 1. Identification of pyrene, 3,4-benzopyrene, naphthobenzopyrene "D," 1,12-benzoperylene, coronene, anthanthrene and perylene from fluorescence spectra in an n-hexane extract: λ_{ex} = 337 (1), 300 (2), 410 (3), 421 (4) nm; 77K, fluoricord.

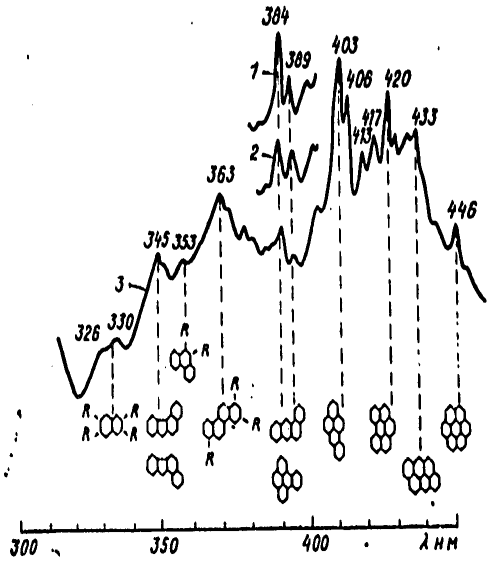

Fig. 2. Identification of a number of aromatic compounds and their substitutes from fluorescence spectra of an n-hexane extract; λ_{ex} = 288 (1), 291 (2), 300 (3) nm; 77 K. Fluoricord.

An example of the photoelectric determination of seven PAH present in prevailing quantities is given in Fig. 1. For determining these PAH we used the method of spectral fractionation of a complex mixture, which led to identification of a large group of aromatic substances.

An invariable component of the range of PAH in aerosols is pyrene, whose characteristic fluorescence spectrum is determined from the strong bands 372, 379, 384, 389, 393 nm with excitation at the strongest maximum of the excitation spectrum 337 nm. By excitation in the band 300 nm it is possible to discriminate spectrally 3,4-benzopyrene (403, 427 nm), naphthobenzopyrene"D" (413 nm) [naphthobenzopyrene "D" is 8,9-benzonaphthopyrene [2", 1":3,4], 1,12 benzoperylene (417, 420, 423 nm) and coronene (432, 446, 455 nm). Excitation at 410 nm is optimum for discriminating anthanthrene (434, 441, 461, 466 nm), whereas excitation at 421 nm is best for discriminating perylene (447, 454, 476 nm) from a similar complex mixture of PAH. These seven aromatic compounds determine fluorescence in the visible region of the spectrum. For discriminating tetraphene (384 nm) and 1,2 benzopyrene (389 nm) we use optimum excitation with λ_{ex} = 288 and 291 nm respectively (Fig. 2). Their identification is also confirmed by the narrow-band fluorescence and phosphorescence spectra. With λ_{ex} = 345-355 nm one observes

the presence of 3-methyl, 3-ethyl and other pyrene substitutes. It was established by an investigation of the excitation spectra of short-wave fluorescence (320-380 nm) that the narrow-band structure in the region 320-340 nm belongs to substitutes of naphthalene; the strong band with the maximum at 345 nm can be identified with the fluorescence of benzofluorenes or their homologues; the bands in the region 353, 363 nm belong to the homologues of phenanthrene and chrysene respectively. The absence of few-ring holonuclear structures (naphthalene, fluorene, phenanthrene), identified in many products of pyrolysis and technogenically affected natural environments, can explain their lesser stability. With entry into an open medium such structures are more subject to photochemical transformations than are hydrocarbons with many rings.

Table 1

Content (μg/100 m^3) of Prevailing PAH in Air Samples at Background Station

Время отбора пробы 1	3,4-бенз-пирен 2	Пирен 3	1,12-бенз-перилен 4	Нафто-бензпи-рен «Д» 5	Коронен 6	Антан-трен 7	Пери-лен 8	Σ
29 VIII 1976	0,0135	0,2700	0,0068	0,0034	—	0,0050	0,0050	0,3037
20 IX	0,0094	0,0570	0,0047	0,0030	0,0020	0,0035	0,0025	0,0821
12 XII	0,0245	0,3300	0,0156	0,0060	0,0036	0,0200	0,0147	0,4144
26 I 1977	0,0318	0,3180	0,0262	0,0063	0,0010	0,0240	0,0159	0,4232
25 II	0,0201	0,3250	0,0192	0,0055	0,0010	0,0270	0,0160	0,4238
21 III	0,0096	0,0700	0,0057	0,0010	—	0,0038	0,0010	0,0911
27 IV	0,0089	0,1100	0,0572	0,0018	0,0010	0,0055	—	0,1844
25 VI	0,0038	0,0950	0,0048	0,0010	0,0026	—	0,0010	0,1082
26 VI	0,0036	0,0700	0,0036	0,0009	0,0010	—	0,0025	0,0816
27 VI	0,0072	0,0600	0,0042	0,0009	—	—	—	0,0723
28 VI	0,0057	0,0570	0,0036	0,0009	—	—	—	0,0672
1 VII	0,0073	0,0580	0,0038	0,0010	—	0,0050	0,0010	0,0761
2 VII	0,0010	0,0100	—	—	—	—	—	0,0110
3 VII	0,0015	0,0100	—	—	—	—	—	0,0115
4 VII	0,0022	0,0420	0,0017	0,0010	0,0010	0,0037	0,0025	0,0541
5 VII	0,0096	0,0480	0,0050	0,0019	0,0010	0,0048	0,0032	0,0735
8 VII	0,0034	0,0810	0,0014	0,0009	0,0010	0,0020	0,0014	0,0911
15 VIII	0,0087	0,0870	0,0062	0,0017	0,0041	—	0,0015	0,1036
25 VIII	0,0075	0,0850	0,0070	0,0015	0,0047	—	—	0,1057
6 IX	0,0354	0,1500	0,0248	0,0060	0,0147	0,0200	0,0147	0,2656
15 IX	0,0058	0,2700	0,0096	0,0025	0,0058	0,0041	0,0038	0,3036
24 IX	0,0401	0,2100	0,0143	0,0020	0,0057	0,0040	0,0050	0,2811
4 X	0,0145	0,2900	0,0099	0,0036	0,0035	0,0036	0,0072	0,3323
12 X	0,0335	0,4400	0,0153	0,0025	0,0073	0,0050	0,0090	0,5126

KEY:

1. Time of sampling
2. 3,4-benzopyrene
3. Pyrene
4. 1,12-benzoperylene
5. Naphthobenzopyrene "D"
6. Coronene
7. Anthanthrene
8. Perylene

The table shows that the content of 3,4-benzopyrene in the air at the background station varies in a very wide range from 0.001 to 0.04 μg/100 m^3. The maximum contents of 3,4-benzopyrene and other hydrocarbons were noted in

the winter months. This was evidently associated with the influence of heating systems, whereas the decrease in the quantitative content and qualitative variety of PAH in the air during the period of the summer months is attributable not only to a decrease in their entry into the atmosphere, but also oxidation under the influence of more intensive UV radiation.

Thus, the described method for determining a large range of PAH and their substitutes affords a possibility for the speedy analysis of such compounds without use of complex methods of extraction and subsequent fractionation and can be recommended for background stations in the monitoring system.

BIBLIOGRAPHY

1. Alekseyeva, T. A., Teplitskaya, T. A., "Formulation of Principles for Determining the Type of Molecular Structure of Unknown Compounds of Complex Mixtures," IZV. AN SSSR, SERIYA FIZ. (News of the USSR Academy of Sciences, Physical Series), Vol 42, No 3, 1978.

2. Dikun, P. P., "Detection of Strong Carcinogens 1,2-4,5 and 3,4-9,10 Dibenzopyrenes in Atmospheric Air," VOPROSY ONKOLOGII (Problems in Oncology), Vol 12, No 1, 1966.

3. Dikun, P. P., "Detection of Polycyclic Aromatic Hydrocarbons in Contaminated Atmospheric Air and Other Objects Using Quasilinear Fluorescence Spectra," ZHURNAL PRIKLADNOY SPEKTROSKOPII (Journal of Applied Spectroscopy), Vol 6, No 2, 1967.

4. Levina, R. Ya., SINTEZ I KONTAKTNYYE PREVRASHCHENIYA NEPREDEL'NYKH UGLEVODORODOV (Synthesis and Contact Transformations of Unsaturated Hydrocarbons), Moscow, Izd-vo MGU, 1949.

5. Sil'versteyn, R., Basler, G., Morril, T., SPEKTROMETRICHESKAYA IDENTIFIKATSIYA ORGANICHESKIKH SOYEDINENIY (Spectrometric Identification of Organic Compounds), Moscow, Mir, 1977.

6. Teplitskaya, T. A., KVAZILINEYCHATYYE SPEKTRY LYUMINESTSENTSII KAK METOD ISSLEDOVANIYA SLOZHNYKH PRIRODNYKH ORGANICHESKIKH SMESEY (Quasilinear Luminescence Spectra as a Method for Investigating Complex Natural Organic Mixtures), Moscow, Izd-vo MGU, 1971.

7. Teplitskaya, T. A., Alekseyeva, T. A., Val'dman, M. M., ATLAS KVAZILINEYCHATYKH SPEKTROV LYUMINESTSENTSII AROMATICHESKIKH MOLEKUL (Atlas of Quasilinear Luminescence Spectra of Aromatic Molecules), Moscow, Izd-vo MGU, 1978.

8. Ugrekhelidze, D. Sh., METABOLIZM EKZOGENNYKH ALKANOV I AROMATICHESKIKH UGLEVODORODOV V RASTENIYAKH (Metabolism of Exogenic Alkanes and Aromatic Hydrocarbons in Plants), Tbilisi, Metsniyereba, 1976.

9. Shabad, L. M., O TSIRKULYATSII KANTSEROGENOV V OKRUZHAYUSHCHEY SREDE (Circulation of Carcinogens in the Environment), 1973.

10. Shabad, L. M., Dikun, P. P., ZAGRYAZNENIYE ATMOSFERNOGO VOZDUKHA KANTSEROGENNYM VESHCHESTVOM 3,4-BENZPIRENOM (Contamination of Atmospheric Air by the Carcinogenic Substance 3,4-Benzopyrene), Moscow, Medgiz, 1959.

UDC 551.(558+577.21)

RELATIONSHIP BETWEEN VERTICAL MOVEMENTS IN THE LOWER TROPOSPHERE AND THE CHARACTERISTICS OF STEADY PRECIPITATION

Moscow METEOROLOGIYA I GIDROLOGIYA in Russian No 6, Jun 79 pp 46-51

[Article by Candidate of Physical and Mathematical Sciences V. S. Antonov, Chernovitskiy State University, submitted for publication 2 October 1978]

Abstract: On the basis of an analysis of numerous data on steady precipitation and the computed values of vertical currents it is shown that ascending vertical movements in the lower troposphere are a necessary but inadequate condition for the falling of precipitation. In order to obtain reliable and adequately precise results of computations of steady precipitation it is necessary to take into account the intracloud physical processes, which can be evaluated indirectly on the basis of some atmospheric macroparameters. The article gives the natural dependence between the complex of thermodynamic atmospheric parameters and the intensity of steady precipitation, in which case the guaranteed probability of the correlation exceeds 88%. The choice of parameters for deriving this dependence was substantiated by the kinetic theory of phase transitions of water in the atmosphere.

[Text] Ordered vertical air movements are an important factor in weather formation. Acting in relatively large spaces commensurable with the regions occupied by synoptic formations, and long retaining their direction, ordered vertical movements change atmospheric stratification, lead air masses to a state of saturation and formation of cloud cover, or, vice versa, lead to the destruction of cloud systems and the drying out of the air.

In presently existing methods for predicting steady precipitation the fact of its falling is determined from the state of saturation of some air layer by water vapor and the quantity of precipitation is determined by the quantity of condensed moisture [5-8, 11, 12]. Since the processes of condensation of water vapor in the free atmosphere are associated with the adiabatic cooling of air masses for the most part as a result of upward movement of unit volumes of air, then, naturally, in computing precipitation the greatest attention is devoted to the intensity of this cooling, caused by the velocity of the ascending movements of air masses. For this reason it appears that if we lay aside other factors participating in the processes of precipitation formation, such as the phase transitions of water in the atmosphere, it will be reasonable to postulate the existence of a dependence between vertical currents (their intensity), the intensity factor, and in the last analysis, the quantity of steady precipitation.

First of all we will examine the frequency of recurrence of the sign of the vertical component of the wind velocity vector at any computation point when steady precipitation is present here.

Table 1 gives data on the frequency of recurrence of the sign of vertical currents, expressed in mb/12 hours at the isobaric surfaces 850, 700 and 500 mb, with the presence of steady precipitation at the ground, which was noted at different points of computation of vertical currents in the course of the day and at the time of computation of these currents.

For computing the frequencies of recurrence represented in this table we used data obtained from the synoptic archives of the USSR Hydrometeorological Center and the Kiev Weather Bureau during the period from 1964 to 1972 for stations located in the European USSR. Using precipitation maps we selected points and days for them during which steady precipitation fell (regardless of the period of falling of precipitation on these days). For the points and days selected in this way we copied the vertical currents at the isobaric surfaces 850, 700 and 500 mb, which were computed at the USSR Hydrometeorological Center by the method developed by S. L. Belousov [11], at the beginning and end of days with precipitation. For the mentioned points we computed the mean daily values of the vertical currents as the half-sum of the values of the vertical currents at the beginning and end of days with precipitation.

Then we selected cases when steady precipitation fell at the points of computation of vertical movements at the times of computation of the latter. As a result of such a choice it was found that the total number of computations of vertical currents for each of the three principal isobaric surfaces for the beginning of a day with steady precipitation was 737 cases; for the end of a day with precipitation -- 734 cases, the number of mean daily values of vertical currents at each of the three main isobaric surfaces -- 630 cases, the total number of computations of vertical movements associated with the moment of falling of steady precipitation at the levels

of the 850- and 700-mb isobaric surfaces -- 471 cases. The frequency of recurrence of the sign of vertical currents during precipitation was computed by the well-known method as the ratio of the number of ascending or descending air movements to the total number of computations of vertical currents at any particular isobaric surface for a definite variant of computation of vertical movements on a day with precipitation.

Table 1

Frequency of Recurrence (%) of Sign of Vertical Component of Wind Velocity Vector at Isobaric Surfaces 850, 700, 500 mb With Presence of Precipitation at Ground Falling During the Day and at the Time of Computation of Vertical Currents

Характеристика повторяемости знака вертикальных токов для момента расчета 1	850		700		500	
	2 Вертикальные токи					
	восходящие 3	нисходящие 4	восходящие 3	нисходящие 4	восходящие 3	нисходящие 4
5 Повторяемость знака вертикальных токов, рассчитанных в начале суток с осадками	48,3	51,7	48,8	51,2	42,0	58,0
6 Повторяемость знака вертикальных токов, рассчитанных в конце суток с осадками	44,8	55,2	44,8	55,2	39,9	60,1
7 Повторяемость знака средних вертикальных токов за сутки с осадками	54,0	46,0	53,8	46,2	50,5	49,5
8 Повторяемость знака вертикальных токов, рассчитанных в момент выпадения осадков	71,0	29,0	77,5	22,5	—	—

KEY:

1. Characteristics of frequency of recurrence of sign of vertical currents for time of computations
2. Vertical currents
3. ascending
4. descending
5. Frequency of recurrence of sign of vertical currents computed at beginning of day with precipitation
6. Frequency of recurrence of sign of vertical currents computed at end of day with precipitation
7. Frequency of recurrence of sign of mean vertical currents for day with precipitation
8. Frequency of recurrence of sign of vertical currents computed at time of falling of precipitation

Now we will examine Table 1. It can be seen that ascending air movements at the main isobaric surfaces at the beginning of a day with precipitation are observed in 42-48.8% of the cases, and descending movements -- in 51.2-

58% of the cases. At the end of a day during which precipitation fell, the frequency of recurrence of ascending currents is still less and is 39.9-44.8%; however, the number of cases of descending currents increases to 55.2-60.1%. The frequency of recurrence of the sign of the mean vertical movements for days with precipitation correlates somewhat better with the ideas concerning the relationship between vertical currents and precipitation. Here the number of cases of ascending movements at the main isobaric surfaces is 50.5-54%, and descending currents -- 46-49.5%. However, on the whole, the vertical currents in the lower troposphere as means for the day and computed at the beginning or end of day, almost to an identical degree with precipitation falling during the day, can be both ascending and descending.

This circumstance suggests that either the method for computing vertical currents used at the USSR Hydrometeorological Center incorrectly reflects the macrophysical process or there is no direct relationship between the fact of falling of precipitation and ordered vertical air movements in the form which we considered. The first doubt immediately disappears if we turn to the last row in Table 1. It follows from this table that the ascending vertical air movements, computed at the time of falling of precipitation, are observed in 71% of the cases at the level of the isobaric surface 850 mb and in 77.5% of the cases at the level of the isobaric surface 700 mb. Since the vertical air movements used here are determined by the structure of the pressure field and its changes with time, and the sign of the vertical currents characterizes the mean 12-hour direction of movement of elementary air volumes along the trajectory, therefore, with ascending movements at the end point of the trajectory, that is, at the computation point, if there is adequate moisture content in the ascending air masses there will be a cloud cover, and with appropriate conditions, precipitation as well. Therefore, if we lay aside cases of considerable transformation coolings of air, it seems natural that in the presence of steady precipitation there will be only ascending vertical currents at the computation point. And in actuality, in the data cited in Table 1 on the frequency of recurrence of the sign of vertical currents during precipitation at the time of computation of vertical movements one discovers a predominance of ascending movements. However, this is only a predominance and not a complete coincidence. It can be postulated that in the existing 22.5-29% of the cases of descending currents during precipitation at the time of computation of vertical movements in part there were errors in determining the latter due to failure to take nonadiabatic factors and other considerations into account, and in part there could also be clouds and precipitation when there are small (close to zero) descending vertical currents when there is adequate transformation cooling of air masses.

Thus, it has been shown that if at one point or another there is steady precipitation, at this point during the preceding 12 hours on the average there were ascending air movements. However, the conclusion drawn by no means implies an inverse correlation, that is, if during the preceding

12 hours ascending currents, on the average, were observed over a particular point, steady precipitation must fall at this point, since precipitation is formed in clouds whose formation in the presence of ascending currents in the atmosphere must be ensured an adequate moisture content from the air mass. Moreover, even in the presence of a cloud cover in some layer of the atmosphere and ascending currents there may be no precipitation if the intracloud physical processes are inadequately active and do not lead to a rapid growth of a definite number of cloud particles [1, 9, 10].

For example, in [2] a study was made of the frequency of recurrence of precipitation reaching the earth's surface in dependence on the relationship between the moisture deficit and vertical movements at the 850-mb surface with different air temperatures at this same level. It was found that with positive temperatures, ascending movements ($W \leqslant -10$ mb/12 hours) and a total saturation of the layer with water vapor ($T - T_d = 0°C$) the probability of falling of precipitation at the earth is 50%; with the above-mentioned conditions, but with an air temperature -1, -9°C precipitation was noted at the surface in 69% of the cases; finally, at temperatures of -10°C or below the probability of precipitation attained only 77%.

An analysis of the material presented in the above-mentioned study indicated that there is no correlation between the precipitation reaching the earth's surface, moisture deficit and vertical velocities at some one isobaric surface, in particular, 850 mb, in the case of positive and small (-1, -9°C) negative air temperatures. With air temperatures at the 850-mb isobaric surface of -10°C or less the dependence which we have discussed is discovered more clearly. In the case of total saturation precipitation is not dependent on the intensity and direction of vertical movements. This is evidently attributable to the fact that at temperatures of -10°C and less a process of intensive crystallization begins in clouds; this process causes a transition of the cloud from a droplet into a mixed state. As is well known, in mixed clouds the precipitation-forming processes are very active. However, these clouds can be situated both above and below the 850-mb level. Therefore, despite the considerable inadequacy of air saturation at this level, but in the presence of any vertical currents precipitation will be observed at the earth's surface. On the other hand, if mixed clouds present at the 850-mb level have an insignificant thickness (less than 400 m), precipitation is not formed in them [1, 2]. In this case, with total saturation at the isobaric surface 850 mb, no precipitation will be observed at the earth's surface, regardless of the intensity of the ascending air movements. Thus, it can be concluded that when using two parameters of state of the atmosphere -- moisture deficit and vertical currents -- without allowance for the kinetics of cloud processes it is impossible to obtain high-probability correlations between precipitation and the mentioned parameters; in particular, it is impossible to hope to discover a correlation only between precipitation at the earth's surface and vertical currents.

Now we will examine the correlation between vertical velocity, on the one hand, and intensity, and also daily quantity of precipitation, on the other.

Table 2

Correlation Coefficients r Between Vertical Currents at Isobaric Surfaces 850, 700 and 500 mb, Daily Quantity RR and Intensity I of Steady Precipitation

Изобарическая поверхность, *мб* 1	*r* между *RR* и *W* в пунктах расчета *W*, определенных в начале суток с осадками 2	*r* между *RR* и *W* в пунктах расчета *W*, определенных в конце суток с осадками 3	*r* между *RR* и среднесуточной величиной *W* 4	*r* между *I* и *W* в пунктах расчета *W*, определенных в момент выпадения осадков 5
850	0,22	0,31	0,31	0,37
700	0,21	0,30	0,30	0,57
500	0,22	0,28	0,32	

KEY:

1. Isobaric surface, mb
2. r between RR and W at points of computation of W, determined at beginning of day with precipitation
3. r between between RR and W at points of computation of W, determined at end of day with precipitation
4. r between RR and mean daily W value
5. r between I and W at points of computation of W, determined at time of falling of precipitation

Table 2 gives information on the correlation coefficients between the daily quantity of precipitation and vertical movements at the isobaric surfaces 850, 700 and 500 mb, computed by the S. A. Belousov method at the USSR Hydrometeorological Center for points where in the course of the day there was registry of steady precipitation, and also between the intensity of precipitation and vertical velocity at the isobaric surfaces 850 and 700 mb, which was computed for the times of determination of the intensity of steady precipitation at different points in the European USSR.

For computing the correlation coefficients indicated in Table 2 we used data which we mentioned at the beginning of this article. A peculiarity in the sampling of data for the construction of Table 2 was that at the points where in the course of the day there was steady precipitation there was additional registry of its daily quantity and vertical currents at the above-mentioned isobaric surfaces. For points where at the time of computation of vertical movements the falling of steady precipitation was noted, we determined its intensity, averaged for two hours, using data from pluviographic observations.

It follows from Table 2 that in all the cases which we considered the correlation coefficients between the daily quantity of precipitation or its intensity and vertical currents indicate an absence of a sufficient closeness of the discussed correlations.

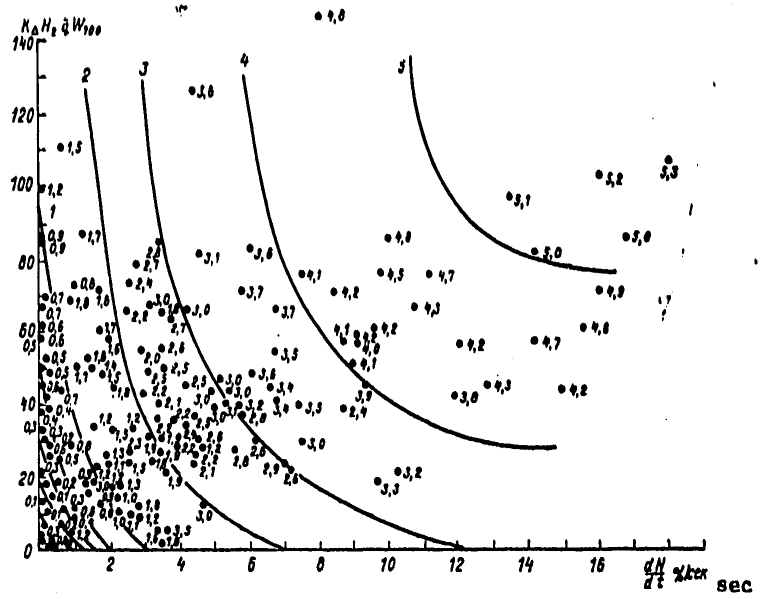

Fig. 1. The figures near the points indicate the intensity of precipitation according to the pluviograph, determined at synchronous times of meteorological and aerological observations.

It must be surmised that the influence of vertical movements on steady precipitation must be manifested complexly, first, through a change in the distribution of other atmospheric parameters, and second, as a result of the effect on intracloud physical processes, for which ordered vertical movements, reflecting the macrophysical atmospheric process, are the background and general condition for the existence of cloud particles. In the investigations [1-4, 9, 10] the authors present the theoretical principles for taking into account intracloud physical processes when determining the fact of falling of precipitation and computing the intensity of steady precipitation from stratiform clouds and establish the physicostatistical correlations between the complex of atmospheric thermodynamic parameters and steady precipitation. Figure 1 shows the dependence between the intensity of steady precipitation falling at the earth's surface I, the averaged total relative number of droplets freezing in a unit time in a unit column of a supercooled stratiform cloud dN/dt and the product of the thickness of the droplet zone of the cloud ΔH_2, the mean liquid-water content of this zone $\bar{q}$, the vertical component of the wind velocity vector at the level AT_{700} W_{700} and the parameter K, characterizing the evaporation of precipitation in the layer below the clouds. In computing the indicated

parameters we did not consider the real cloud layer, but the atmospheric layer where the difference between the temperature and the dew point was two and less degrees ($T - T_d \leqslant 2°C$). The method for computing each of the above-mentioned parameters has been described in detail in [3, 4]. It remains for us only to indicate that the guaranteed probability of computations of the intensity of steady precipitation with the use of the considered graph exceeds 88% and is not dependent on either the geographic region or the season of the year.

BIBLIOGRAPHY

1. Antonov, V. S., "Allowance for Intracloud Physical Processes in the Diagnosis and Prediction of Steady Precipitation," TRUDY LGMI (Transactions of the Leningrad Hydrometeorological Institute), No 14, 1963.

2. Antonov, V. S., "Some Comments on a Nomogram for Computing Steady Precipitation," METEOROLOGIYA I GIDROLOGIYA (Meteorology and Hydrology), No 9, 1963.

3. Antonov, V. S., "Possibility of Creating a Method for Computing the Quantity of Steady Precipitation, Taking into Account the Kinetics of Phase Transitions of Water in the Atmosphere," TRUDY UkrNIGMI (Transactions of the Ukrainian Scientific Research Hydrometeorological Institute), No 126, 1974.

4. Antonov, V. S., Yegorovskaya, G. D., "Physical-Statistical Dependences Between a Complex of Thermodynamic Parameters of the Atmosphere and the Intensity of Steady Precipitation," TRUDY UkrNIGMI, No 134, 1976.

5. Bachurina, A. A., "Present Status of the Method for Predicting Precipitation," METEOROLOGIYA I GIDROLOGIYA, No 12, 1962.

6. Bachurina, A. A., Orlova, Ye. M., "Analysis of the Modern Method for Predicting Precipitation and Further Prospects for its Development," TRUDY VSESOYUZNOGO METEOROLOGICHESKOGO SOVESHCHANIYA (Transactions of the All-Union Meteorological Conference), Vol III, 1963.

7. Kadyshnikov, V. M., "Pseudoadiabatic Model of Steady Precipitation in Short-Range Weather Forecasting," METEOROLOGIYA I GIDROLOGIYA, No 12, 1968.

8. Kadyshnikov, V. M., "Computation of Precipitation Using a Hydrodynamic Model of the Atmosphere," METEOROLOGIYA I GIDROLOGIYA, No 2, 1975.

9. Kachurin, L. G., et al., "Analysis of Zones of Precipitation from Frontal Clouds of Stratiform Types," TRUDY LGMI, Nos 5-6, 1956.

10. Kachurin, L. G., "Formation of Precipitation in Clouds With Small Vertical Currents," IZV. AN SSSR, SERIYA GEOFIZ. (News of the USSR Academy of Sciences, Geophysical Series), No 2, 1956.

11. RUKOVODSTVO PO KRATKOSROCHNYM PROGNOZAM POGODY (Manual on Short-Range Weather Forecasting), Parts I and II, Leningrad, Gidrometeoizdat, 1965.

12. Bushby, F. H., Timpson, M. S., "A 10-Level Atmospheric Model and Frontal Rain," QUART. J. ROY. METEOROL. SOC., No 395, 1967.

UDC 551.(501.776:521.31)(47)(263)

OPTICAL DENSITY OF CUMULUS CLOUDS IN THE TEMPERATE LATITUDES OF THE EUROPEAN USSR AND THE TROPICAL ZONE OF THE ATLANTIC

Moscow METEOROLOGIYA I GIDROLOGIYA in Russian No 6, Jun 79 pp 52-56

[Article by Candidate of Physical and Mathematical Sciences R. G. Timanovskaya, Main Geophysical Observatory, submitted for publication 15 September 1978]

Abstract: This paper presents the results of generalization of data on the attenuation of radiation by cumulus clouds. It is shown that cumulus clouds, whatever may be their coverage in the heavens over either the land or over the ocean, always contain a definite quantity of semitransparent elements. When there are few clouds (cloud cover less than 5/10) the semitransparent elements predominate over optically dense parts of cumulus clouds.

[Text] Statistical actinometry, which has been developed during recent years [7], has opened up great possibilities for investigating the state of the cloud-covered sky by means of simple and readily available techniques, which include actinometric radiation detectors -- actinometers and the Yu. D. Yanishevskiy pyranometers.

As demonstrated in [3-7], using such sensors it is possible to determine from the surface of the earth (ocean) a number of characteristics of the cloud cover, such as its extent in the heavens (tenths), linear dimensions of cloud inhomogeneities, optical thickness - transmissivity relative to the solar radiation incident on the upper boundary of the cloud.

One of the results of the mentioned studies is the conclusion that cumulus clouds to a definite degree are transparent for incident solar radiation. Such a conclusion was somewhat unexpected because before these investigations it was assumed that cumulus clouds as lower-level clouds are not transparent for direct radiation.

The conclusion drawn later in [7, 8] that cumulus clouds are semitransparent was confirmed by experimental results obtained by both the authors of the mentioned studies and by other researchers [4, 9].

Extensive observational data have now been accumulated on direct solar radiation under cumulus cloud cover conditions, and accordingly, information has been accumulated on the attenuation of direct radiation by cumulus clouds, from which it is possible to make qualitative judgments concerning the optical thicknesses of these clouds.

The purpose of this article is to present for discussion the results of generalizations concerning the attenuation of direct radiation by cumulus clouds, and accordingly, on their "optical" thicknesses.

It was demonstrated in [3, 9] that the source of such information is the differential distribution functions for the relative fluxes of direct radiation S^*, that is, $p(S^*)$. These functions are computed using data from continuous records of direct radiation. The duration of the records is 1.5-2 hours; the discreteness of the readings (reading of ordinates from the traces) is about 10-15 sec. The validity of such an approach to the processing of the traces has been discussed in detail in [10].

Here, as in [10], by the "relative flux" S^* is meant the measured direct radiation at the moment in time t - S(t), normalized to the radiation of the cloudless sky $S_0(t)$, computed for this time:

$$S^*(t)=S(t)[S_0(t)]^{-1}. \quad (1)$$

As a result of such normalization there is exclusion of the influence of solar altitude (diurnal variation of the $h_\odot$ value) on the statistical characteristics of direct radiation, including on the function $p(S^*)$.

It was demonstrated in [7] that with a cumulus cloud cover the fluxes $S^*(t)$, regardless of time of day, vary from 0 under conditions of total coverage of the solar disk by the dense parts of cumulus clouds to 1 under conditions of an open solar disk. The presence of values $0<S^*<1$, as is characteristic for the conditions of cumulus clouds, is specifically evidence that cumulus clouds transmit direct solar radiation partially incident on them. It is logical to expect that with a small coverage of cumulus clouds in the heavens there should be a predominance of the fraction of semitransparent cloud elements in the cloud inhomogeneities.

Using the $p(S^*)$ functions it was possible to ascertain the percentage relationship between dense and semitransparent elements of the cloud layer in dependence on the tenths of coverage by cumulus clouds.

In accordance with [5], the tenths of cloud cover is easily determined using the formula

$$n = 1 - p(S^* \geqslant 0{,}9), \qquad (2)$$

where $p(S^* \geqslant 0.9)$ is the total frequency of recurrence of the fluxes $S^* \geqslant 0.9$ during the period T, determined using the function $p(S^*)$. Here it is assumed that the possible variability of S^* values from 0.9 to 1 is attributable to the influence of atmospheric transparency, and accordingly, the value $p(S^* \geqslant 0.9)$ corresponds to the conditions of a cloud-free sky, that is, to the sum of the clearings between clouds during the time T.

It is also logical to assume that $p(S^* \approx 0)$ corresponds to the total frequency of recurrence of optically dense (nontransparent to direct solar radiation) parts of cumulus clouds n'_{dense} during this same period T, that is

$$n'_{dense} = p(S^* \approx 0). \qquad (3)$$

It is evident that the tenths of semitransparent elements n'_{semi} is determined as the difference in the values n and n'_{dense}:

$$n'_{semi} = n - n'_{dense}. \qquad (4)$$

Table 1, on the basis of observational data collected in the Moscow area, gives the mean values n'_{semi} and n'_{dense} for each tenth of coverage by cumulus clouds.

Table 1

Relationship Between Dense and Semitransparent Elements of Cumulus Clouds in Dependence on Their Coverage n in the Heavens According to Observations in the Moscow Region

	1 Балл облаков n							
	2	3	4	5	6	7	8	9
2 $n'_{пл}$	0	0,05	0,16	0,22	0,31	0,40	0,58	0,84
3 $n'_{полу}$	0,20	0,25	0,24	0,28	0,29	0,30	0,22	0,06

KEY:

1. Tenths of cloud cover, n
2. dense
3. semitransparent

These data were obtained as a result of generalization of the traces of direct solar radiation with a total duration of 380 hours, which corresponds to the cloud space penetrated during this time at the altitude of cumulus clouds ($H \simeq 1$ km), about 15,000 km. The registry of fluxes was predominantly when there were Cu hum and Cu med clouds.

The cited data show that with any n cumulus clouds contain semitransparent elements, as is indirectly confirmed by the photograph in Fig. 1.

Fig. 1. Photograph of a cumulus cloud taken from the earth's surface and illustrating the process of screening of the solar disk by the edge of a cloud. The solar disk is clearly seen. At this moment the S^* value was equal to 0.2.

Table 2

Percentage Relationship Between Dense and Semitransparent Elements of Cu Clouds With Their Different Coverages in the Heavens

	1 Балл облаков n							
	2	3	4	5	6	7	8	9
2 $n'_{пл}$	0	20	33	43	53	60	72	89
3 $n'_{по}$	100	80	67	57	47	40	28	11

KEY:

1. Tenths of cloud cover n
2. dense
3. semitransparent

When there are few clouds ($n \leqslant 2$) they are usually completely semitransparent for direct radiation; with $2 < n \leqslant 5$ cumulus clouds in large part are also semitransparent since in all cases $n'_{dense} < n'_{semi}$; in the case of a considerable cloud cover -- with $n > 5$ -- the total frequency of recurrence of dense cloud elements considerably exceeds the corresponding values for semitransparent elements.

Table 1 also shows that with $3 \leqslant n \leqslant 8$ the total frequency of recurrence of semitransparent elements is identical in absolute value. An analysis of the relative values $n_{semi} = n'_{semi}\, n^{-1}$ and $n_{dense} = n'_{dense} n^{-1}$ shows that

with an increase in n the relative importance of the dense parts of the cumulus clouds increases, whereas the relative importance of the semitransparent parts decreases (see Table 2).

Table 2 also shows that in the case of a small quantity of cumulus clouds in the heavens (with $n < 3$) the cloud inhomogeneities themselves are semitransparent. In the remaining cases, evidently, the semitransparent elements occur both in the peripheral parts of the cloud inhomogeneities and in cloud inhomogeneities of small horizontal extent, which usually are always present in the heavens regardless of the extent of cloud coverage.

The general relationship of the n_{dense} and n_{semi} values with large n of cumulus clouds, when $2 \leqslant n \leqslant 9$, can be described by the following equations:

$$n_{dense} = 1.2\ n - 0.2, \quad (5)$$
$$n_{semi} = 10 - 0.8\ n, \quad (6)$$

where n is in tenths.

Table 3

Relationship Between Dense and Semitransparent Sectors of Cumulus Clouds in Dependence on Their Coverage in the Heavens in the Moscow Area and in the Tropical Zone of the Atlantic

Количество облаков *n*, *баллы* 1	2 Суша (Подмосковье)			3 Океан (НИСП «Эрнст Кренкель»)		
	суммарная длительность регистрограмм, *мин* 4	% плотных частей облаков 5	% полупрозрачных частей облаков 6	суммарная длительность регистрограмм, *мин* 4	% плотных частей облаков 5	% полупрозрачных частей облаков 6
2	30	0	100	2	10	90
3	30	20	80	16	31	69
4	60	33	67	—	—	—
5	70	43	57	10	25	75
6	68	53	47	8	44	56
7	50	60	40	12	52	48
8	40	72	28	—	—	—
9	32	89	11	—	—	—

KEY:

1. Cloud coverage, n, tenths
2. Land (Moscow area)
3. Ocean (scientific research weather ship "Ernst Krenkel'")
4. Total duration of traces, min
5. % of dense parts of clouds
6. % of semitransparent parts of clouds

As was noted above, all the cited data are characteristic for the Moscow area. It is of definite interest to compare these data with other regions of the USSR or the earth.

During the TROPEKS-74 expedition aboard the "Ernst Krenkel'" ship there was continuous registry of direct solar radiation by an actinometer with direct pointing on the sun [2].

The processing of the resulting traces by the method described above also made it possible to obtain information on cumulus clouds for the tropical region of the Atlantic with the coordinates $\varphi = 65°N$, $\lambda = 20°W$ (ICZ region), the site where the ship was anchored on this expedition (see Table 3).

It can be seen clearly that in this region of the Atlantic the cumulus clouds are also semitransparent for direct solar radiation. Due to the small volume of data it was not possible to trace a clear dependence of n_{dense} and n_{semi} on n; it was only possible to trace a general tendency for an increase in n_{dense}, and accordingly, a decrease in n_{semi} with an increase in n.

Nevertheless, it can be seen clearly from the cited data that cumulus clouds in the ICZ, with respect to their optical thicknesses (transmissivity of solar radiation), virtually do not differ from the cumulus clouds in the temperate latitudes of the European USSR when there is a corresponding coverage in the heavens, whereas with respect to their linear dimensions (horizontal and vertical) these clouds differ substantially in the mentioned regions of the earth [1, 11].

This conclusion somewhat contradicts the results published in a number of papers in the collection of articles [11]. This contradiction is evidently attributable to the fact that the method for investigating the transmissivity of solar radiation by cumulus clouds used by the author of this article did not provide for an investigation of individual clouds, as was done on the TROPEKS-74 expedition aboard an aircraft, but the entire spectrum of cloud inhomogeneities which during a time interval from 1.5 to 5 hours entered the field of view of the radiation detector (actinometer) carried aboard the ship.

The following conclusions can be drawn on the basis of what has been said above.

1. Cumulus clouds Cu hum and Cu med, whatever may be their coverage in the heavens over the land or over the ocean, always contain a definite number of semitransparent elements. When there are few cumulus clouds ($n < 3$), the clouds themselves are semitransparent to radiation fluxes; in the remaining cases the semitransparent elements occur both in the peripheral parts of the cloud inhomogeneities and in clouds with small dimensions.

2. Both over the land and over the ocean in the ICZ region, when cumulus clouds have a coverage up to 5/10, semitransparent elements predominate (in sum) over the optically dense parts of the cloud inhomogeneities.

3. With respect to the transmissivity of solar radiation the ICZ cumulus clouds Cu hum and Cu med do not differ from those in the temperate latitudes of the European USSR.

BIBLIOGRAPHY

1. Gudimenko, A. V., Rudneva, L. B., Timanovskaya, R. G., Timanovskiy, D. F., "Linear Dimensions of Cumulus Clouds According to Data from Surface Measurements of Radiation Fluxes," TRUDY GGO (Transactions of the Main Geophysical Observatory), No 388, 1977.

2. Dyubkin, I. A., Timanovskaya, R. G., Timanovskiy, D. F., Morachevskiy, A. V., "Transparency Coefficient for the Cloudy Atmosphere," TRUDY GGO, No 388, 1977.

3. Kasatkina, O. I., et al., "On the Problem of Objective Analysis of Cloud Cover Characteristics," METEOROLOGIYA I GIDROLOGIYA (Meteorology and Hydrology), No 8, 1972.

4. Mullamaa, O. A. R., et al., STOKHASTICHESKAYA STRUKTURA POLEY OBLACHNOSTI I RADIATSII (Stochastic Structure of the Cloud Cover and Radiation Fields), Tartu, 1972.

5. Rudneva, L. V., Timanovskaya, R. K., "On the Problem of Automation of Cloud Cover Observations," TRUDY GGO, No 388, 1977.

6. Timanovskaya, R. G., "Statistical Structure of Fluxes of Direct and Total Solar Radiation at the Earth's Surface in the Presence of Cumulus Clouds," TRUDY GGO, No 297, 1973.

7. Timanovskaya, R. G., Feygel'son, Ye. M., "Solar Radiation Fluxes at the Earth's Surface in the Presence of Cumulus Clouds," METEOROLOGIYA I GIDROLOGIYA, No 11, 1970.

8. Timanovskaya, R. G., Timanovskiy, D. F., "Determination of Cloud Coverage from the Continuous Registry of Direct Radiation," TRUDY GGO, No 345, 1975.

9. Timanovskaya, R. G., Feygel'son, Ye. M., "Some Parameters of Cumulus Clouds Obtained from Photographs of the Cloud-Covered Sky and from Surface Actinometric Measurements," TEPLOOBMEN V ATMOSFERE (Heat Exchange in the Atmosphere), Moscow, Nauka, 1972.

10. Timanovskaya, R. G., Feygel'son, Ye. M., "On a Method for Studying the Statistical Structure of Surface Fluxes of Solar Radiation Under Cloudy Conditions," TEPLOOBMEN V ATMOSFERE, Moscow, Nauka, 1972.

11. TROPEKS-74: TRUDY MEZHVEDOMSTVENNOY EKSPEDITSII PO PROGRAMME MEZHDUNARODNOGO ATLANTICHESKOGO EKSPERIMENTA (Tropeks-74: Transactions of the Interdepartmental Expedition Under the Program of the International Atlantic Experiment), Vol 1, Leningrad, Gidrometeoizdat, 1976.

UDC 551.461.6

NUMERICAL METHOD FOR SOLVING THE PROBLEM OF FREE OSCILLATIONS OF THE WORLD OCEAN IN A BAROTROPIC APPROXIMATION

Moscow METEOROLOGIYA I GIDROLOGIYA in Russian No 6, Jun 79 pp 57-66

[Article by A. V. Protasov, Computation Center Siberian Department USSR Academy of Sciences, submitted for publication 4 August 1978]

Abstract: The article examines a numerical method for computing free oscillations of the world ocean in a barotropic approximation. It is based on a combination of the method of simultaneous iterations of a group of vectors and the method of inverse iterations. In carrying out the inverse iterations use is made of a direct algorithm for solution of the derived system of complex algebraic equations.

[Text] Introduction. The investigation of the mechanism of appearance of tidal waves in the world ocean [3] is closely related to the problem of free oscillations. Until recently these investigations were carried out for the most part using rather simplified analytical models for basins which are far in their configuration from real basins in the world ocean. The results obtained in this work have really been of a qualitative character.

In the numerical solution of the problem of free oscillations of the world ocean, even with use of very simple models, a number of significant difficulties arise. These are related to the poor conditionality of the problem in eigenvalues and the lack of effective numerical methods for its solution. The poor conditionality of the problem of free oscillations is attributable to the fact that the operator spectrum falls in a quite broad range and its eigenvalues are very close in absolute value. It is necessary to find several eigenvalues and the corresponding eigenfunctions falling within the spectral interval. Therefore, the use of known iteration methods, using direct iterations of the operator, for solution of a partial spectral problem, is in large part ineffective due to the inadequate convergence rate.

One of the first results of numerical computation of free oscillations for individual basins of the world ocean was the numerical results obtained by Platzman [10]. He examined the linear barotropic model without allowance for frictional forces, whereas the eigenvalues and eigenfunctions were found using the Lantsosh method [6].

In this paper we will examine a solution of the spectral problem for a difference analogue of the tidal operator on the basis of one of the modifications of the simultaneous iterations method [9]. This method makes it possible to carry out iterations of the corresponding subspaces, which has a number of advantages when there are close eigenvalues. The special structure of the operator of the considered model makes it possible to write a direct inversion algorithm for its difference analogue, which will ensure a rapid rate of convergence of the proposed method and will make it possible to solve effectively the problem of tidal waves in the world ocean without frictional forces being taken into account.

Now we will examine a linearized model of the dynamics of tides in a barotropic world ocean in a spherical coordinate system (ϑ, ψ) [3]

$$\begin{aligned} &\frac{\partial u}{\partial t} + lv + \frac{g}{a\sin\vartheta}\frac{\partial \zeta}{\partial \psi} = f_1, \\ &\frac{\partial v}{\partial t} - lu + \frac{g}{a}\frac{\partial \zeta}{\partial \vartheta} = f_2, \\ &\frac{\partial \zeta}{\partial t} + \frac{1}{a\sin\vartheta}\left[\frac{\partial Du}{\partial \psi} + \frac{\partial \sin\vartheta\, Dv}{\partial \vartheta}\right] = 0. \end{aligned} \tag{1}$$

where u and v are components of the velocity vector $\vec{u}$, ζ is the level excess, f_1 and f_2 are the projections of the moment of the tide-generating force, l is the Coriolis parameter, g is the acceleration of free falling, $D = D(\vartheta, \psi)$ is depth, a is the earth's radius.

Problem (1) will be solved in the region G bounded by the contour Γ, representing the stylized boundary of the world ocean and formed from segments of coordinate lines. For closing the system of equations (1) we will assume that at the boundary Γ the velocity vector component normal to the boundary Γ becomes equal to zero, that is

$$u_n = 0 \text{ at } \Gamma, \tag{2}$$

Introducing into consideration the operator

$$A = \left\| \begin{array}{cc|c} 0 & l & \frac{g}{a\sin\vartheta}\frac{\partial}{\partial\psi} \\ -l & 0 & \frac{g}{a}\frac{\partial}{\partial\vartheta} \\ \hline \frac{1}{a\sin\vartheta}\frac{\partial (D\cdot)}{\partial\psi} & \frac{1}{a\sin\vartheta}\frac{\partial(\sin\vartheta D\cdot)}{\partial\vartheta} & 0 \end{array} \right\| \tag{3}$$

and the vector-functions

$$\vec{\varphi}=\begin{pmatrix} u \\ v \\ \zeta \end{pmatrix}, \quad \vec{f}=\begin{pmatrix} f_1 \\ f_2 \\ 0 \end{pmatrix},$$

the system of equations (1) is written in operator form

$$\frac{\partial \vec{\varphi}}{\partial t}+A\vec{\varphi}=\vec{f}. \tag{4}$$

Now we will examine the Hilbert space of the vector-functions Φ with the scalar product

$$(\vec{a}, \vec{b})_{\Phi}=\sum_{i=1}^{3}\int_{G} d_i a_i b_i dG, \tag{5}$$

where a_i, b_i ($i = 1, 2, 3$) are the components of the vector-functions $\vec{a}$, $\vec{b}$ $\in \Phi$ in the region G, d_i ($i = 1, 2, 3$) are weighting coefficients, selected in such a way that by using the functional (5) it was possible to determine the energy of system (1), that is, $d_1 = d_2 = D$ and $d_3 = g$, and an element of volume $dG = a^2 \sin \vartheta \, d\vartheta \, d\psi$.

The set of quite smooth vector-functions $\vec{\varphi} \in \Phi$, satisfying condition (2), forms the region of determination $\overline{\Phi}(A)$ of the operator A. It is easy to see that the operator A, determined by expression (3), is antisymmetric in the sense of the scalar product (5), that is

$$(A\vec{\varphi}, \vec{\varphi}^*)_{\Phi}=-(\vec{\varphi}, A\vec{\varphi}^*)_{\Phi}, \tag{6}$$

where $\vec{\varphi}^* = (u^*, v^*, \zeta^*)$ is an arbitrary function with quite smooth components.

It follows from equation (6) that the spectrum of the operator A is situated on a fictitious axis.

Proceeding from the method for formulating finite-difference approximations on the basis of determination of a generalized solution [2, 5] for the problem (1)-(2) and using displaced grids in the process, we obtain the following system of finite-difference equations, written in vector-matrix form

$$\frac{d\vec{\varphi}^h}{dt}+A^h\vec{\varphi}^h=\vec{f}^h, \tag{7}$$

where the matrix operator A^h has the form

$$A^h = \begin{pmatrix} L & H \\ W & 0 \end{pmatrix}, \tag{8}$$

and the matrix operators L, H and W approximate the corresponding differential operators in the representation (3) with a second order of accuracy on a four-point template. It follows from the method for forming the finite-difference approximation that the difference operator A^h will also be antisymmetric in the sense of the scalar product, being an analogue of (5)

$$(\vec{\varphi}^h, \vec{\psi}^{h*})_{\Phi^h} = (\tilde{D}_h \vec{\varphi}^h, \vec{\psi}^{h*}),$$

where (,) is the Euclidean scalar product in the space $\vec{\Phi}^h$ of the grid functions $\vec{\varphi}^h$, $\vec{\varphi}^{h*}$, $\tilde{D}_h$ is the corresponding diagonal matrix of weights.

For the matrix operator A^h we will formulate the scalar problem

$$A^h \vec{\psi} = \lambda \vec{\psi}. \tag{9}$$

We will examine this problem in unitary space $\tilde{\vec{\Phi}}^h$, representing a complex expansion of the space of real vectors $\vec{\Phi}^h$ [1]. In this case any vector $\vec{\psi} \in \vec{\Phi}^h$ is unambiguously represented in the form

$$\vec{\psi} = \vec{\psi}_1 + i\vec{\psi}_2, \quad \vec{\psi}_1, \vec{\psi}_2 \in \Phi^h, \tag{10}$$

and the scalar product in the space $\tilde{\vec{\Phi}}^h$ is determined in the following way:

$$(\vec{z}_1, \vec{z}_2)_{\tilde{\Phi}^h} = (\vec{x}_1, \vec{x}_2)_{\Phi^h} + (\vec{y}_1, \vec{y}_2)_{\Phi^h} + i\,[(\vec{y}_1, \vec{x}_2)_{\Phi^h} - (\vec{x}_1, \vec{y}_2)_{\Phi^h}],$$

$$\vec{z}_1 = \vec{x}_1 + i\vec{y}_1, \quad \vec{z}_2 = \vec{x}_2 + i\vec{y}_2, \quad \vec{x}_1, \vec{y}_1, \vec{x}_2, \vec{y}_2 \in \Phi^h.$$

The eigenvalues of the matrix A^H are purely fictitious and the eigenvectors of the problem (9) with corresponding normalization satisfy the orthogonality condition

$$(\vec{\psi}_p, \vec{\psi}_q)_{\tilde{\Phi}^h} = \delta_{pq},$$

where δ_{pq} is the Kronecker symbol, p and q are the numbers of the eigenvectors. This follows from the property of antisymmetry for the matrix A^h [9].

Assume that we must determine several eigenvectors and the corresponding eigenvalues of the problem (9), close in absolute value to some prestipulated number γ_1, that is, find several eigenvalues less in absolute value and the corresponding eigenvectors of the problem

$$(A^h - i\gamma_1 E)\vec{\psi} = i\mu\vec{\psi} \tag{11}$$

in the space $\tilde{\vec{\Phi}}^h$, where E is the identity operator. Taking into account the representation (10) of the vectors from the space $\tilde{\vec{\Phi}}^h$, the problem (11) is written in the form

$$\begin{pmatrix} A^h & \eta_1 E \\ -\eta_1 E & A^h \end{pmatrix}\begin{pmatrix} \vec{\psi}_1 \\ \vec{\psi}_2 \end{pmatrix} = \begin{pmatrix} 0 & -\mu E \\ \mu E & 0 \end{pmatrix}\begin{pmatrix} \vec{\psi}_1 \\ \vec{\psi}_2 \end{pmatrix}. \tag{12}$$

Multiplying equation (12) by the operator

$$B = \begin{pmatrix} A^h & \eta_1 E \\ -\eta_1 E & A^h \end{pmatrix}, \tag{13}$$

we arrive at the problem

$$A_B \vec{z} = \nu \vec{z}, \tag{14}$$

where

$$A_B = -B \cdot B, \ \vec{z} = \begin{pmatrix} \vec{\psi}_1 \\ \vec{\psi}_2 \end{pmatrix}, \ \nu = \mu^2. \tag{15}$$

Thus, if the dimensionality of the unitary space Φ^h is equal to n, instead of the problem (9) in this space we have the equivalent spectral problem (14) in the real space R of the dimensionality 2 with the real symmetric matrix A_B in the scalar product

$$(\vec{z}, \vec{w})_R = (D_R, \vec{z}, \vec{w}), \ \vec{z}, \vec{w} \in R, \ D_R = \begin{pmatrix} \tilde{D}_h & 0 \\ 0 & \tilde{D}_h \end{pmatrix}. \tag{16}$$

By solving the partial spectral problem (14), we thereby find the orthogonal base of the invariant subspace of the B matrix. Since the B matrix has the structure (13), and the eigenvectors of the A^h matrix have the form (15), it is easy to see that the vector components $\vec{\psi}_1^k$ and $\vec{\psi}_2^k$ z^k of the A_B matrix corresponding to different eigenvalues will also be the orthogonal base of the invariant subspaces of the dimensionality two of the A^h matrix in the space Φ^h, and the eigenvectors of the A matrix will have the form (10).

A modification of the iteration process, known as the simultaneous iterations method [9], has been developed for solving the partial spectral problem (14). The essence of the proposed method is as follows.

Assume that in the space R we have some linear subspace R_m, generated by the base, orthogonal in the sense of the scalar product (16), such that the projections of the first m eigenvectors A_B onto this subspace are different from zero. For convenience in further reasonings we will examine the base vectors as vector-columns of the matrix Φ_0^j of the dimensionality 2n x m, where j is the number of the iteration interval. An iteration with the number j consists of five main stages.

1. From the base Φ_0^j we form the matrix Φ_1^j of the dimensionality 2n x 2m

$$\Phi_1^j = [\Phi_0^j, \ F(A_B)], \tag{17}$$

where $F(\Lambda_B)$ is some function of the matrix A_B, leaving invariant the characteristic linear subspaces of the matrix A_B.

2. We separate the linearly independent vector-columns by orthogonalization of the column of the Φ_1^j matrix. As a result we arrive at a matrix Φ_2^j of the dimensionality $2n \times n_j$ $(m \leqslant n_j \leqslant 2m)$, whose columns are orthogonal (the first m columns coincide with the corresponding columns of the matrix Φ_0^j) and generate the subspace $R_{n_j} \subset R$.

3. In the subspace R_{n_j} we will examine the functional

$$J_j = \frac{\vec{c}^T \Phi_2^{jT} D_R A_B \Phi_2^j \vec{c}}{\vec{c}^T \vec{c}}, \tag{18}$$

where $\vec{c} = (c_1, c_2, \ldots, c_{n_j})^T$ is a vector-column of the coefficients of expansion of an arbitrary $\vec{x} \in R_{n_j}$ along the base Φ_2^j, and the superscript T denotes transposing. We will find the stationary points of the functional (18) in the set of coefficients c_i, solving the total spectral problem for the symmetric matrix $B^j = \Phi_2^{jT} D_R A_B \Phi_2^j$ [4], that is

$$B^j C^j = C^j \Lambda^j. \tag{19}$$

Here C^j is a matrix formed from the orthonormalized eigenvectors of the matrix B^j, and Λ^j is a diagonal matrix of the corresponding eigenvalues.

4. We shift from the base Φ_2^j to the base Φ_3^j using the transformation matrix C^j using the formula

$$\Phi_3^j = \Phi_2^j C^j.$$

5. Selecting m vectors from the base Φ_3^j, corresponding to the minimum eigenvalues of the matrix B^j, we arrive at the new base Φ_0^{j+1}.

The described process of repetition to convergence, that is, until the subspace generated by the base Φ_0^j is invariant relative to the matrix A_B and its dimensionality is equal to m.

Since in each iteration $j (j > 1)$ we retain in the base the vectors obtained in the preceding iteration, it follows from forming of the matrix B^j in the spectral problem (19) that it has the form

$$B^j = \begin{pmatrix} \tilde{\Lambda}^{j-1} & Q \\ Q^T & \tilde{F} \end{pmatrix},$$

where Q and $\tilde{F}$ are some real matrices and $\tilde{\Lambda}^{j-1} = \operatorname{diag}\{\nu_1^j - 1, \quad \nu_2^{j-1}, \ldots, \nu_m^{j-1}\}$ is a diagonal matrix formed from the first m eigenvalues, obtained in the iteration with the number $j - 1$ and arranged in an increasing order.

We have the following inequalities

$$\nu_1^j \leq \nu_1^{j-1},\ \nu_2^j \leq \nu_2^{j-1},\ \ldots,\ \nu_m^j \leq \nu_m^{j-1}, \tag{20}$$

that is, iterations of eigenvalues with identical numbers form nonincreasing sequences, and the limiting elements of these sequences will be the eigenvalues of the initial problem (14). The proof of this assertion is based on the division theorem for symmetric matrices [6] and the minimax principle [8].

It still remains to examine the problem of choice of the function $F(A_B)$ from (17) in the iteration process. Taking into account that we must determine the lower eigenvalues of the A_B matrix, the $F(A_B)$ function must be selected in such a way that first of all it will suppress the components corresponding to the higher eigenvalues of the A_B matrix. Therefore, a simple method for forming the $F(A_B)\,\Phi_0^j$ vectors in (17) is the application of one or more intervals of known iteration methods employed for determining the minimum eigenvalue of the A_B matrix [6]. In this respect the most preferable method is the inverse iterations method [6]. In the problem which we considered the special form of the operator A, and in the last analysis, the A^h matrix, makes it possible to invert the matrix operator B, determined by the equation (13). In actuality, the organization of one interval of the inverse iterations from the A_B matrix requires solutions of a system of equations of the type

$$\begin{pmatrix} A^h & \eta E \\ -\eta E & A^h \end{pmatrix}\begin{pmatrix} \vec{x} \\ \vec{y} \end{pmatrix} = \begin{pmatrix} \vec{F}_1 \\ \vec{F}_2 \end{pmatrix}$$

or, which is the very same, the system of equations

$$\begin{pmatrix} L - i\eta E_1 & H \\ W & -i\eta E_2 \end{pmatrix}(\vec{x} + i\vec{y}) = \vec{F}_1 + i\vec{F}_2, \tag{21}$$

where E_1 or E_2 are unit matrices of the corresponding dimensionality, and $\vec{F}_1$ and $\vec{F}_2$ are real vectors from the space Φ^h, determined by the base vectors from Φ_0^j, and the matrices L, H and W were determined in (8).

We introduce the new notations:

$$\vec{x} + i\vec{y} = \begin{pmatrix} \vec{x}_u \\ \vec{x}_\zeta \end{pmatrix},\quad \vec{F}_1 + i\vec{F}_2 = \begin{pmatrix} \vec{F}_u \\ \vec{F}_\zeta \end{pmatrix}$$

and making similar transformations, the system of equations (21) is written in the form

$$\begin{aligned} (L - i\eta E_1)\,\vec{x}_u + H\vec{x}_\zeta &= \vec{F}_u, \\ -(i\eta E_2 + W(L - i\eta E_1)^{-1} H)\,\vec{x}_\zeta &= \vec{F}_\zeta - W(L - i\eta E_1)^{-1}\vec{F}_u. \end{aligned} \tag{22}$$

With known $\vec{x}_\zeta$ the solution $\vec{x}_u$ of the first of the equations (22) is determined directly, since the operator $L - i\eta E_1$ is block-diagonal, with ordinary second-order square blocks. In the solution of the second equation from (22) we are dealing with a block - three-diagonal complex matrix

$$\tilde{A} = -(i\eta E_2 + W(L - i\eta E_1)^{-1} H), \tag{23}$$

that is

$$\tilde{A}\vec{x}_\zeta = \vec{q}, \tag{24}$$

where

$$\vec{q} = \vec{F}_\zeta - W(L - i\eta E_1)^{-1}\vec{F}_u,$$

$$\tilde{A} = \left\| \begin{array}{ccccccc} A_1 & B_1 & & & & & 0 \\ C_2 & A_2 & B_2 & & & & \\ & C_3 & A_3 & B_3 & & & \\ & & \cdot & \cdot & & & \\ & & & \cdot & \cdot & & \\ & & & & \cdot & \cdot & \\ 0 & & & & C_{N-1} & A_{N-1} & B_{N-1} \\ & & & & & C_N & A_N \end{array} \right\|. \tag{25}$$

Here A_i are square and B_i and C_i are rectangular complex matrices, the specific form of which is determined by the rule of ordering of points in the grid region and a finite-difference approximation of the problem (1)-(2). The number of square blocks in the $\tilde{A}$ matrix is equal to the number of sections $\theta = \theta_i$ (or $\psi = \psi^j$) of the grid region and the dimensionality N_i of each square block A_i is equal to the number of points in the grid region in the corresponding section.

For solving the system of equations (24) we prepare a direct algorithm for the inversion of the matrix (25) using its expansion into the product of the unitary matrix and the upper triangular matrix. Use is made of a block variant of the Hausholder method with a partial sampling of the "leading" column [7].

We use the method of realizing one interval of the inverse iterations directly for solution of the system of equations (7) with stipulated values of the tide-generating force, and in particular, this makes possible the quite effective determination of periodic solutions of the problem (7) with a periodic (in time) right part $\vec{f}^h$ with an arbitrary period τ of oscillations, that is, numerically solve the problem of tidal waves in the world ocean [3]. In actuality, assume that the right-hand side of the system of equations (7) is stipulated in the form

$$\vec{f}^h = e^{-i\omega t}\vec{f}_0^h, \tag{26}$$

where $\vec{f}_0^h$ is a grid vector-function not dependent on the variable t, and $\omega = 2\pi/\tau$. We will seek solution of the problem (8) in the form

$$\vec{\varphi}^h = e^{-i\omega t}\vec{\varphi}_0^h. \tag{27}$$

Substituting expressions (26) and (27) into (7), we obtain the equation

$$-i\omega\vec{\varphi}_0^h + A^h\vec{\varphi}_0^h = \vec{f}_0^h, \tag{28}$$

whose form, with an accuracy to the notations, coincides with (21).

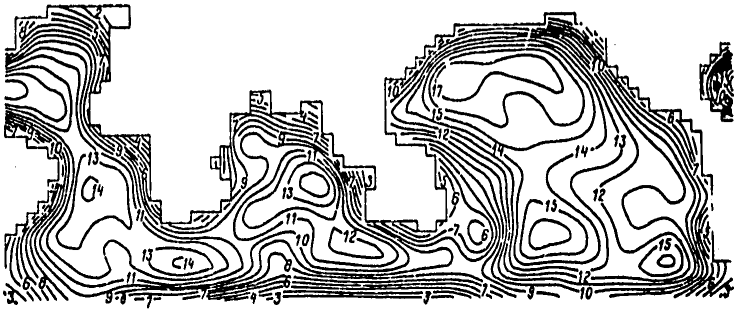

Fig. 1. Region of solution of problem of free oscillations and isolines of smoothed depths of the world ocean.

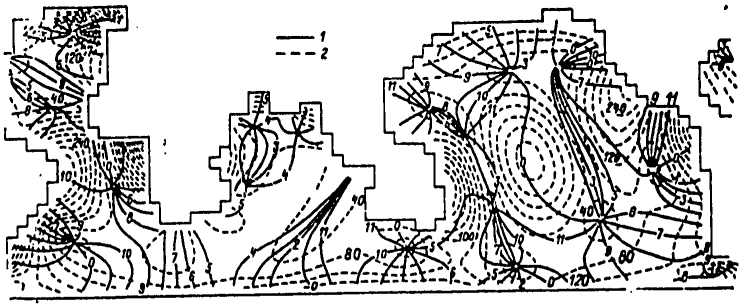

Fig. 2. Main semidiurnal wave M_2. 1) cotidal lines each 30°, 2) isoamplitudes

Numerical Experiments

In order to carry out numerical computations using the model described above the region G was selected in the form represented in Fig. 1. In this same figure we show isolines of smoothed depths of the world ocean. The numbers

of the isolines correspond to a uniform breakdown into 18 parts between the maximum (max(D) = 5.2 km) and minimum (min(D) = 1 km) depth values. The grid regions were constructed with use of uniform intervals $\Delta\theta = \Delta\psi = 5°$. With this resolution the matrix A in formula (25) has the order 1427.

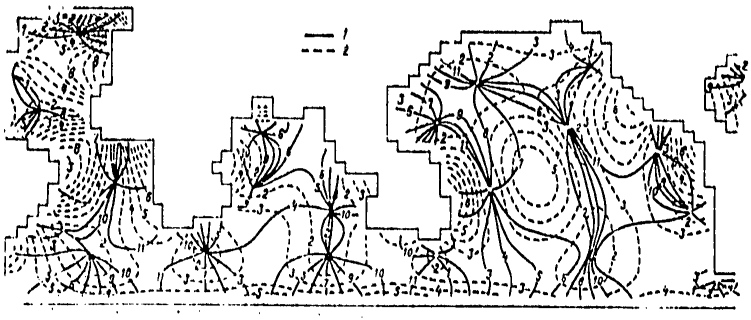

Fig. 3. Cotidal lines (1) and isoamplitudes (2) of computed eigenfunction with period of oscillations τ = 12.3562 hours.

The computations indicated an adequate effectiveness of the proposed method and the pattern of the fields of isophasal and cotidal lines of the computed M_2 wave qualitatively coincides with known experimental and numerical ideas concerning its structure [3], [11]. We note that since in the considered model friction is absent, the values of the isoamplitudes were exaggerated.

Table 1

Модули собственных чисел 1	Периоды колебаний собственных функций τ, ч 2	Модули собственных чисел 1	Периоды колебаний собственных функций τ, ч 2
1,517703	11,5000	1,446935	12,0622
1,505195	11,5954	1,412512	12,3562
1,490266	11,7115	1,385716	12,5951
1,472138	11,8557	1,374438	12,6985
1,453413	12,0085		

KEY:
1. Moduli of eigenvalues
2. Periods of oscillations of eigenfunctions τ, hours

In computing the eigenfunctions of the difference operator A^h in the iteration process m was selected equal to 14. In different variants of the computations the convergence was attained on the average after 10 iterations. The criterion for ending of the computations was not only a coincidence of the eigenvalues obtained in two successive iterations, but also the condition of invariance of the corresponding subspace with the base vectors from Φ_0^j in formula (17). It was assumed that the invariance is observed if the corresponding Gram matrix of the normalized vectors from Φ_1^j, determined in (17), has the rank m, that is, if with an adequate degree of accuracy of m eigenvalues the Gram matrices are equal to two and the others are equal to zero. In addition, it follows from formula (15)

that the spectrum of the A_β matrix must be multiple. This is also one of the criteria for ending the iterations.

The use of inverse iterations in combination with the simultaneous iterations method for a group of vectors not only ensures a rapid convergence, but also to some degree gives a definite guarantee that in the computed interval there are no other eigenvalues other than those which have been found.

As an example we will cite two variants of computations of eigenvalues of the operator A^h with $m = 14$ for $\eta = 1.405143905 \cdot 10^{-4}$ and $\eta = 1.454444 \cdot 10^{-4}$, that is, for frequencies in the neighborhood of the M_2 and S_2 waves respectively. Among the 28 eigenfunctions found in these two variants, only 18 were different, that is, the intervals of the computed eigenvalues were superposed on one another. Table 1 gives the moduli of the computed eigenvalues and the corresponding periods of oscillations of the eigenfunctions of the A^h operator. Figure 3 illustrates one of the eigenfunctions with a period of oscillations $\tau = 12.3562$ hours.

In this article we have for the most part examined the computation aspects of solution of the partial spectral problem for discrete analogues of the linearized tidal operators. The application of this method for studying the dynamics of tidal oscillations on the basis of a geophysical interpretation of the results of numerical experiments will be discussed in special publications.

The author expresses appreciation to G. I. Marchuk and B. A. Kagan for formulating the problem and constant attention to the work and to V. V. Penenko for assistance in developing the method.

BIBLIOGRAPHY

1. Gantmakher, F. R., TEORIYA MATRITS (Matrix Theory), Nauka, 1967.

2. Ladyzhenskaya, O. A., KRAYEVYYE ZADACHI MATEMATICHESKOY FIZIKI (Boundary Value Problems in Mathematical Physics), Nauka, 1973.

3. Marchuk, G. I., Kagan, B. A., OKEANSKIYE PRILIVY. MATEMATICHESKIYE MODELI I CHISLENNYYE EKSPERIMENTY (Ocean Tides. Mathematical Models and Numerical Experiments), Leningrad, Gidrometeoizdat, 1977.

4. Mikhlin, S. G., VARIATSIONNYYE METODY V MATEMATICHESKOY FIZIKE (Variation Methods in Mathematical Physics), Nauka, 1970.

5. Penenko, V. V., "Computation Aspects of Modeling of the Dynamics of Atmospheric Processes and Evaluation of the Influence of Different Factors on Atmospheric Dynamics," NEKOTORYYE PROBLEMY VYCHISLITEL'NOY I PRIKLADNOY MATEMATIKI (Some Problems in Computation and Applied Mathematics), Novosibirsk, Nauka, 1975.

6. Wilkinson, J. H., ALGEBRAICHESKAYA PROBLEMA SOBSTVENNYKH ZNACHENIY (Algebraic Problem of Eigenvalues), Nauka, 1970.

7. Wilkinson and Reinsch, SPRAVOCHNIK ALGORITMOV NA YAZYKE ALGOL (Handbook of Algorithms in ALGOL Language), LINEYNAYA ALGEBRA (Linear Algebra), Moscow, Mashinostroyeniye, 1976.

8. Faddeyev, D. K., Faddeyeva, V. N., VYCHISLITEL'NYYE METODY LINEYNOY ALGEBRY (Computation Methods of Linear Algebra), Moscow-Leningrad, Fizmatgiz, 1963.

9. Faddeyev, D. K., Faddeyeva, V. N., VYCHISLITEL'NYYE METODY LINEYNOY ALGEBRY: ZAPISKI NAUCHNYKH SEMINAROV LOMI (Computation Methods in Linear Algebra: Notes of Scientific Seminars of the Leningrad Division of the Mathematics Institute), edited by V. V. Voyevodin, Leningrad, Nauka, Vol 54, 1975.

10. Platzman, G. W., "Normal Modes of the Atlantic and Indian Oceans," J. PHYS. OCEANOGR., Vol 5, No 2, 1975.

11. Zahel, W., "Mathematical and Physical Characteristics and Recent Results of Ocean Models," LECTURE NOTES IN PHYSICS, COMPUTING METHODS IN APPLIED SCIENCES. SECOND INTERNATIONAL SYMPOSIUM, December 15-19, 1975, Springer-Verlag, Berlin-Heidelburg-New York, 1976.

UDC 551.46.062.5(262.54)

WATER EXCHANGE BETWEEN THE SEA OF AZOV AND THE BLACK SEA WITH OPERATION OF A REGULATING STRUCTURE IN KERCH STRAIT

Moscow METEOROLOGIYA I GIDROLOGIYA in Russian No 6, Jun 79 pp 67-73

[Article by Candidate of Geographical Sciences I. A. Shlygin, State Oceanographic Institute, submitted for publication 5 January 1979]

Abstract: By the method of mathematical modeling of the water and salt balances in the Sea of Azov the author has computed the parameters of water exchange through the Kerch hydraulic complex. It was possible to determine the statistical characteristics, variability and guaranteed probability of the magnitudes of Sea of Azov and Black Sea flows in different stages in the process of regulating sea salinity. The article gives the guaranteed probabilities of the total time during which discharge openings are opened for the passage of migratory fish with an accompanying wind flow during the spring and autumn.

[Text] Water and salt exchange through Kerch Strait is of fundamental importance in forming the hydrological regime of the Sea of Azov. It not only exerts a direct influence on sea salinity (the fraction of salt exchange with the Black Sea is 97% of the salt balance of the Sea of Azov), but also exerts a decisive effect on the chemical and biological bases of productivity, and also on the extent of areas of different salinity, which in turn limit the habitats and development of different species of fish.

Modern negative changes in the hydrological regime of the Sea of Azov have occurred as a result of the totality of natural and anthropogenic factors, expressed in a reduction in the inflow of fresh water (the nonreturned withdrawals alone amount to 9-12 km^3/year) and changes, in this connection, in the characteristics of water exchange through Kerch Strait. The ratio of the quantity of inflow of Black Sea waters to runoff from the Sea of Azov

in a natural period was 0.68; during the last eight years it was 0.85 [5]. Changes in the sea regime were expressed in a disruption of the balance of biogenous substances, a deterioration in the oxygen regime, and most importantly, an increase in the mean salinity of sea water from 10.5°/oo under natural conditions to 12.4°/oo during the last eight years. Thus, a study of the characteristics of water exchange is necessary for an investigation of the entire complex of hydrological, hydrochemical and biological changes in the sea regime.

The modern parameters of water exchange, as well as its changes by periods, are retrospective; the statistical characteristics are given in [1, 5].

At the same time, in order to optimize the hydrological regime of the Sea of Azov, there are plans for carrying out a whole complex of water management measures, postulating a change in the water balance components of the sea. Among these measures the most important are the shifting of runoff from other basins and regulation of water exchange through Kerch Strait. In both cases there is a change in the conditions for water exchange between the Sea of Azov and the Black Sea. However, with a certain degree of probability it can be postulated that whatever may be the influence exerted on river runoff (increase in withdrawal, shifting of direction of stream flow, etc.) on a scale not exceeding the present-day changes in river runoff, the general patterns in variation of water exchange through Kerch Strait will remain unchanged. It would be a different matter with the construction of a regulating structure, when the artificial restriction of entry of saline Black Sea water and the controllable discharge of water and salts from the Sea of Azov will first make it possible to reduce the salinity of the Sea of Azov and subsequently maintain it at the optimum level.

The problems involved in a change in sea salinity in a case of regulated water exchange were first examined in [6, 7, 9]. Computations of regulation of the salinity and level of the Sea of Azov have been made by the method of mathematical modeling of the water and salt balances of the sea [9]. In the computations use was made of river runoff and apparent evaporation series obtained by Ye. A. Asarin and A. M. Naumov at the Gidroproyekt by the statistical tests method; the statistical parameters of the natural series adopted in the modeling are given in Table 1.

The annual quantities of natural runoff were modeled using the D. Ya. Ratkovich scheme [8]. The intra-annual distribution of runoff was ascertained by analogy with the distribution of equal annual volumes of the observed untransformed runoff. The total prospective withdrawal, determined taking into account the dispatcher graphs of reservoir operation, was superposed on the series obtained in this way. The water consumption in the basin was taken in the basin in accordance with the "Sea of Azov Scheme" (residual inflow 28 km^3), and also artificially increased by 2 and 4 km^3. As a result, we obtained three inflow variants, each with 25 30-year records in each.

Table 1

Statistical Parameters of Natural Runoff and Apparent Evaporation Used in Modeling (According to Ye. A. Asarin and A. M. Naumov)

Река (створ, участок) 1	Среднее многолетнее значение, км³ 2	C_v	C_s
3 р. Дон, Цимла	21,6	0,34	2 C_v
4 р. Дон, участок Цимла — Азовское море	6,3	0,62	2 C_v
5 р. Кубань, Краснодар	13,4	0,17	2 C_v
6 Видимое испарение	20,03	0,18	0,0

KEY:

1. River (station, reach)
2. Mean long-term value, km^3
3. Don River, Tsimla
4. Don River, reach Tsimla-Sea of Azov
5. Kuban' River, Krasnodar
6. Apparent evaporation

The monthly values of apparent evaporation were obtained by multiplying the total annual value of the element by a coefficient constant for each month. The latter was determined from long-term data on the intra-annual distribution of precipitation and evaporation.

The discharges through the hydraulic complex were determined using hydraulic dependences for a bottom spillway with a broad apron (a total of 34 water-discharge spans). The level drop in the pools of the hydraulic complex was determined by the algebraic summation of the balance level, formed by river runoff, precipitation and evaporation -- for the Sea of Azov pool, and the mean monthly level -- for the Black Sea pool, and a special level-differences correction. The latter was obtained by V. P. Belov and Yu. G. Filippov [4] by the hydrodynamic method using standard wind fields [3].

The computations were made using 30-year runoff and apparent evaporation series with time intervals corresponding to the "lifetime" of standard wind fields (from 6 to 48 hours). The time for computing one 30-year series on a "Minsk-22" electronic computer is 12 minutes.

The process of regulating salinity of the Sea of Azov is accomplished in three stages.

1. The mean sea salinity for each computation interval is greater than $10.5^{o}/oo$. The water accumulates in the Sea of Azov to the upper reading (+10 cm abs.). When this reading is exceeded there is a discharge of the excess Sea of Azov waters. However, if the quantity of water entering the sea is less than the quantity evaporating and the sea level drops, upon reaching the reading -60 cm abs. the Black Sea water is admitted. Since

under average conditions the fresh balance of the sea is positive, with predominantly discharge of Sea of Azov water there is a decrease in the salt reserve and a decrease in sea salinity.

2. Upon attaining a salinity of 10.5°/oo the additional withdrawal of fresh water is possible. Therefore, in the next computation interval a correction is subtracted from the projected river runoff; this correction is equal to the volume of the additional withdrawals for each computation interval (the volume of these withdrawals is up to 6 km^3 annually).

3. However, if with additional withdrawal of river water the salinity continues to drop, with its decrease to 9.5°/oo there is a discharge of the overflow sea prism. In the next computation intervals, when the level in the Sea of Azov pool exceeds the level of the Black Sea pool, there is a further discharge of Sea of Azov water; with the opposite situation there is entry of Black Sea water. Such mutually opposite inflows of water occur up to the time of an increase in Sea of Azov salinity to 9.5°/oo.

From the point of view of an investigation of water exchange, stages 1 and 2 are equally important and henceforth will be considered jointly.

In modeling the regulating process, regardless of the stage of decrease in sea salinity, there was modeling of spring and autumn passage of fish through the hydraulic complexes. It was assumed that the passage of the migratory fish through the dam occurs in April-May from the Black Sea into the Sea of Azov and in October-November in the opposite direction with an accompanying wind flow. For this purpose the level drops near the dam created by the wind were used [4]. In the event of formation of level differences associated with "accompanying" winds, seven openings in the dam are opened (length of the spillway front 100 m) and the fish are able to pass through with the accompanying wind current, that is, the same as under natural conditions. The volume of fish passing through was taken into account in the further analysis as a component part of the water exchange. At the same time, we ascertained the total time during which the spillway openings were open for the passage of fish.

The computed volumes of flows of Sea of Azov and Black Sea waters through the hydraulic complex during each computation interval were summed for obtaining the monthly and annual water exchange values (V_A and V_{BS} respectively). The analysis was made using the total annual water exchange values for all series (a total of 75 records).

It was postulated that the work of the hydraulic complex will begin in 1990. Therefore, Table 2 gives the mean values and dispersions of water exchange through the hydraulic complex with the realization of a mean projected inflow of river waters in a volume of 28 km^3/year during the last 17 years of the investigated 30-year periods. This table also gives the mean values of these characteristics with an inflow of 26 and 24 km^3/year. According to the data in [1], the present quantities of water

exchange are $\bar{V}_{BS}$ = 33.5 km^3, σ^2 = 24.0, $\bar{V}_A$ = 48.8 km^3, σ^2 = 49.0.

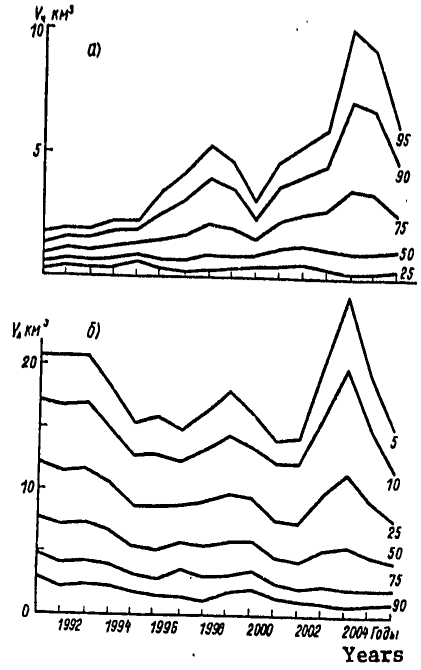

Fig. 1. Chronological graph of equally guaranteed volumes of Black Sea (a) and Sea of Azov (b) flows.

Accordingly, with regulation there will be a considerable decrease in the volume of water exchange (especially the inflow of Black Sea waters). The ratio of the volumes of inflow of Black Sea waters to outflow from the Sea of Azov decreases from 0.7 to 0.2. Such a radical transformation of water exchange unquestionably will change the overall picture of formation of hydrological elements in the sea.

Figure 1 shows graphs of the chronological variation of water exchange volumes of different guaranteed probability, constructed on the assumption of moderate asymmetry (C_s = 2 C_v) of the series of water exchange volumes. In computing the guaranteed probability we took into account the nature of the dependence of water exchange components on river runoff; with the minimum values of river runoff there are minimum V_A and maximum V_{BS} values. By analogy with runoff they are assigned a high guaranteed probability.

Table 2

Mean Values (km^3) and Dispersion of a Series of Values for Water Exchange Through the Kerch Hydraulic Complex for a Mean River Runoff 28 km^3. Onset of Regulation -- 1990

Год 1	Приток из Черного моря 2		Отток в Черное море 3	
	$\bar{V}_{Ч}$ BS	σ^2	$\bar{V}_A$	σ^2
1990	0,4	0,12	9,6	26,7
1991	0,9	0,45	8,8	47,1
1992	0,8	0,18	8,3	30,7
1993	0,8	0,45	9,4	45,4
1994	1,0	0,49	6,7	15,2
1995	1,1	0,33	6,4	21,2
1996	1,2	2,93	6,6	19,3
1997	1,3	1,80	7,0	16,7
1998	1,9	6,23	6,7	33,1
1999	1,1	0,57	7,9	27,5
2000	1,3	1,55	6,5	20,3
2001	2,1	4,11	4,8	17,1
2002	1,7	2,15	6,1	23,0
2003	2,2	7,17	8,2	71,4
2004	3,1	22,42	8,6	87,0
2005	2,0	4,31	4,9	15,4
2006	1,9	5,38	6,2	30,1
Среднее 4	1,5	4,26	7,2	32,6
Среднее при стоке 26 км³ 5	1,6	2,82	6,3	24,9
Среднее при стоке 24 км³ 6	2,2	5,43	5,3	20,6

KEY:

1. Year
2. Inflow from Black Sea
3. Outflow into Black Sea
4. Mean
5. Mean for runoff 26 km^3
6. Mean for runoff 24 km^3

With a general insignificant increase in the mean V_{BS} values and a decrease in V_A in the course of the investigated series, associated with a general decrease in salinity, it is possible to discriminate two variability maxima falling in 1997 and 2003. The second maximum is greater than the first.

The appearance of these maxima is attributable to the fact that in 1997 active releases will begin in one case(third regulation stage). In 2003 there will be four such cases. In the remaining 21 cases of the investigated variant the stability is stabilized in the range 9.5-10.5°/oo by means of an increase in the water intakes.

Figure 2 shows the guaranteed probability of the annual volumes of water exchange and river runoff.

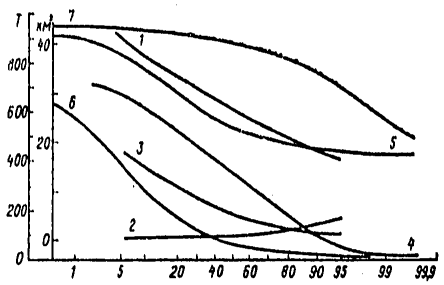

Fig. 2. Guaranteed probability of river runoff (1), runoff of Sea of Azov (3) and inflow of Black Sea (2) waters, and also T_{BS} and T_A values in the first and second stages of regulation (4, 5) and during time of active water releases (6, 7).

In the analysis an attempt was made to determine the dependence of the V_A and V_{BS} values on river runoff and apparent evaporation (by analogy with [1, 5]). However, it was not possible to detect stable correlations for the annual values of the mentioned parameters. The reason for this is that the construction of a hydraulic complex in Kerch Strait will lead to the transformation of the Sea of Azov into a reservoir of the long-term regulating type with a useful regulating volume 18.5 km^3 (between the readings +10 and -60 cm abs.). The annual runoff of the rivers is 25-30 km^3, less 17-23 km^3 of apparent evaporation, giving an excess of the fresh balance 5-10 km^3. This volume can be completely accumulated by the sea.

Therefore, an analysis was made of the mean V_{riv}, V_{BS} and V_A values for each record in the first and second stages in regulation and in the third stage separately. There was found to be a rather stable relationship between the mean values of the water exchange components and mean river runoff; the nature of the dependence for these two cases is substantially different.

In the stage of a decrease in salinity and with its stabilization by means of the withdrawal of river water the dependences of water exchange on river runoff are nonlinear and are described by the exponential equations

$$V_A = 0{,}0478\, V_p^{1.0499} \times \times e^{0.0585\, V_p}, \quad (1)$$

$$V_Ч = 1{,}023 \cdot 10^{10} V_p^{-8.1946} \times e^{0.1495\, V_p}, \quad (2)$$

[A = Sea of Azov; Ч = Black Sea; p = river]

which are valid in the range of V_{river} variations from 20 to 34 km^3.

The multiple correlation coefficient for expression (1) is equal to 0.98; for expression (2) it is equal to 0.70, which is unquestionably significant, since with a 5% significance level under these conditions the coefficient becomes significant if it exceeds 0.32, whereas with a 1% significance level it is equal to 0.38.

The nonlinearity of the correlations is manifested most clearly in the range of V_{river} values close to 20 km^3. In this case the fresh sea balance approaches zero and in order to stabilize the level the need arises for changing the operating regime of the hydraulic complex -- to increase the admissions of Black Sea waters.

In the stage of active entry of water the dependences of the water exchange components on river runoff have a linear form:

$$V_A = 0.74\ V_{river} - 12.42 \quad (3)$$
$$V_{BS} = 7.24 - 0.22\ V_{river}. \quad (4)$$

The linear correlation coefficient for equation (3) is equal to 0.96; for equation (4) -- 0.85.

The linear dependences of V_A and V_{BS} on runoff and their nature (direct for Sea of Azov flow and inverse for Black Sea flow) show that in the case of free water entries through the hydraulic complex under the conditions for regulation of salinity the water exchange regime approaches a natural regime.

One of the important problems involved in the influence of the regulation of water exchange on the hydrobiological conditions of the sea is the problem of the possibility of the passage of migrating fish through the dam. The conditions for the modeling of the passage of fish were indicated above.

The objective possibilities of the passage of migrating fish are determined primarily by the time during which the spillway openings were open for their passage with an accompanying wind flow. The duration of the individual situations favoring the passage of fish is determined by the duration of favorable types of wind fields [3] and varies, as indicated, from 6 to 48 hours. The total time for the season is essentially dependent on the stage of the sea freshening process. In the first and second stages of salinity decrease this time is a function of the mean river runoff and sea salinity (Fig. 3). In the case of high salinity values the time for opening of the floodgates to a high degree is dependent on the river runoff (that is, the balance level of the Sea of Azov). The parameters of closeness of the graphic dependences are 0.73-0.91. In the third stage of the regulation process it was not possible to detect correlations between the time of opening of the openings in the dam for the passage of fish and the parameters of the water and salt balances. This is attributable to the fact that in this stage the balance level varies about its mean long-term value

(-30 cm abs.). However, in the process of decrease in salinity the level stands near the upper readings (+10 cm) and its variability is considerably less. Figure 2 shows curves of the guaranteed probability of the T_{BS} and T_A values in the stage of a decrease in salinity (4 and 5) and in the process of its stabilization. For the T_{BS} and T_A values in the third stage of regulation the theoretical and empirical guaranteed probability curves (6 and 7 in Fig. 2) virtually coincide. For T_{BS} and T_A, obtained in the first and second stages of the process of decrease in salinity (curves 4 and 5), due to the strong asymmetry of the series, empirical guaranteed probability curves were constructed. The mean T_{BS} value in the first and second stages of regulation was 95 hours (σ = 68), T_A -- 880 hours (σ = 61 hours), in the third stage of regulation these values are equal to $\overline{T}_{BS}$ = 360 hours (σ = 204), $\overline{T}_A$ = 504 hours (σ = 130).

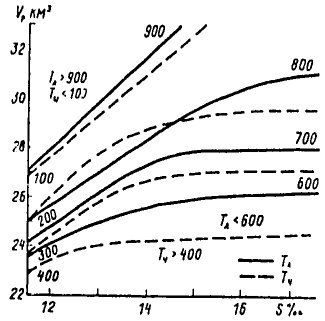

Fig. 3. Dependence of the total time of opening of flood gates of hydraulic complex for passage of fish in spring (T_{BS}) and autumn (T_A) on river runoff and sea salinity in first and second regulation stages.

An analysis of the guaranteed probability curves shows that regardless of the values of the water balance components the objective possibilities of passage through of fish with the accompanying wind current remain.

BIBLIOGRAPHY

1. Al'tman, E. N., "Investigation of Water Exchange Between the Black Sea and the Sea of Azov," SBORNIK RABOT LYuM GOIN (Collection of Articles of the Southern Seas Laboratory of the State Oceanographic Institute), No 11, 1972.

2. Al'tman, E. N., "Structure of Currents in Kerch Strait," TRUDY GOIN (Transactions of the State Oceanographic Institute), No 125, 1975.

3. Belov, V. P., "Wind Regime and Wind Waves in the Sea of Azov," TRUDY GOIN, No 139, 1978.

4. Belov, V. P., Filippov, Yu. G., "Principal Features of the Dynamics of Waters in the Sea of Azov and Kerch Strait," TRUDY GOIN, No 139, 1978.

5. Belov, V. P., Filippov, Yu. G., Shlygin, I. A., "Computation of Water Exchange Through Kerch Strait," METEOROLOGIYA I GIDROLOGIYA (Meteorology and Hydrology), No 2, 1978.

6. Gontarev, N. P., Shlygin, I. A., "Present-Day Hydrodynamic Problems of the Sea of Azov and Possible Ways to Solve Them," TRUDY GOIN, No 139, 1977.

7. Gontarev, N. P., Shlygin, I. A., "Salinity of the Sea of Azov With Regulated Water Exchange Through Kerch Strait," IZV. SEVERO-KAVKAZSKOGO NAUCHNOGO TSENTRA VYSSHEY SHKOLY (News of the Northern Caucasus Scientific Center of the Higher School), No 1, 1978.

8. Ratkovich, D. Ya., "Modeling of Mutually Dependent Hydrological Series," VODNYYE RESURSY (Water Resources), No 1, 1977.

9. Shlygin, I. A., "On a Method for Computing Regulation of Salinity in the Sea of Azov by the Kerch Hydraulic Complex," TRUDY GOIN, No 137, 1978.

UDC 532.517.4

TEMPERATURE-STRATIFIED CURRENT IN A WATER BODY WITH THROUGH FLOW

Moscow METEOROLOGIYA I GIDROLOGIYA in Russian No 6, Jun 79 pp 74-79

[Article by Candidate of Physical and Mathematical Sciences V. I. Kvon, Hydrodynamics Institute, Siberian Department USSR Academy of Sciences, submitted for publication 5 September 1978]

Abtract: A study was made of a temperature-stratified current in a flow-through water body arising at the time of discharge of heated water. The coefficients of vertical turbulent exchange are determined using a two-parameter model of turbulence containing an equation for turbulent energy and an equation for the rate of dissipation of this energy. The method for numerical solution of the problem is briefly described. An example of practical computations is given.

[Text] An important element in the model of stratified turbulent currents is a turbulence model. Different turbulence models have been proposed for studying stratified currents ([4, 8, 11] and others). In particular, in [4] use is made of a simple and rather universal two-parameter turbulence model for the mathematical modeling of surface turbulence in the ocean. In this paper we also use a two-parameter model of turbulence in studying a temperature-stratified current in a water body with through flow.

Formulation of Problem

A temperature-stratified turbulent current of water in a water body is described by a system of equations [1, 6]

$$\frac{\partial u_1}{\partial t} + u_1 \frac{\partial u_1}{\partial x_1} - l u_2 = -g \frac{\partial}{\partial x_1}\left(z + \frac{1}{\rho_0}\int_{x_3}^{z_0} \rho\, dx_3\right) + \frac{\partial}{\partial x_3} K \frac{\partial u_1}{\partial x_3}, \tag{1}$$

$$\frac{\partial u_2}{\partial t} + u_2 \frac{\partial u_2}{\partial x_2} + l u_1 = -g \frac{\partial}{\partial x_2}\left(z + \frac{1}{\rho_0}\int_{x_3}^{z_0} \rho\, dx_3\right) + \frac{\partial}{\partial x_3} K \frac{\partial u_2}{\partial x_3}, \tag{2}$$

$$\frac{\partial u_\alpha}{\partial x_\alpha} = 0, \quad \rho = f(T), \tag{3}$$

$$\frac{\partial T}{\partial t} + u_\alpha \frac{\partial T}{\partial x_\alpha} = \frac{\partial}{\partial x_3} K_T \frac{\partial T}{\partial x_3}. \tag{4}$$

Here t is time; $x_\alpha (\alpha = 1, 2, 3)$ are the axes of a rectangular coordinate system, with the x_3 axis being directed vertically upward; u_α are the components of the velocity vector; ρ is water density; f is a stipulated temperature function; z is the deviation of the free water surface from the undisturbed horizontal position z^0; ρ_0 is some constant (mean) density value; g is the acceleration of free falling; ℓ is the Coriolis parameter; K and K_T are the coefficients of total viscosity and thermal conductivity.

The following boundary conditions are used for the system of equations (1)-(4). On a lateral cylindrical surface

$$\left.\begin{aligned} &u_n = 0 \text{ for } \vec{x} \in \Sigma_0 \\ &u_n = f_n(x, t) \text{ for } \vec{x} \in \Sigma_1 \\ &u_1 = f_1(\vec{x}, t),\ u_2 = f_2(\vec{x}, t),\ T = k_3 T_3(t) + f_T(\vec{x}, t) \quad \text{for } \vec{x} \in \Sigma_2 \end{aligned}\right\} \tag{5}$$

At a water surface with $x_3 = z^0$

$$\frac{\partial z}{\partial t} = u_3,\ K\frac{\partial \vec{u}}{\partial x_3} = \frac{\vec{\tau}}{\rho_0},\ c_p \rho_0 K_T \frac{\partial T}{\partial x_3} = -k_T (T - T_E). \tag{6}$$

At the bottom with $x_3 = z_0(x_1, x_2)$

$$u_3 = u_1 \frac{\partial z_0}{\partial x_1} + u_2 \frac{\partial z_0}{\partial x_2},\ K\frac{\partial \vec{u}}{\partial x_3} = k_b |\vec{u}| \vec{u},\ \frac{\partial T}{\partial x_3} = 0 \tag{7}$$

Here

$$\vec{x} = (x_1, x_2, x_3),\ \vec{u} = (u_1, u_2),\ \vec{\tau} = (\tau_1, \tau_2),$$

τ_1 and τ_2 are wind shearing stresses; u_n is the velocity component normal to the shoreline; k_b is the coefficient of bottom shearing stress [2]; k_T is the heat exchange coefficient; T_E is equilibrium temperature; f with the subscripts are stipulated functions; Σ_0 is the solid shore part of the boundary Σ; Σ_1 is the liquid part of Σ in which the water flows from the water body (water intake); Σ_2 is the liquid part of the boundary Σ at which the water flows into the water body (water discharge), k_3 is a proportionality factor stipulating a linear correlation between the temperature at the water outlet and the temperature $T_3(t)$ at the water intake. When $k_3 = 0$ condition (5) stipulates the water temperature at the water outlet.

The coefficients of vertical turbulent exchange in (1)-(4) are determined on the basis of the following turbulence model [4, 8]:

$$\frac{\partial e}{\partial t} = \frac{\partial}{\partial x_3} K \frac{\partial e}{\partial x_3} + p - \varepsilon, \tag{8}$$

$$\frac{\partial \varepsilon}{\partial t} = \frac{\partial}{\partial x_3} K_1 \frac{\partial \varepsilon}{\partial x_3} + \frac{\varepsilon}{e} (c_1 p - c_2 \varepsilon), \tag{9}$$

where

$$p = K^* \left[\left(\frac{\partial u_1}{\partial x_3} \right)^2 + \left(\frac{\partial u_2}{\partial x_3} \right)^2 \right] (1 - \alpha_T \mathrm{Ri}),$$

$$\mathrm{Ri} = - \frac{g \partial \rho / \partial x_3}{\rho_0 \left[\left(\frac{\partial u_1}{\partial x_3} \right)^2 + \left(\frac{\partial u_2}{\partial x_3} \right)^2 \right]},$$

e is the energy of turbulence; ε is the rate of dissipation of this energy; K^* is the coefficient of turbulent viscosity [4, 8],

$$K^* = \alpha \frac{e^2}{\varepsilon}; \tag{10}$$

α_T is the ratio of the coefficient of turbulent thermal conductivity to the coefficient of turbulent viscosity ($K_T = \alpha_T K^* + \lambda$, where λ is the coefficient of molecular thermal conductivity); c_1, c_2 and α are empirical coefficients [2, 9, 10].

The total viscosity in (1)-(8) is determined through the coefficient of turbulent viscosity by the expression

$$K = K^* + \nu,$$

where ν is the coefficient of kinematic viscosity. The coefficient $K_\varepsilon = \alpha_\varepsilon K^* + \nu$, α_ε is a constant [9].

The following boundary conditions are used for the system (8) and (9).

At the water surface

$$K \frac{\partial e}{\partial x_3} = k_e \left| \frac{\vec{\tau}}{\rho_0} \right|^{3/2}, \quad \varepsilon = c_\varepsilon \frac{e^{3/2}}{y^0}. \tag{11}$$

At the bottom

$$\frac{\partial e}{\partial x_3} = 0, \quad \varepsilon = c_\varepsilon \frac{e^{3/2}}{y_0}. \tag{12}$$

Here k_e and c_ε are constants [2, 3]; y^0 and y_0 are the roughnesses of the water surface and bottom respectively.

In addition to the boundary conditions for system (1)-(4) and (8), (9) it is necessary to stipulate the initial conditions, representing the initial distributions of the sought-for current parameters. The function f(T) in (3) is determined from the dependence [12]

$$f(T) = \rho_0[1 - 6{,}8 \cdot 10^{-6}(T-4)^2]. \tag{1.3}$$

The formulated problem is solved numerically with use of implicit difference schemes. We will briefly describe the solution method. In order to approximate the equations of motion (1) and (2) in time in the interval $n\tau \leqslant t \leqslant (n+1)\tau$ we use a stabilizing correction scheme [7]. In the first fractional interval the levels of the free surface z are computed in a certain n-th layer in time (τ is the time interval). In the second fractional interval there is a correction for stability. In order to determine the level of the free surface in the upper (n + 1)-st time layer we use integration of the continuity equation (3) with depth. With the substitution of expressions for velocities (in this case determined in the second fractional interval) into this equation we obtain an equation for a level surface [5]. The difference equations for momentum and heat transfer are written using directed differences [5]. The difference operators in the vertical direction are approximated with a second order of accuracy [2]. The coefficients on the derivatives are computed in the n-th layer in time. The difference equations for the turbulence parameters are solved numerically by the fitting method [7]. In solving the difference equations for momentum (in the first fractional interval) and heat transfer and the equations for a level surface use is made of the Gauss-Seidel method. In this case the fitting method is used for the heat transfer equation in the direction of the x_3 axis and the matrix fitting method is employed for the equations of motion [7].

Results of Numerical Modeling

Employing the computation algorithm described above we carried out computations of a temperature-stratified current in the cooling pool at the Ekibastuzskaya GRES-2 power station. The horizontal dimensions of this pool are approximately 7 km in length and 6.5 km in width. The average depth of this water body is 7.6 m and the maximum depth is 12 m. In the example of the computations the discharge of heated water is accomplished by two surface water outlets and the intake of cooled water by one deep water intake. The computations were made for the meteorological conditions of a hot ten-day period in the absence of a wind. The following input data were stipulated: discharge in both water outlets -- 125 m^3/sec each, discharge in the water intake -- 250 m^3/sec, equilibrium temperature -- 22.7°C, heat transfer coefficient k_T = 19.21 Cal/(m^2·hour·°C). The following values were used in condition (5): proportionality factor k_3 = 1, temperature drop in the condensers at the thermal electric power station f_T = 10°C. The initial condition corresponded to a state of rest. The initial water temperature was equal to the equilibrium temperature.

Figure 1 shows the isotherms and velocity fields (u_1, u_2) at the surface (at left) and at the bottom (at right) when there is a steady hydrothermal regime in the water body, corresponding to 22 days of physical time. In this figure the double arrow indicates the sites of the water outlets and intake;

the velocity vectors, indicated by simple arrows, show only the direction of circulation due to the relative smallness of its absolute value. At the lower water outlet the discharge of heated water occurs at an angle of 30° to the shoreline. A narrow zone of heated water flows from this outlet at the bottom along the shore. At the water surface it is possible to trace jet streams caused by the surface discharge of heated water. In the shore region near the water intake the warm surface water, moving toward the shore, subsides and flows along the bottom in the opposite direction. Accordingly, near the water intake the maximum stratification is not observed at the shore itself, but at some distance from it. An analysis of the depth-averaged velocity field indicated that the averaged current has a large eddy zone in the central part of the water body.

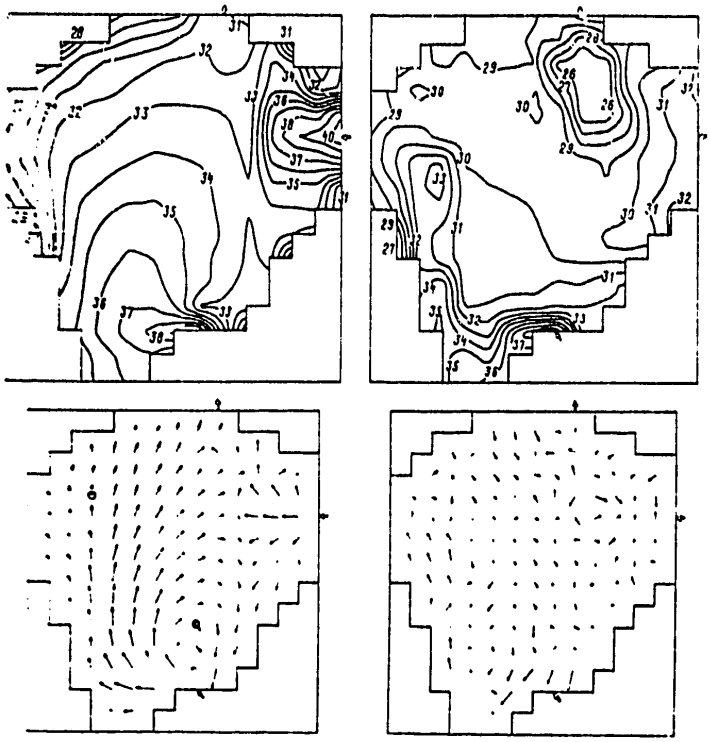

Fig. 1.

The length scale of the velocity vectors can be judged using the data in Fig. 2, which gives the distributions of the horizontal velocity components (u_1, u_2), the coefficient of turbulent viscosity and the temperature at two verticals. The positions of these verticals are indicated in Fig. 1 by small circles. It can be seen that both near the water outlets (dark

circle in Fig. 1, solid curves in Fig. 2) and far from them (open circle, dashed curves) a temperature stratification is present. At both verticals the velocities change sign with depth (curves 1 correspond to the velocity u_1, curves 2 correspond to the velocity u_2). Appreciable turbulent fluctuations are observed only in the surface layer of the water body. Below this layer vertical diffuse exchange occurs by molecular processes (see Fig. 2). Here the turbulent fluctuations are suppressed by Archimedes forces caused by stable water stratification (see equations (8) and (9), the terms $\alpha_T Ri$ in them).

Figure 3 shows a curve of change in water temperature at the water intake with time. This temperature is the principal characteristic of the cooling capability of the cooling pool.

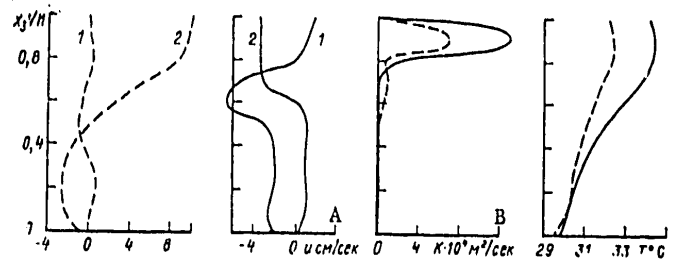

Fig. 2

KEY:

A) cm/sec

B) m^2/sec

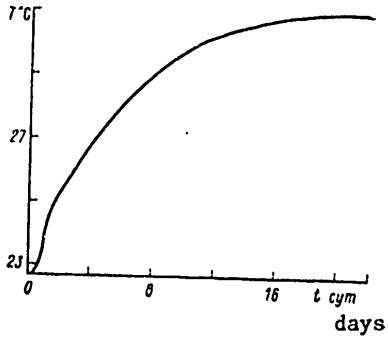

Fig. 3

We recall that in the computations the temperature drop between the water outlet and water intake was stipulated. In this case in the absence of heat exchange through the water surface the water temperature in the water body would increase without limit. The setting-in of a stationary hydrothermal regime with time means that the heat discharged into the water body

no longer accumulates in it and fully escapes into the atmosphere through the water surface.

BIBLIOGRAPHY

1. Vasil'yev, O. F., Kvon, V. I., Makarov, I. I., "Hydrothermal Regime of Cooling Pools at Thermal and Atomic Electric Power Stations," IZV. AN SSSR, ENERGETIKA I TRANSPORT. (News of the USSR Academy of Sciences, Power and Transportation), No 4, 1976.

2. Ignatova, G. Sh., Kvon, V. I., "A Hydrodynamic Slip Model in a Turbulent Current," METEOROLOGIYA I GIDROLOGIYA (Meteorology and Hydrology), No 7, 1978.

3. Kitaygorodskiy, S. A., Miropol'skiy, Yu. Z., "Dissipation of Turbulent Energy in the Surface Layer of the Sea," IZV. AN SSSR, FIZIKA ATMOSFERY I OKEANA (News of the USSR Academy of Sciences, Physics of the Atmosphere and Ocean), Vol IV, No 6, 1968.

4. Marchuk, G. I., Kochergin, V. P., Klimok, V. I., Sukhorukov, V. A., "Mathematical Modeling of Surface Turbulence in the Ocean," IZV. AN SSSR, FIZIKA ATMOSFERY I OKEANA, Vol 12, No 8, 1976.

5. Sarkisyan, A. S., OSNOVY TEORII I RASCHETA OKEANICHESKIKH TECHENIY (Principles of Theory and Computation of Ocean Currents), Leningrad, Gidrometeoizdat, 1966.

6. Fel'zenbaum, A. I., "Dynamics of Sea Currents," GIDROMEKHANIKA-1968 (Hydromechanics-1968), Moscow, 1970.

7. Yanenko, N. N., METOD DROBNYKH SHAGOV RESHENIYA MNOGOMERNYKH ZADACH MATEMATICHESKOY FIZIKI (Fractional Intervals Method for Solving Multi-dimensional Problems in Mathematical Physics), Novosibirsk, Nauka, 1967.

8. Chen, Ch. T., Rodi, W., "A Mathematical Model for Stratified Turbulent Flows and its Application to Buoyant Tets," PROCEEDINGS XVIth CONGRESS OF THE IAHR, Sao Paulo, Brazil, Vol 3, 1975.

9. Jones, W. P., Launder, B. E., "The Calculation of Low Reynolds Number Phenomena With a Two-Equation Model of Turbulence," INT. J. HEAT AND MASS TRANSFER, Vol 16, No 6, 1973.

10. Launder, B. E., "Comments on 'Improved Form of the Low Reynolds Number k-ε Turbulence Model' by G. H. Hoffman," THE PHYSICS OF FLUIDS, Vol 19, No 5, 1976.

11. Mellor, G. L., Durbin, P. A., "The Structure and Dynamics of the Ocean Surface Mixed Layer," J. PHYS. OCEANOGR., Vol 5, 1975.

12. Simons, T. J., "Development of a Three-Dimensional Numerical Model of the Great Lakes," CANADA CENTER FOR INLAND WATERS, SCIENTIFIC SERIES, No 12, Burlington, 1973.

UDC 556.(166+048)

METHOD FOR COMPUTING WATER DISCHARGES

Moscow METEOROLOGIYA I GIDROLOGIYA in Russian No 6, Jun 79 pp 80-84

[Article by E. S. Khersonskiy, State Hydrological Institute, submitted for publication 23 November 1978]

Abstract: The author proposes a method for computing the maximum discharges of rain-induced high waters and spring floods. A formula is given for computing the observed discharges and their guaranteed probability values.

[Text] One of the important aspects of hydrological support for the planning, construction and operation of hydraulic structures is computation of maximum runoff when there is a shortage or lack of observational data.

At the present time computations of the maximum runoff of spring floods and rain-induced high waters are made using empirical and semiempirical formulas of different types: reduction and volume formulas and formulas based on allowance for the maximum intensity of rain and on the hydromechanical theory of surface runoff of water [3]. Without dwelling on certain merits and shortcomings of these formulas, we will note two of their common characteristics. First, as the principal arguments in them use is made of the area of the drainage basin, layer or intensity of precipitation and the runoff coefficient. Second, they were developed for computing maximum water discharges with a rare frequency of recurrence. Therefore, an objective checking of computation errors on the basis of observational data to all intents and purposes is unrealistic.

In this paper an attempt is made to develop a more general computation scheme which while retaining the merits of the existing methods would meet two principal requirements: first, make it possible to determine the maximum discharges of spring floods and rain-induced high waters with a stipulated excess probability and second, make it possible to give an objective evaluation of the computed characteristics on the basis of observational data in the example of real floods and high waters.

A detailed analysis of existing methods for computing maximum runoff and the theoretical premises indicated that in the considered computation scheme it is feasible to use the following arguments: length of the channel network, basin slope, runoff coefficient, layer and intensity of precipitation (snow reserves).

The length L or the density γ of the channel network, in contrast to the area of the drainage basin, carries information not only on the volume of the falling precipitation (snow reserves), but also on the peculiarities of structure of the hydrographic net, being the joint product of geology and climate and formed in the course of the historical time period [1]. The mean slope i of the drainage basin reflects the relief category [4] and in generalized form indirectly characterizes the hydrodynamic peculiarities of water flow along the slopes of the river basin.

Whereas the length of the channel network and the mean slope are relatively stable characteristics of a drainage basin (in a relatively short historical period), the layer and intensity of precipitation (snow reserves) are quite variable during the course of the warm season and from year to year. Therefore, in the considered computation scheme it seems feasible to use the characteristics of the measured values of the latter, which would make it possible to convert from precipitation (snow reserves) of a given excess probability to the maximum discharges of the corresponding guaranteed probability. A theoretical analysis indicated that for the characteristics of flood-forming precipitation it is sounder (in contrast to existing methods) to use the generalized precipitation parameter N, including its layer H and the intensity $\bar{a}$ simultaneously:

$$N = \bar{a}H. \tag{1}$$

Since $\bar{a} = H/t$, where t is the duration of the rain, then

$$N = \frac{H^2}{t}. \tag{2}$$

In accordance with existing methods, the runoff coefficient φ is determined in dependence on the computed guaranteed probability. It seems most correct to find its values by independent methods. For example, an analysis of observational data for 400 periods of high water at stations in the central part of the Baykal-Amur Railroad Line zone indicated that the runoff coefficient for one and the same stations decreases from the beginning to the end of the warm season [2]. This is associated with an increase in the water-holding capacity of the ground as it thaws during the warm season. An indirect characteristic of heat accumulation is the sum of positive mean daily air temperatures $\sum + t°$, with which the runoff coefficient is also rather closely related. At the same time, this φ value is also related to the general precipitation parameter N. Thus, the runoff coefficient can be

computed on the basis of the stipulated characteristics $\sum + t°$ and N for any high water period on the rivers of the permafrost zone. A similar approach is possible for an independent determination of the runoff coefficient in other regions of the country.

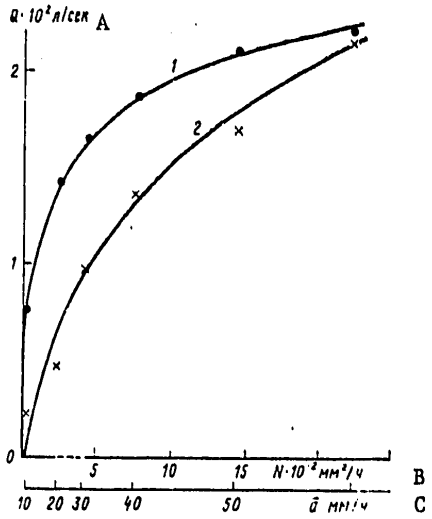

Fig. 1. Curves of the dependence $Q_{max} = f(N)$, $f(a)$, maximum discharge, on generalized precipitation parameter (mean intensity of precipitation) on the basis of sprinkling data in flumes $F = 2\ m^2$.

KEY:

A. liters/sec
B. mm^2/hour
C. mm/hour

Whereas the N parameter reflects the dynamics of feeding of water into the drainage basin, the combination of the generalized precipitation parameter and the mean basin slope determines the dynamics of discharge of the water from the slopes into the channel network. Hence $Q = f(N, i)$. An analysis of data from experimental sprinkling in flumes (Fig. 1) and data from long-term observations on the rivers studied by the Kolymskaya Water Balance Station and the Mogotskiy Heat and Water Balance Polygon of the Baykal-Amur Expedition of the State Hydrological Institute during 1975-1977 (Fig. 2) indicated that $Q = f(N^i)$.

Thus, the proposed computation scheme for determining maximum runoff can be expressed in the form of the following models:

a) for the maximum discharge of rain water runoff

$$Q_{max_д} = L\varphi N^i + Q_{пр}, \quad (3)$$

[Д = rain(water); пр = pre-high water] where $Q_{max_{rain}}$ is in m^3/sec, L is in km; N is in mm^2/sec; i is in fractions of unity; Q_{pre} is the pre-high-water water discharge, in m^3/sec;

b) for the maximum discharge of spring high water

$$Q_{max_{сн}} = L\varphi N^i_{сн} + Q_{пр}, \quad (4)$$

[CH = snow] where N_{snow} is a generalized parameter of snow reserves, equal to

$$N_{snow} = S^2/t; \quad (5)$$

here S is the water reserve in the snow, mm, $t_т$ is the duration of snow thawing, sec;

c) for the maximum discharge of mixed snow- and rain-induced high waters

$$Q_{max_{сд}} = L\varphi (N + N_{сн})^i + Q_{пр}. \quad (6)$$

[CD = s-r = snow-rain]

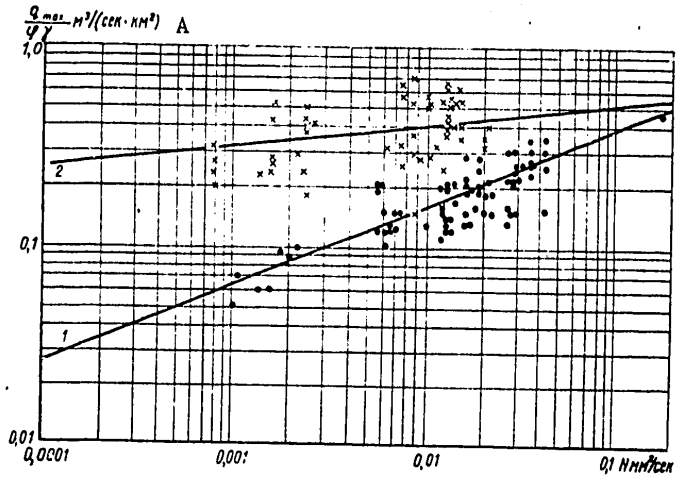

Fig. 2. Curves of dependence $q_{max}/\gamma\varphi = f(N)$ of maximum runoff modulus on generalized precipitation parameter. 1) Kolymskaya water balance station, $i_{mean} = 0.40$; 2) Mogotskiy experimental polygon State Hydrological Institute. A) $m^3/(sec \cdot km^2)$; B) mm^2/sec

Converting to runoff moduli, we have

$$q_{\max_{Д}} = \gamma\varphi N^{l} + q_{пр}, \tag{7}$$

$$q_{\max_{СН}} = \gamma\varphi N_{СН}^{l} + q_{пр}, \tag{8}$$

$$q_{\max_{СД}} = \gamma\varphi (N + N_{СН})^{l} + q_{пр}. \tag{9}$$

[Д = rain; SH = snow; СД = snow-rain; пр = pre(high-water discharge]

Table 1

Computation of Maximum Water Discharges for Different Adopted Intervals of Rainfall Duration

	t ч 1				t сут 2			
	20	21	25	30	10	11	12	15
	H=60 мм; i=0,10; φ=0,5; γ=1,0				H=100 мм; i=0,10; φ=0,5; γ=1,0			
H^2/t	0,050	0,048	0,040	0,033	0,012	0,0105	0,0097	0,0077
$(H^2/t)^l$	0,740	0,738	0,728	0,711	0,643	0,634	0,631	0,617
q м^3/(сек·км^2) 3	0,37	0,369	0,364	0,356	0,32	0,317	0,316	0,309
$\frac{\Delta q}{q_{20}} \cdot 100\%$	—	0	1,6	3,8	$\frac{q_n - q_{10}}{q_{10}} \cdot 100\%$	1,6	1,9	3,4

KEY:

1. hours
2. days
3. sec·km^2

One of the peculiarities of the proposed method is that there is simultaneous use of elements of the volume formulas and the formulas for limiting intensity in the form of the parameter $N = \bar{a}H$. Thus, the precipitation layer H is the main argument in the volume formulas and the intensity of precipitation $\bar{a}$ is the principal argument in the formulas for limiting intensity.

The practical use of formulas (3), (4) and (6)-(9) for determining the maximum water discharges does not involve special difficulties, since the hydrographic characteristics of the drainage basin L, γ and i can be determined quite simply from large-scale maps and the N parameter can be determined on the basis of observational data for the nearest meteorological stations. The possible subjective approach and the errors in determining

the duration of rainfall have no serious effect on the accuracy of the computations (Table 1). The possible computation errors for all intents and purposes will not exceed 20% even with errors in determining rainfall duration from 10 to 15 days and basin slopes to 0.50. The reason for this is the dominating role in the formation of maximum water discharge played by such hydrographic and morphological characteristics as density of the river network and basin slope.

The errors in determining the maximum discharges of rain-induced high waters by the use of formulas (3) and (7) were evaluated by means of comparison of 66 computed discharges with measurements in 1976-1977 in six river basins of the Mogotskiy heat and water balance polygon of the Baykal-Amur expedition of the State Hydrological Institute (central segment of the Baykal-Amur Railroad), having the following characteristics: area of basin -- from 3 to 100 km^2, slope -- 0.15-0.18, channel network density -- 0.8-1.0 km/km^2. The correlation coefficient between the computed and measured maximum discharges was 0.99.

In addition, formulas (3) and (7) were also checked using observational data for the period from 1950 through 1975 on three watercourses of the Kolymskaya water balance station: Kontaktovyy Nizhniy ($F = 21.2$ km^2), Kontaktovyy Sredniy ($F = 14.2$ km^2) and Vstrecha ($F = 5.4$ km^2). Their characteristics are: slope 0.30-0.65 and density of the channel network 2.0-3.5 km/km^2. These differ substantially from the similar characteristics of drainage basins in the Mogotskiy polygon. The correlation coefficients between the computed and measured maximum water discharges were equal to: for the Kontaktovyy Nizhniy -- 0.93, Kontaktovyy Sredniy -- 0.85, Vstrecha -- 0.64. The curve of distributions of deviations of the measured and computed discharges for the Kontaktovyy Nizhniy is shown in Fig. 3.

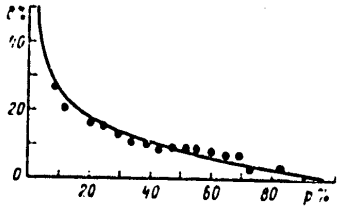

Fig. 3. Distribution of deviations of Q_{meas} from Q_{comp}. Kontaktovyy Nizhniy stream. $F = 21.2$ km, $\delta_{mean} = 11\%$, $C_v = 0.89$, $C_s = 1.75$.

The checking of formulas (4) and (8) for computing the maximum discharges of spring high water on the basis of long-term observational data for the Valdayskaya Scientific Research Hydrological Laboratory imeni V. A. Uryvayev indicated that the computation errors do not exceed 30%. In this case the runoff coefficients were not computed by an independent method and were adopted on the basis of factual data, which is not entirely correct.

Thus, the proposed method has a number of advantages over existing methods: first, it makes it possible to compute the maximum discharges of rain-induced high waters and spring floods, and also mixed feeding by snow and rain of different excess probability on the basis of use of the small volume of available information, and second, it makes it possible to obtain more precise results. Without question, it must be tested using a great volume of data from field observations in different regions of the country with different natural conditions.

One of the objectives of further investigations is a more rigorous theoretical substantiation of the proposed method.

BIBLIOGRAPHY

1. Alekseyev, G. A., "Computation of the Maximum Runoff of Melt and Rain Water Using Data from Hydrometric Observations on Adjacent Rivers," VODNYYE RESURSY (Water Resources), No 4, 1977.

2. Vasilenko, N. G., Khersonskiy, E. S., "Coefficients of High-Water Runoff on Rivers in the Central Sector of the Baykal-Amur Railroad," TRUDY GGI (Transactions of the State Hydrological Institute), No 254, 1978.

3. Sokolovskiy, D. L., RECHNOY STOK (River Runoff), Leningrad, Gidrometeoizdat, 1968.

4. UKAZANIYA PO OPREDELENIYU RASCHETNYKH MAKSIMAL'NYKH RASKHODOV TALYKH VOD SN 356-66 (Instructions on Determination of the Computed Maximum Discharges of Melt Water SN 356-66), Leningrad, Gidrometeoizdat, 1966.

UDC 551.524:633.842(478.9)(477)

INFLUENCE OF AIR TEMPERATURE ON THE YIELD OF PEPPERS

Moscow METEOROLOGIYA I GIDROLOGIYA in Russian No 6, Jun 79 pp 85-89

[Article by L. Ye. Bozhko, Odessa Hydrometeorological Institute, submitted for publication 28 November 1978]

Abstract: A study was made of the influence of air temperature on change in the yield of vegetable pepper under conditions of irrigation in the Moldavian SSR and in the southern Ukrainian SSR.

[Text] The cultivation of peppers became common in our country in the late 1930's when the canning industry began to develop. The principal regions of its cultivation in the European USSR are the Moldavian SSR, the southern oblasts of the Ukrainian SSR and RSFSR, and the northern boundary of commercial cultivation runs along the line Bryansk-Tambov-Kuybyshev. The total area in peppers at the kolkhoz and sovkhoz farms in the Soviet Union is 50% of the areas occupied by this crop in the world.

Peppers are characterized by increased requirements on heat and moisture, far greater even than for tomatoes and eggplants. Peppers will not tolerate arid conditions and therefore in most regions it is cultivated under irrigated conditions. In the opinion of some authors [1, 2, 7] peppers grow and develop well at an air temperature above 15°C; at 13°C its growth and development are slowed, the flowers, buds and young fruits drop off, and at 10°C growth ceases completely. It is damaged by frosts of any intensity at any age. During spring the seedlings perish completely even when there are insignificant frosts, whereas during the autumn the fruits lose commercial value. Peppers require the most heat during budding and mass flowering. During the fruit-bearing period peppers react less sharply to a decrease in air temperature, but on the other hand the moisture requirements increase. With a decrease in soil moisture content below 75% during the fruit-bearing period there is an increase in the distortion and bitterness of the fruits and a worsening of their commercial appearance.

In the European USSR the varieties with the greatest commercial importance are Novocherkasskiy 35, Bolgarskiy 079, Moldavskiy Belyy, Yubileynyy 307, Moldova 118, and others. Everywhere peppers are cultivated as a transplant

crop. The setting out of the seedling takes place when the air temperature passes through 13-15°C. In Moldavia and in the southern oblasts of the Ukraine the transplanting takes place in the second ten-day period of May; to the north of the line Chernovtsy-Znamenka-Izyum -- at the end of May. The mean long-term date of flowering is observed during the third ten-day period of June - early July, and technical ripeness -- in late July-early August respectively. The last harvesting of fruits is limited by autumn frosts and occurs in late September-early October. The duration of the growing season averages 145 days; the duration of the fruit-bearing season is 80 days. There are 8-12 harvestings during the fruit-bearing season. The greater part of the harvest falls in the third-eighth harvestings.

During the period from the transplanting to the flowering of the peppers (middle-maturing varieties) there must be a sum of 2,500-2,800°C of active temperatures above 15°C. The guaranteed probability of growing season heat for peppers in the Moldavian SSR and in the southern oblasts of the Ukraine is 85-90%, in the southeastern oblasts of the Ukraine -- 75-85%, and to the north of the line Chernovtsy-Znamenka-Izyum -- 65-75%. Due to the different guaranteed probability of heat, there is a different mean level of the yield of peppers. Its highest mean yields are in Moldavia, Odesskaya, Nikolayevskaya, Khersonskaya Oblasts and in Krymskaya Oblast -- 200-260 centners/hectare. In the southeastern oblasts of the Ukraine the mean yield is 150-190 centners/hectare. In the remaining regions it is 130-150 centners/hectare. The yield in all regions varies in a wide range from year to year.

Few studies have been devoted to determining the agrometeorological reasons for the considerable variations in the yield of peppers.

We examined data on the yield of peppers and the agrometeorological conditions for its growth during a period of 18-20 years. An analysis of the yield variability was made by the V. N. Obukhov method [5]. As is well known, the dynamics of increase in the yield of agricultural crops is governed by an increase in the technical level of agriculture, against whose background there are random variations of yield associated for the most part with weather conditions. Such studies made for winter and spring wheat, barley, sunflower and oats [3-6] are known.

For the considered territory the temporal change in yield ($y = f(t)$, where y is yield, t is time) was approximated either by a straight-line equation or by a second-degree polynomial. The coefficient a in the equations characterizes the mean annual yield increment. It should be noted here that the mean annual increment in the equations for the tendency to a change with time (trend) can be determined not only by the level of agricultural cultivation, but also to some degree by the weather conditions in individual years [3-6].

An analysis of the dynamics of the tendency to a change in the yield of peppers (Table 1) shows that the increment in its yield in different regions of the investigated territory is nonuniform. It was greatest in the

Moldavian SSR, Odesskaya, Khersonskaya and Nikolayevskaya Oblasts (42-65%). There is a lower increment in the remaining oblasts of the Ukraine, especially in Crimean SSR, where it was only 16%. It should be noted that during recent years in some oblasts, especially southeastern oblasts, the rate of the increment decreased. The decrease in the rate of yield increment during recent years can be attributed to some degree to a disruption of the irrigation regime (a shortage of water for irrigation in the Crimea) and also a change in the physical properties of the soil as a result of their salinization.

Table 1

Equations for Trend Lines and Change in Mean Oblast Yield of Peppers During Period from 1956 Through 1973

Республика, область 1	Уравнения линий трендов 2	3 Урожай, ц/га: начало периода 6	3 Урожай, ц/га: конец периода 7	4 Прирост урожая за весь период: ц/га centners	4 Прирост урожая за весь период: %	5 Коэффициент вариации
8 Молдавская ССР	$y=0{,}17x^2+20{,}4x+46{,}9$	193	318	115	52	0,23
9 Области УССР						
10 Одесская	$y=1{,}9x+154{,}9$	198	311	113	47	0,18
11 Херсонская	$y=3{,}6x+148{,}2$	180	235	46	21	0,14
12 Николаевская	$y=1{,}6x+180{,}8$	130	269	139	49	0,16
13 Крымская	$y=1{,}6x+210{,}1$	253	291	38	16	0,19
14 Запорожская	$y=0{,}9x^2+24{,}5x+54{,}8$	99	146	47	47	0,24
15 Донецкая	$y=1{,}2x+139{,}6$	98	183	85	48	0,31
16 Ворошиловградская	$y=3{,}4x^2+58{,}2x+19{,}5$	96	159	63	56	0,32
17 Днепропетровская	$y=2{,}7x+138{,}8$	96	185	90	98	0,22
18 Кировоградская	$y=1{,}3x+154{,}8$	83	188	105	101	0,24

KEY:

1. Republic, oblast
2. Trend line equations
3. Yield, centners/hectare
4. Increment in yield during entire period
5. Variation coefficient
6. Beginning of period
7. End of period
8. Moldavian SSR
9. Oblasts of Ukrainian SSR
10. Odesskaya
11. Khersonskaya
12. Nikolayevskaya
13. Krymskaya
14. Zaporozhskaya
15. Donetskaya
16. Voroshilovogradskaya
17. Dnepropetrovskaya
18. Kirovogradskaya

Using the method employed earlier in evaluating the climatic variability of the yield of winter and spring wheat, spring barley, sunflowers and oats [3, 4, 6], we computed the climatic variability of the yield of peppers C_p (Table 1).

$$C_p = \frac{1}{\bar{y}}\sqrt{\frac{\sum_{i=1}^{n}(y_i-\bar{y})^2-\sum_{i=1}^{n}(\hat{y}_i-\bar{y})^2}{n-1}}.$$

Here C_p is the variation coefficient, y_i is the yield for a specific year, $\bar{y}$ is the mean yield, $\hat{y}_i$ is the dynamic mean yield value, n is the number of investigated years.

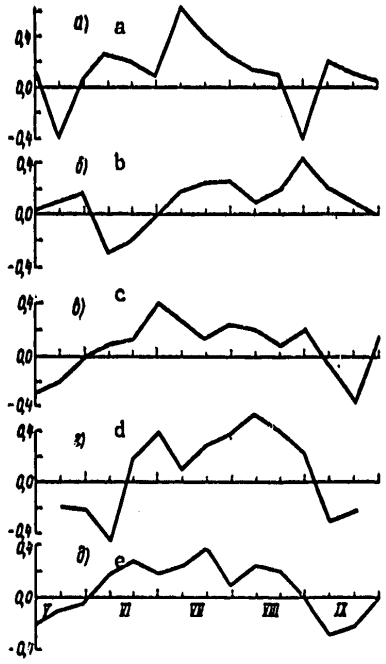

Fig. 1. Dynamics of correlation coefficients between deviations of yield of peppers and mean ten-day air temperature. a) Donetskaya and Zaporozhskaya Oblasts; b) Voroshilovgradskaya Oblast; c) Moldavskaya SSR, Odesskaya, Khersonskaya and Nikolayevskaya Oblasts; d) Dnepropetrovskaya and Kirovogradskaya Oblasts; e) Krymskaya Oblast

An investigation of the variability of the yield with time shows that relatively stable yields of peppers are observed in the Moldavian SSR, Krymskaya, Odesskaya and Khersonskaya Oblasts. Considerable yield variations were observed in Zaporozhskaya, Donetskaya and Voroshilovgradskaya Oblasts, where the C_p values are maximum (0.24-0.32).

What factors are responsible for the considerable yield deviations from the trend line? As mentioned above, in the entire considered territory peppers are cultivated under irrigated conditions. We did not feel that it was

possible to evaluate the influence of the irrigation regime. It can be surmised that under irrigation conditions the moisture supply of sown crops is adequate. Therefore, we examined only the distribution of air temperature. Quantitative investigations of the interrelationship between deviations of the yield of peppers from the trend line and the anomaly of the mean 10-day air temperature made it possible to detect the influence of air temperature during the period from May through the second ten-day period in September on yield.

Figure 1 shows that not in all regions is the influence of the thermal factor on the change in crop yield the same. For the Moldavian SSR, southern and southeastern oblasts of the UkrSSR the period of greatest positive influence of air temperature on change in yield falls at the end of June and July; for Kirovogradskaya and Dnepropetrovskaya Oblasts -- in July and early August.

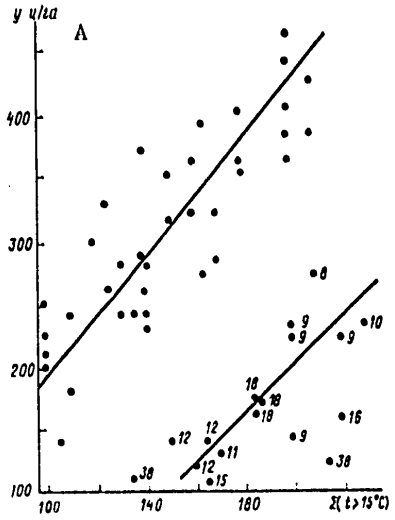

Fig. 2. Correlation between yield of peppers (y) and sum of air temperature above 15°C (x) during critical period.

KEY:

A. y centners/hectare

A high air temperature in June exerts a negative influence on the magnitude of the yield in these regions. To some extent this is associated with the times of transplanting of peppers. In Moldavia and in the southern oblasts of the Ukraine, where transplanting occurs in the second ten-day period in May, by June the plants begin to vegetate actively. In Kirovogradskaya and Dnepropetrovskaya Oblasts the transplanting occurs later and in June the

plants are acclimatized. Therefore, it is natural that the high temperatures of the beginning of June exert a negative influence on the yield of peppers, especially when the irrigation is not carried out in time. An increase in the period between waterings in the period of fruit-bearing up to 20 days or more and any sum of precipitation during this period of less than 10 mm also has the effect that the air temperature begins to exert a negative influence on the magnitude of the yield (in Zaporozhskaya Oblast -- in the third ten-day period of July and the first ten-day period of August (Fig. 1a); the third ten-day period of August and the beginning of September -- in Donetskaya Oblast (Fig. 1c).

A correlation analysis of the anomaly of the mean ten-day air temperature and deviations of the yield from the trend line shows that over the entire territory the factor of greatest importance for crop yield is air temperature in the budding period and the mass flowering of pepper plants. This period lasts about 30 days and is called the critical period. With respect to calendar periods, as a long-term average this period is observed in late June-July. The special correlation coefficients are highest precisely during this period and vary in the range from 0.42 in Krymskaya Oblast to 0.65 in Dnepropetrovskaya Oblast. Proceeding on this basis, we attempted to determine the dependence of the yield of peppers on the sum of the mean daily temperature above 15°C during the period 10 days before to 20 days after the phase of flowering of the plants. This dependence is represented in Fig. 2 and is characterized by two concentrations of dots. A more detailed analysis of this correlation indicated that low yields in the case of an adequate air temperature sum are obtained as a result of the withering of plants damaged by the fungus Verticillum albo - atrum R and the virus affecting the buds. A considerable decrease in the yield is already noted when 8% of the plants are affected. The greatest damage to the plants occurs in years with marked transitions from moist cool periods to dry and hot periods [2, 7]. The correlation between the yield of peppers and an air temperature sum above 15°C during the critical period is linear and is expressed by the straight line equation

$$y = 1.86x + 189,$$

where x is the temperature sum above 15°C during the critical period, n = 82, r = 0.77±0.03, E_y = ±21 centners/hectare.

The error in the equation is 9% of the mean level (236 centners/hectare).

It should be noted that in all categories of farms the yield will be lower than in the seed-selection stations. The corresponding coefficients were established for conversion from the yield at the seed-selection stations to the mean oblast yield (Table 2). The coefficients were different for different oblasts. The greatest value of the coefficient is for Moldavia and its lowest value is in the southeastern oblasts of the Ukrainian SSR. This is evidently attributable to the different levels of agricultural engineering. In Moldavia the coefficient is highest, close to the level of the seed-selection station.

The equation which we derived -- the dependence between the yield of peppers and the air temperature sum -- can be used for predicting the yield of peppers. Since the period of fruit bearing of peppers lasts from 60 to 90 days, the advance time of the forecast is 2-2.5 months.

Table 2

Ratio of Mean Oblast Yield of Peppers to its Yield at State Seed-Selection Stations

Republic, Oblast	$\bar{y}/\bar{y}_{SSSS}$
Moldavskaya SSR	0.80
Oblasts of UkrSSR	
Odesskaya	0.50
Dnepropetrovskaya	0.45
Zaporozhskaya	0.40
Krymskaya	0.56

BIBLIOGRAPHY

1. Bozhko, L. Ye., "Requirements of Peppers on Temperature Conditions," METEOROLOGIYA, KLIMATOLOGIYA I GIDROLOGIYA (Meteorology, Climatology and Hydrology), No 2, 1966.

2. Zaginaylo, N. N., "Peppers," OVOSHCHEVODSTVO MOLDAVII (Cultivation of Vegetables in Moldavia), Kishinev, Kartya Moldovenyaske, 1972.

3. Kogan, F. N.,"Yield of Grain Crops in the Nonchernozem Zone of the European Territory of the USSR and Possibilities of its Prediction on the Basis of Weather Data," TRUDY GIDROMETTSENTRA SSSR (Transactions of the USSR Hydrometeorological Center), No 174, 1977.

4. Mel'nik, Yu. S., "Allowance for Agrometeorological Conditions and Level of Sophistication of Agricultural Mechanization in Predicting the Yield of Sunflowers," TRUDY GIDROMETTSENTRA SSSR (Transactions of the USSR Hydrometeorological Center), No 174, 1977.

5. Obukhov, V. M., UROZHAYNOST' I METEOROLOGICHESKIYE FAKTORY (Crop Yield and Meteorological Factors), Moscow, Gosplanizdat, 1949.

6. Pasov, V. M., "Climatic Variability of the Yield of Winter Wheat," METEOROLOGIYA I GIDROLOGIYA (Meteorology and Hydrology), No 2, 1973.

7. Filov, A. I., PERTSY I BAKLAZHANY (Peppers and Eggplants), Moscow-Leningrad, Sel'khozizdat, 1956.

UDC 551.509.314:633.15(497.2)

STATISTICAL STRUCTURE OF THE FIELD OF PHENOLOGICAL PHENOMENA FOR CORN IN BULGARIA

Moscow METEOROLOGIYA I GIDROLOGIYA in Russian No 6, Jun 79 pp 90-96

[Article by Ye. Khershkovich, N. Slavov, M. Vandova, M. Yordanova and P. Ivanov, Institute of Hydrology and Meteorology, Sofia, submitted for publication 28 November 1978]

Abstract: For the purpose of studying the optimum density of the network of phenological stations a study was made of the statistical structure of the phenological phenomena for corn in the low-lying part of the territory of the country (up to 400 m above sea level). The investigation was made using structural and covariation functions of the interphase periods of corn on the basis of data for 25 stations making observations in different climatic regions of the country in 1960-1975. The authors have determined the random and "microclimatic" errors of the corresponding functions. The errors in optimum interpolation and extrapolation were ascertained. It is concluded that the use of the statistical structure of the field of phenological phenomena makes possible a scientific validation of the optimum density of stations making phenological observations.

[Text] In an article entitled "Statistical Structure of the Field of Phenological Phenomena in Bulgaria" [7] an attempt was made to investigate the optimum density of siting of phenological stations in the country, for this purpose using an objective method -- study of the statistical structure of the field of the observed element. Our investigation is devoted to this same objective, employing the same method, but with a different approach and other initial data.

In order to study the peculiarities of phenological phenomena, governed by their dependence on many conditions, not only on the environment, but also on the plants themselves, the cultivation method, etc., the duration of the interphase periods of corn was adopted as the basic material for the investigation. The influence of the variety and agrotechnology on the duration of the interphase periods was not taken into account, since in the investigation we used the computed dates of onset of the phenological phases by means of indices derived from the great volume of observational data for a definite group of hybrids.

We studied the duration of the interphase periods: sowing-sprouting, sprouting-ear formation, ear formation-milky ripeness, milky ripeness-wax ripeness, wax ripeness-total ripeness by the method developed by N. Slavov [5]. The duration of the interphase periods was determined on the basis of data for 25 stations situated in different climatic regions of the country, at an elevation as great as 400 m above sea level, during a 15-year period (1960-1975). For each phase we obtained 325 combinations of two stations with a different distance between the stations, and for six phases -- 1,950 combinations. For some distances there were few cases, which exerted an influence on the results.

The investigation of the statistical structure of the field of phenological phenomena was carried out with respect to the structural and covariation functions -- normalized and not normalized.

In determining the structural and covariation functions we used the deviations f' -- the deviations of the duration of the interphase periods from their mean values f, computed for this same period.

The structural $\tilde{b}_f(\ell)$ and covariation $\tilde{m}_f(\ell)$ functions were regarded as functions of the distance ℓ between the observation points.

The duration (in days) of the interphase periods of corn, averaged for the country, the standard deviations and their maximum and minimum values, are given in Table 1.

Table 2 gives the values of the normalized structural and covariation functions by distance gradations, mean distances and the number of cases on the basis of which they were obtained.

According to [2], in order for the field of phenological observations to be uniform and isotropic relative to these functions, there must be satisfaction of the condition

$$b_f(l) + 2m_f(l) = 2m_f(0) = b_f(\infty),\ \beta_f(l) + \mu_f(l) = 1.$$

An analysis of the resulting values of the structural and covariation functions indicated that this condition is not fully satisfied. This is because the considered functions were computed with errors, attributable both to the limitation of the series which are used in the study and to

the errors in the initial data caused by random and "microclimatic" errors. However, the data in Table 2, obtained after eliminating most of the errors by means of computing the corrected functions, show that the field of phenological phenomena can to a considerable degree be considered uniform and isotropic.

In Fig. 1 it is possible to trace the change in the structural and covariation functions.

Table 1

Mean Duration of Interphase Periods of Corn for Country (D, days) and Their Standard Deviation (σ)

Д	σ			Д	σ			Д	σ		
	ср. 1	макс. 2	мин. 3		ср. 1	макс. 2	мин. 3		ср. 1	макс. 2	мин. 3
4 Сев—всходы				5 Всходы — выметывание				6 Выметывание — молочная спелость			
18	5	6	3	66	10	12	8	26	2	3	1
7 Молочная спелость — восковая спелость				8 Восковая спелость — полная спелость				9 Всходы — полная спелость			
17	2	3	1	14	2	3	1	124	10	13	8

KEY:

1. mean
2. maximum
3. minimum
4. Sowing-sprouting
5. Sprouting-ear formation
6. Ear formation-milky ripeness
7. Milky ripeness-wax ripeness
8. Wax ripeness-total ripeness
9. Sprouting-total ripeness

In this paper we determined the random and "microclimatic" errors by means of extrapolation of the structural $\tilde{b}_f(l)$ and covariation $\tilde{m}_f(l)$ functions to $l = 0$ using the graphs shown in Fig. 1.

Table 3 gives the computed (by two methods) values of the standard deviations σ_0^2 of the random and "microclimatic" errors and their measure $\delta^2 = \sigma_0^2 / \sigma_f^2$. The values of the measure of errors show that the computed duration of the interphase periods is accompanied by errors which constitute 10-18% of the natural variability of the interphase periods. Only the variability of the sowing-sprouting interphase period, as was expected, was maximum -- 40% of the natural variability. This period is dependent to a

considerable degree on environmental factors and although the most important of them, heat and moisture, were taken into account in computing its duration, it can be said that as a result of the great number of factors exerting an influence on its duration, the data for this station cannot be representative for other places, even with minimum distances.

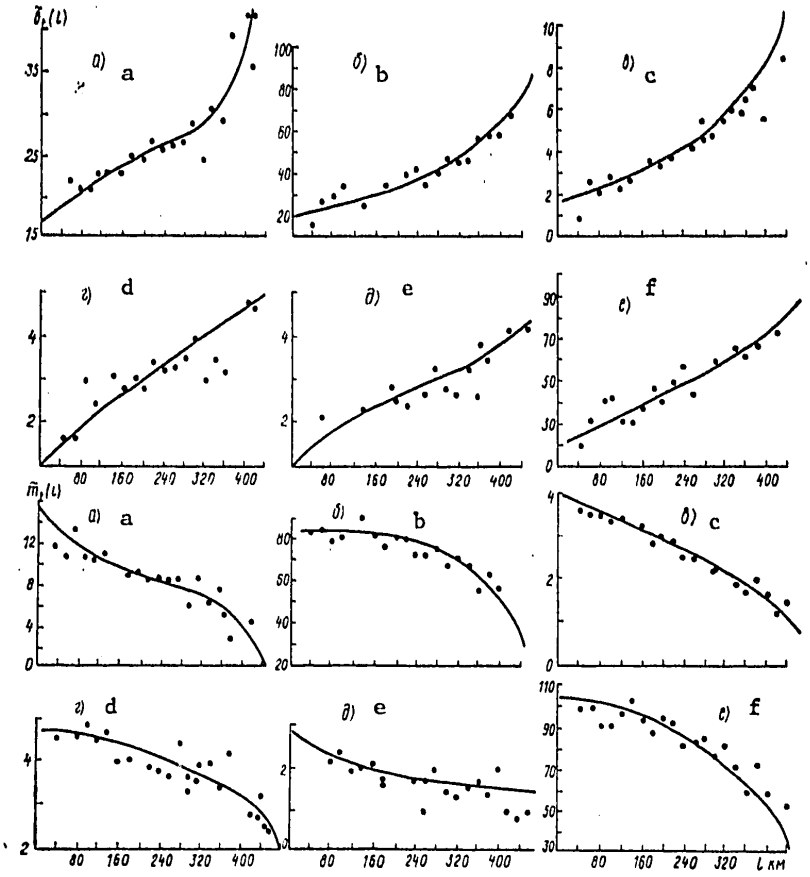

Fig. 1. Structural ($\tilde{b}_f(L)$) and covariation ($\tilde{m}_f(L)$) functions of duration of interphase periods of corn. a) sowing - sprouting; b) sprouting - ear formation; c) ear formation - milky ripeness; d) milky - wax ripeness; e) wax ripeness - total ripeness; f) sprouting - total ripeness

Since the normalized covariation function $\tilde{\mu}_f(L)$ (correlation coefficient) was used as the basic criterion in determining the errors in optimum interpolation and the admissible distances for interpolation between the observation points, it was analyzed more carefully (Fig. 2). The values of

the correlation coefficient decrease with an increase in the distance between pairs of stations. With all interphase periods to a distance of 60-80 km this coefficient decreases relatively rapidly -- from 0.95, 0.90 to 0.80. This also relates to the interphase period sowing-sprouting, but with the difference that the empirical correlation coefficient, with a zero distance, is here 0.70, whereas at 60-80 km it decreases to 0.50. The relatively small correlation coefficient for the data for one station with this interphase period indicates a great variability of its duration from year to year.

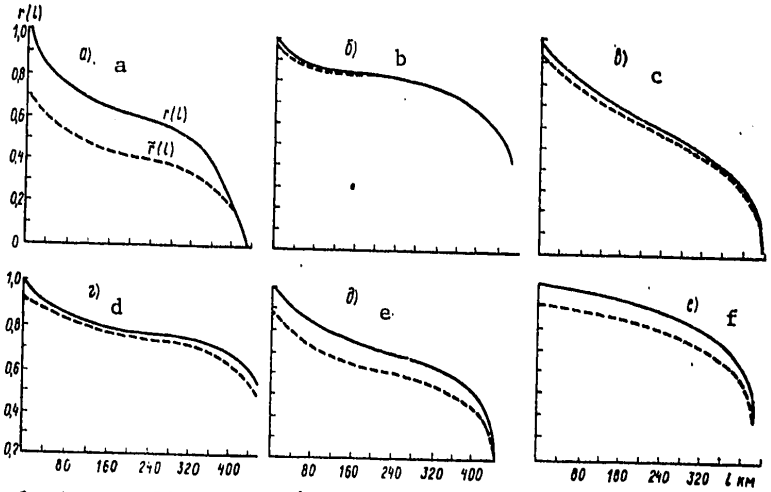

Fig. 2. Correlation coefficient $r(\ell)$ of duration of interphase periods of corn. a) sowing - sprouting; b) sprouting - ear formation; c) ear formation - milky ripeness; d) milky - wax ripeness; e) wax - total ripeness; f) sprouting - total ripeness; $r(\ell)$ -- theoretical curve; $\tilde{r}(\ell)$ — empirical curve.

With distances from 80 to 280-300 km the correlation coefficient for all interphase periods remains relatively high, at one level, after which it decreases rapidly.

The empirically computed correlation coefficients $\tilde{r}(\ell)$ in absolute value are less than the theoretical $r(\ell)$ correlation coefficients as a result of the random and "microclimatic" errors which are involved. Despite this, their values when $\ell = 0$, obtained by means of extrapolation of the empirical curve $\tilde{r}(\ell)$, are extremely high, 0.90 and above. With some interphase periods $\tilde{r}(\ell)$ is close to $r(\ell)$ or equal to it. In Fig. 2 it is possible to trace the variation of the corrected correlation coefficients, with which there is elimination of the influence of random and "microclimatic" errors using known formulas. The measure of error of the random and "microclimatic" errors $\delta 2$, obtained with correction of the empirical correlation coefficients by computation, for all the interphase periods is extremely close to that obtained in Table 3.

Table 2

Normalized Structural and Covariation Functions of Duration of Interphase Periods of Corn

Градация расстояний км	Число случаев $m_f(l)$	$\tilde{\gamma}_f(l)$	$\tilde{\mu}_f(l)$	$\tilde{\gamma}_f(l)+\tilde{\mu}_f(l)$	$\tilde{\gamma}_f(l)$	$\tilde{\mu}_f(l)$	$\tilde{\gamma}_f(l)+\tilde{\mu}_f(l)$	$\tilde{\beta}_f(l)$	$\tilde{\mu}_f(l)$	$\tilde{\beta}_f(l)+\tilde{\mu}_f(l)$
1	2	Сев — всходы 3			4 Всходы — выметывание			Выметывание — молочная спелость 5		
21—40	3	0,40	0,60	1,00	0,09	0,91	1,00	0,12	0,91	1,03
41—60	18	0,52	0,51	1,03	0,15	0,87	1,02	0,25	0,76	1,01
61—80	17	0,53	0,48	1,01	0,16	0,84	1,00	0,22	0,81	1,03
81—100	16	0,51	0,51	1,02	0,18	0,83	1,01	0,29	0,72	1,01
101—120	20	0,53	0,49	1,02	0,14	0,87	1,01	0,23	0,78	1,01
121—140	17	0,54	0,48	1,02	0,12	0,89	1,01	0,29	0,72	1,01
141—160	25	0,57	0,44	1,01	0,16	0,85	1,01	0,31	0,70	1,01
161—180	21	0,59	0,43	1,02	0,19	0,82	1,01	0,39	0,63	1,02
181—200	26	0,57	0,42	0,99	0,17	0,84	1,01	0,35	0,66	1,01
201—220	24	0,60	0,42	1,02	0,19	0,81	1,00	0,39	0,63	1,02
221—240	20	0,62	0,41	1,03	0,23	0,79	1,02	0,46	0,56	1,02
241—260	18	0,60	0,44	1,04	0,20	0,81	1,01	0,47	0,57	1,04
261—280	20	0,62	0,40	1,02	0,22	0,79	1,01	0,55	0,47	1,02
281—300	9	0,69	0,32	1,01	0,27	0,74	1,01	0,52	0,50	1,02
301—320	10	0,62	0,40	1,02	0,26	0,75	1,01	0,57	0,48	1,05
321—340	13	0,71	0,30	1,01	0,26	0,76	1,02	0,62	0,40	1,02
341—360	7	0,67	0,35	1,02	0,35	0,66	1,01	0,66	0,40	1,06
361—380	7	0,89	0,12	1,01	0,32	0,70	1,02	0,61	0,42	1,03
381—400	2	1,00	0,01	1,01	0,35	0,67	1,02	0,67	0,38	1,05
401—420	4	0,83	0,18	1,01	0,44	0,57	1,01	0,83	0,27	1,10
421—440	2	1,00	0,08	1,08	0,31	0,68	1,01	0,75	0,29	1,04
441—460	1	0,93	0,14	1,07	0,88	0,12	1,00	0,99	0,12	1,11
		Молочная спелость — восковая спелость 6			Восковая спелость — полная спелость 7			Всходы — полная спелость 8		
21—40	3	0,14	0,90	1,04	0,21	0,82	1,03	0,11	0,90	1,01
41—60	18	0,18	0,84	1,02	0,36	0,64	1,00	0,15	0,86	1,01
61—80	17	0,26	0,84	1,10	0,33	0,73	1,06	0,19	0,83	1,02
81—100	16	0,22	0,84	1,06	0,42	0,69	1,11	0,21	0,80	1,01
101—120	20	0,23	0,81	1,04	0,38	0,68	1,06	0,15	0,87	1,02
121—140	17	0,26	0,79	1,05	0,39	0,67	1,06	0,14	0,88	1,02
141—160	25	0,28	0,76	1,04	0,36	0,71	1,07	0,18	0,83	1,01
161—180	21	0,30	0,76	1,06	0,51	0,55	1,06	0,22	0,80	1,02
181—200	26	0,29	0,76	1,05	0,44	0,60	1,04	0,18	0,83	1,01
201—220	24	0,35	0,79	1,14	0,46	0,64	1,10	0,23	0,79	1,02
221—240	20	0,37	0,73	1,10	0,50	0,58	1,08	0,26	0,76	1,02
241—260	18	0,41	0,70	1,11	0,48	0,59	1,07	0,21	0,80	1,01
261—280	20	0,31	0,73	1,04	0,47	0,58	1,05	0,26	0,75	1,01
281—300	9	0,41	0,67	1,08	0,53	0,52	1,05	0,30	0,72	1,02
301—320	10	0,27	0,77	1,04	0,55	0,54	1,09	0,25	0,76	1,01
321—340	13	0,36	0,71	1,07	0,56	0,51	1,07	0,31	0,71	1,02
341—360	7	0,43	0,67	1,10	0,53	0,52	1,05	0,34	0,67	1,01
361—380	7	0,43	0,69	1,12	0,58	0,48	1,06	0,41	0,71	1,12
381—400	2	0,33	0,73	1,06	0,67	0,44	1,11	0,51	0,51	1,02
401—420	4	0,59	0,64	1,23	0,80	0,33	1,13	0,42	0,58	1,00
421—440	2	0,49	0,57	1,06	0,70	0,31	1,01	0,40	0,61	1,01
441—460	1	1,19	0,34	1,53	0,78	0,35	1,13	0,75	0,75	1,00

KEY TO TABLE 2

1. Distance gradation, km
2. Number of cases
3. Sowing-sprouting
4. Sprouting-ear formation
5. Ear formation - milky ripeness
6. Milky ripeness - wax ripeness
7. Wax ripeness - total ripeness
8. Sprouting - total ripeness

Table 3

Random and "Microclimatic" Errors in Duration of Mean Interphase Corn Periods

	Сев — всходы 1	Всходы — выметывание 2	Выметывание — молочная спелость 3	Молочная спелость — восковая спелость 4	Восковая спелость — полная спелость 5	Всходы — полная спелость 6
7						
σ_0^2 по $b_f(l)$	8,5	11	0,8	0,5	0,5	10
σ_0^2 по $\tilde{m}_f(l)$	9	12	1,1	0,5	0,4	9
δ^2	0,4	0,12	0,18	0,1	0,13	0,1

KEY:

1. Sowing-sprouting
2. Sprouting-ear formation
3. Ear formation-milky ripeness
4. Milky ripeness-wax ripeness
5. Wax ripeness-total ripeness
6. Sprouting-total ripeness
7. for

Using data on the measure of random and "microclimatic" errors δ^2 and the corrected values of the correlation coefficient $r(l)$ we computed the measure of errors $S^2(l)$ in optimum interpolation using the formula

$$S^2(l) = \frac{\delta^2}{2} + 1 - \frac{2r^2\left(\frac{l}{2}\right)}{1 + r(l)}.$$

As assumed in study of the statistical structure of the field of the known element (1), in this analysis we also use the condition that optimum interpolation can be admissible when the measure of errors in optimum interpolation does not exceed half the natural variability of the mean duration of the interphase periods and is greater than the measure of random errors δ.

Table 4

Correlation Coefficient r(ℓ), Measure of Errors in Optimum Interpolation S(ℓ) and Extrapolation Errors E (Days, %) of the Duration of Interphase Periods

l км	1 Сев — всходы				2 Всходы — выметывание				3 Выметывание — молочная спелость			
	r (l)	S (l)	E, дни 4	E/D %	r (l)	S (l)	E, дни 4	E/D %	r (l)	S (l)	E, дни 4	E/D %
40	0,83	0,57	3	17	0,94	0,28	3	4	0,88	0,32	1	4
80	0,73	0,64	3	17	0,90	0,35	4	6	0,80	0,40	1	4
120	0,67	0,71	4	22	0,89	0,36	4	6	0,75	0,48	1	4
160	0,61	0,74	4	22	0,87	0,42	5	8	0,70	0,52	1	4
200	0,60	0,77	4	22	0,86	0,45	5	8	0,64	0,55	2	8
240	0,58	0,80	4	22	0,85	0,45	5	8	0,60	0,56	2	8
280	0,56	0,83	4	22	0,83	0,46	6	9	0,54	0,58	2	8
320	0,50	0,85	4	22	0,79	0,46	6	9	0,48	0,60	2	8
360	0,38	0,83	5	28	0,76	0,44	6	9	0,41	0,61	2	8
400	0,21	0,78	5	28	0,70	0,42	7	11	0,31	0,63	2	8
	5 Молочная спелость — восковая спелость				6 Восковая спелость — полная спелость							
40	0,96	0,26	1	6	0,90	0,37	1	7				
80	0,91	0,30	1	6	0,82	0,42	1	7				
120	0,89	0,36	1	6	0,78	0,51	1	7				
160	0,87	0,40	1	6	0,74	0,55	1	7				
200	0,85	0,41	1	6	0,70	0,56	1	7				
240	0,84	0,44	1	6	0,67	0,58	1	7				
280	0,80	0,44	1	6	0,64	0,61	2	14				
320	0,78	0,45	1	6	0,61	0,62	2	14				
360	0,75	0,46	1	6	0,55	0,66	2	14				
400	0,70	0,45	1	6	0,46	0,63	2	14				

KEY:

1. Sowing-sprouting
2. Sprouting-ear formation
3. Ear formation-wax ripeness
4. Days
5. Milky ripeness-wax ripeness
6. Wax ripeness-total ripeness

We also determined the mean square errors which could arise in extrapolation at different distances from the observation point using the formula

$$E = \bar{\sigma}_f \sqrt{1 - |r_f(l)|^2},$$

where $\bar{\sigma}$ is the standard deviation of the mean duration of the interphase periods, rf(ℓ) is the corrected correlation coefficient at different distances.

Table 4 gives the values of the corrected correlation coefficient r(ℓ), measure of errors in optimum interpolation S(ℓ) and in absolute (days) and relative (%) values the mean square errors E in extrapolation for the corresponding distances.

The data in Table 4 show that except for the interphase sowing-sprouting period, for all other interphase periods optimum interpolation is admissible in the case of considerable distances -- from 120 to 400 km from the observation point, and the mean square error in extrapolation even to 400 km is more than 14-15% of the values of the interphase periods.

It can be assumed in general that for the nonmountainous part of the country, to an elevation of 400 m above sea level, a good correlation is manifested between the duration of the interphase periods of corn in days (except for the sowing-sprouting period) at great distances. Here, as in [7], it must be emphasized that this correlation is manifested at great distances only under the condition that the localities for which the data of the observational point are extrapolated are situated in level and open places, similar to the site of the observation point.

The one-sided results obtained in two investigations of the statistical structure of the field of phenological phenomena can serve as a basis for developing a new structure of the network of phenological stations in the country and a new method for making observations of phenological phenomena.

BIBLIOGRAPHY

1. Alekseyev, G. A., OB"YEKTIVNYYE METODY VYRAVNIVANIYA I NORMALIZATSII KORRELYATSIONNYKH SVYAZEY (Objective Methods for Evening-Out and Normalizing Correlations), Leningrad, 1971.

2. Gandin, L. S., OB"YEKTIVNYY ANALIZ METEOROLOGICHESKIKH POLEY (Objective Analysis of Meteorological Fields), Leningrad, 1963.

3. Zakhariyev, V., "On the Statistical Structure of the Surface Temperature Field Over Bulgaria," IZV. NA IKhM (News of the Institute of Hydrology and Meteorology), Vol XII, 1968.

4. Kyuchukova, M., "On the Statistical Structure of the Dew Point Spread Field in Bulgaria," KHIDROLOGIYA I METEOROLOGIYA (Hydrology and Meteorology), No 1, 1976.

5. Slavov, N., "On a Method for Predicting the Development of Crops in Bulgaria," SELSKOSTOPANSKA NAUKA (Agricultural Science), No 3, 1974.

6. S"beva, M., "Statistical Structure of the Humidity Field in Bulgaria," KHIDROLOGIYA I METEOROLOGIYA, No 1, 1976.

7. Khershkovich, Ye., Ganeva, B., Yordanova, M., Vandova, M., Ivanov, P., "On the Statistical Structure of the Fields of Phenological Phenomena in Bulgaria," KHIDROLOGIYA I METEOROLOGIYA, No 6, 1976.

UDC 551.509.313

POSSIBILITY OF RESONANCE EXCITATION OF LARGE-SCALE WAVES

Moscow METEOROLOGIYA I GIDROLOGIYA in Russian No 6, Jun 79 pp 97-99

[Article by Doctor of Physical and Mathematical Sciences A. I. Ivanovskiy and A. A. Krivolutskiy, Central Aerological Observatory, submitted for publication 28 August 1978]

Abstract: In this article it is demonstrated that the application of the linear theory of tides makes it possible to detect the resonance properties of the atmosphere as an oscillatory system. In the presence of "centers" in the atmosphere modulating atmospheric parameters in longitude there can be excitation of traveling planetary waves — Rossby waves. Estimates made for the case of absorption of variations of the flux of solar radiation caused by solar rotation ($T \approx 27$ days) in longitude inhomogeneities of ozone in the earth's atmosphere give a value of the resonance amplitude for individual resonance modes of about 10-15 mb.

[Text] The application of the linear theory of tides makes it possible in explicit form to detect the resonance properties of the earth's atmosphere as an oscillatory system. For this purpose we will examine a system of equations in hydrodynamics and thermodynamics (on a sphere), linearized relative to the mean state of the atmosphere

$$\frac{\partial u}{\partial t} + \frac{\bar{u}}{a \sin \vartheta} \frac{\partial u}{\partial \varphi} + v \left(2\omega \cos \vartheta + \frac{1}{a} \frac{\partial u}{\partial \vartheta} + \frac{\bar{u}}{a} \operatorname{ctg} \vartheta \right) = - \frac{1}{a \rho \sin \vartheta} \frac{\partial p}{\partial \varphi} - \frac{\nu}{H^2} u,$$

$$\frac{\partial v}{\partial t} + \frac{\bar{u}}{a \sin \vartheta} \frac{\partial v}{\partial \varphi} - u \left(2\omega \cos \vartheta + \frac{\bar{u}}{a} \operatorname{ctg} \vartheta \right) = - \frac{1}{a \rho} \frac{\partial p'}{\partial \vartheta} - \frac{\nu}{H^2} v,$$

$$\frac{\sigma}{\partial x} \frac{p'}{P} = \frac{T'}{T},$$

$$\frac{dP}{dt} - \gamma \frac{kT}{m} \frac{d\rho}{dt} + (\gamma - 1) q = 0,$$

$$\frac{d\rho}{dt} + \rho \left(\chi - \frac{\partial w}{\partial x} H \right) + \rho \frac{\partial w}{\partial x} H = 0, \qquad (1)$$

where

$$\chi = \frac{1}{a \sin \vartheta} \left\{ \frac{\partial}{\partial \vartheta} (v \sin \vartheta) + \frac{\partial u}{\partial \varphi} \right\}$$

is the plane divergence of velocity; u, v, w are the wind velocity components; φ is longitude; ϑ is colatitude; H is scale height; $x = z/H$; p', T' are disturbances of pressure and temperature; ρ is density; $\gamma = c_p/c_v$; ν is the vertical coefficient of turbulent viscosity; a is the earth's radius; $\bar{u} = a\alpha(\vartheta)$ is the climatological wind profile; q is an external source.

System (1) is more general than that used in the linear theory of tides [1]. We note that the linearization of the initial equations appears justified (also like the introduction of viscosity of the "dry friction" type) in the case of examination of large-scale (background) processes.

We will seek the solution (1) in the form of traveling waves:

$$u = U(x, \vartheta) e^{i\sigma t + is\varphi},$$

$$v = V(x, \vartheta) e^{i\sigma t + is\varphi},$$

where σ is the frequency of the process, s is the longitude wave number.

Then χ after transformations assumes the form

$$\chi = \frac{1}{2\omega a^2} \hat{F} \left(\frac{p'}{l'} \right) + \frac{\partial w}{\partial x} H,$$

where

$$\hat{F} = \frac{\partial}{\partial \mu} \frac{f(1-\mu^2) gH \left(\frac{\partial}{\partial \mu} - \bar{a} \right)}{F_1 F_2} + \frac{s\mu F_2 gH \left(\frac{\partial}{\sigma \mu} - \bar{\alpha} \right) - s\mu F_1 gH - \frac{fsgH}{1-\mu^2}}{F_1 F_2 \left(\frac{f^2}{F_1 F_2} - \mu^2 \right)},$$

$$\mu = \cos \vartheta, \quad \bar{a} = -\frac{2\omega \mu a^2 a}{\sqrt{1-\mu^2} gH}, \quad f = \frac{\sigma'}{2\omega}, \quad \sigma' = \sigma + S \frac{a}{\sin \vartheta} + l \frac{\nu}{H^2},$$

$$F_1 = 1 + \frac{a}{\omega \sin \vartheta}, \quad F_2 = 1 + \frac{\frac{\partial a}{\partial \vartheta} + a \operatorname{ctg} \vartheta}{2\omega \cos \vartheta}.$$

For Blinova-Haurwitz circulation

$$a = \delta \omega \sin \vartheta, \qquad F_1 = F_2 = 1 + \delta, \quad f = \frac{1}{2\omega} \left(\sigma + s\omega\delta + l \frac{\nu}{H^2} \right).$$

The F operator coincides with the classical operator of tides, if in the latter $f = \sigma/2\omega$ is replaced by $\frac{\sigma + s\delta\omega + l\frac{\nu}{H^2}}{2\omega(1+\delta)}$, and ω is replaced by $\omega(1+\delta)$.

After transformations for a sufficiently thin layer of the atmosphere the system (1) is reduced to the equation

$$\sigma\left[\left(1-\frac{\beta A}{H}\frac{\gamma-1}{\gamma}\right)\frac{p'}{P}+\frac{\gamma-1}{\gamma}\frac{A}{H}\frac{\partial}{\partial x}\frac{p'}{P}\right]-\sigma'\left[\left(1-\frac{\beta A}{H}\right)\frac{\partial}{\partial x}\frac{p'}{P}+\frac{A}{H}\frac{\partial^2}{\partial x^2}\frac{p'}{P}\right]+ \quad (2)$$

$$+\frac{1}{2\omega a^2}\hat{F}\left(\frac{p'}{P}\right)+iQ=0,$$

where

$$A=\frac{\bar{T}}{\left(\frac{\partial\bar{T}}{\partial z}+\Gamma_a\right)} \qquad Q=(\gamma-1)\frac{A}{H}\left(\frac{\partial}{\partial x}\frac{q}{P}+\frac{\dot{q}}{P}\right), \qquad \beta=1+\frac{\partial H}{\partial z},$$

(the line at top indicates vertical averaging in some layer).

Representing the solution and source in the form of a series of eigenfunctions of the operator $\hat{F}$, after separation of the variables we obtain a residual equation in the form

$$\frac{2}{\sigma'}\left[\left(1-\beta\frac{A}{H}\frac{\gamma-1}{\gamma}\right)X_n^s+\frac{\gamma-1}{\gamma}\frac{A}{H}\frac{dX_n^s}{dx}\right]- \quad (3)$$

$$-\left[\left(1-\frac{\beta A}{H}\right)\frac{dX_n^s}{dx}+\frac{A}{H}\frac{d^2X_n^s}{dx^2}\right]-\frac{gH\lambda_n^s}{4a^2\omega^2F^2}X_n^s+\frac{iR_n^s}{\sigma'}=0,$$

where λ_n^s is the separation constant; R_n^s, X_n^s are the amplitudes of oscillations of the source and pressure of a definite wave mode.

Solving (3) with the boundary conditions for radiation at infinity (Wilkes) and $w = 0$ at the earth's surface, after transformations it can be found that at the earth's surface in the neighborhood $h_n^s \approx \gamma H$ the "fundamental" resonance [1] is

$$X_n^s=i\frac{\gamma(2-\gamma)H\omega(1+\delta)}{\sigma'\frac{\partial h_n^s}{\partial f}\left(\sigma-\sigma_p^{n,s}+i\frac{\nu}{H^2}\right)}\int_0^\infty e^{\frac{\gamma-1}{\gamma}\xi}\frac{}{P(\xi)}R_n^s(\xi)\,d\xi, \quad (4)$$

where $h_n^s=\frac{4a^2\omega^2}{g\lambda_n^s}$ is the "equivalent depth" of the atmosphere, $\sigma_{res}^{n,s}$ is the resonance frequency,

$$\sigma_p^{n,s}\approx -\delta s+\frac{2\omega s}{n(n+1)}.$$

[p = res(onance)]

In the case $\sigma\approx\sigma_{res}^{n,s}$ the X_n^s value will evidently be maximum (resonance) and limited by the value ν/H^2.

It must be noted that the representation of the source in the form of a traveling wave $\sim e^{i(\sigma t+s\varphi}$ is correct when there are longitude inhomogeneities and variations with time. Then the amplitude of the effect will be proportional to the value $A_s \cos(s\varphi)A_\omega\cos(\sigma t)$, that is, is a standing wave. It can be represented in the form of the sum of two waves traveling in opposite directions:

$$A_1 A_2 \cos(s\varphi)\cos(\sigma t) = \frac{A_1 A_2}{2}\cos(\sigma t + s\varphi) + \frac{A_1 A_2}{2}\cos(\sigma t - s\varphi).$$

But the oscillatory properties of the atmosphere are such [1] that only one of them can be resonance ($h_n^s \approx \gamma H$). Thus, on fixed "centers," modulating atmospheric parameters, there can be generation of waves traveling along a circle of latitude -- Rossby waves (in the presence of source variations with time).

For evaluating such data we will examine a thermal source -- periodic heating of the atmosphere as a result of the absorption of solar radiation, modulated by solar radiation ($T \approx 27$ days). In our opinion, this is the external source most studied at the present time [5].

As the absorbent we will examine ozone, whose total content has a longitudinal periodicity -- "ozone waves" [4].

Taking into account absorption in the Huggins and Chappuis bands (computing the R_n^s values in (4)) and taking the relative amplitudes of the fluctuations of solar radiation A_σ and the total ozone content A_{O_3}: $A_\sigma = 0.06\%$ [5], $A_s = A_{O_3} = 15\%$ [3], we find, as a result of computations, that the amplitudes of the individual (resonance) modes at resonance can be 10-15 mb.

An analysis shows that conditions for precise resonance are possible in the lower stratosphere. The oscillations arising there then, without significant attenuation, penetrate into the troposphere (tide). In this connection, the coefficient ν, participating in the evaluations, corresponds to this region of altitudes $\nu = 5 \cdot 10^4$ cm^2/sec [3].

It must be remembered that the value $\sigma - \sigma_{res}^{n,s}$, determining the closeness of the frequency of the external effect to the characteristic frequency of the atmosphere, will change slowly with time (δ has a quasi-annual period). Therefore, the source can successively excite an entire set of wave modes, whose superpositioning (solution) will give a complex picture of atmospheric response to an external effect, whose prediction is possible only on the basis of mathematical modeling.

Our computations and evaluations give basis for considering the further development of the resonance mechanism to be promising.

The principal points, mathematical model and evaluations of the resonance amplitudes have been presented in greater detail in [2].

BIBLIOGRAPHY

1. Dikiy, L. A., KOLEBANIYA ZEMNOY ATMOSFERY (Oscillations of the Earth's Atmosphere), Leningrad, Gidrometeoizdat, 1969.

2. Ivanovskiy, A. I., Krivolutskiy, A. A., "Resonance Model of Solar-Atmospheric Relationships," Deposited at the All-Union Institute of Scientific and Technical Information, No 1343-76, 1976.

3. Karol', I. L., VYSOTNYYE SAMOLETY I STRATOSFERA (High-Altitude Aircraft and the Stratosphere), Leningrad, Gidrometeoizdat, 1974.

4. Khrgian, A. Kh., FIZIKA ATMOSFERNOGO OZONA (Physics of Atmospheric Ozone), Leningrad, Gidrometeoizdat, 1973.

5. Heath, Donald F., "Space Observation of the Variability of Solar Irradiance in the Near and Far Ultraviolet," JGR, Vol 78, No 16 [year not given].

UDC 551.594.21(574.51)

UNUSUAL OCCURRENCE OF A WINTER THUNDERSTORM IN ALMA-ATA

Moscow METEOROLOGIYA I GIDROLOGIYA in Russian No 6, Jun 79 pp 100-101

[Article by Candidates of Geographical Sciences R. S. Golubov and A. A. Skakov, Kazakh Scientific Research Hydrometeorological Institute, submitted for publication 15 May 1978]

Abstract: The article describes the synoptic and thermodynamic conditions under which an intensive thunderstorm was observed for the first time during winter.

[Text] On 25 December 1977, at Alma-Ata, during the intensive falling of snow, at 0520 and 0540 hours Moscow time there were severe thunderstorm discharges accompanied by loud rolling of thunder. During the existing 60-year period of observations such a phenomenon was observed for the first time in winter in Alma-Ata. [Here we do not take into account the thunderstorm observed at Alma-Ata on 27 February 1973 because the synoptic processes of late February belong to the spring period.]

In this connection it is of unquestionable scientific interest to analyze the mentioned case.

It follows from a comparison of the weather maps that between 0300 and 0600 a cold front passed through Alma-Ata which is well expressed in temperature contrasts. This frontal separation was accompanied by an extensive zone of precipitation. In order to determine the time of passage of the front through the city more precisely we analyzed data on the temperature change at the Alma-Ata Hydrometeorological Observatory (AAHMO) (city), the airport and at three high-mountain stations situated at elevations of about 1,900, 2,300, 3,000 m and situated to the south of the AAHMO at a distance of 20-23 km. It follows from all these data that the cooling began between 0500 and 0600 hours, according to data from the Aerometeorological Center (AMC) where observations were made each 15 minutes, at 0535 hours Moscow time. Thus, the beginning of the thunderstorm almost coincided with the time of passage of the front through Alma-Ata. The front had a very steep inclination; in accordance with the time of observations at

the meteorological stations, the cooling began almost simultaneously from the ground surface to an altitude of 3,000 m (Mynzhilki station).

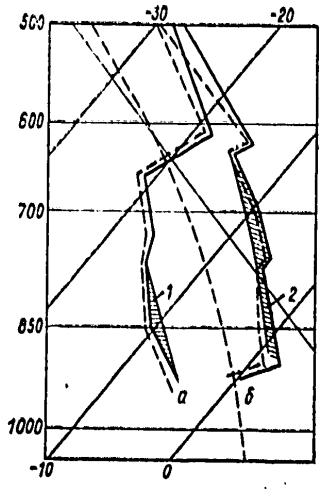

Fig. 1. Aerological diagrams. Alma-Ata, 27 December 1977. a) 0900 hours; b) 0300 hours. 1) unstable stratification; 2) stable stratification

For a still clearer demonstration of what we have said, Fig. 1 gives aerological diagrams for 0300 and 0900 Moscow time. It follows from these data that a cooling from 0300 to 0900 hours was simultaneously propagated to the 500-mb surface. It was especially significant to the 700-mb surface (approximately 10°C in 6 hours). It follows from Figure 1 that at the time of formation of a thunderstorm to the 750-mb surface (by the particle method) an unstable stratification was observed (1). According to data in the aerological diagram, at 0300 hours in the layer 615-500 mb there was convective instability

$$\left(\partial\theta'/\partial z = -1.1^{\circ}C\right).$$

The convective instability was also observed according to the aerological diagram in the layer 0-850 mb ($\partial\theta'/\partial z = -1.5^{\circ}C$). All this is confirmed by the presence of Cb at the moment of passage of the front according to data for the AAHMO meteorological station in the city. At the same time, at the airport, according to data of the AMC meteorological station, thunderstorm discharges were not observed there. The clouds were of the stratocumulus and stratonimbus types. We note that vertical sounding of the atmosphere is carried out in the neighborhood of the AAHMO (in the city).

After analyzing all that has been said, the following conclusions can be drawn:

1) thunderstorm discharges in the neighborhood of the city on 25 December 1977 occurred as a result of passage of a well-expressed cold front with a very steep slope, favoring intensive vertical movements, intensified by

mountain ranges, as a result of which an unstable state of the atmosphere developed;
2) in order to predict this phenomenon in the cold season of the year it is possible to employ only those methods which are capable of predicting the stratification curve reliably at the time of passage of a front;
3) the thunderstorm developed with very low specific humidity values at the ground level (about 3.0-3.5 g/kg).

UDC 551.508.95:535.343.4

SPECTROSCOPIC METHOD FOR DETERMINING ATMOSPHERIC CO_2 CONTENT

Moscow METEOROLOGIYA I GIDROLOGIYA in Russian No 6, Jun 79 pp 102-105

[Article by R. M. Akimenko, Candidates of Physical and Mathematical Sciences V. A. Aref'yev and N. Ye. Kamenogradskiy, N. I. Sizov and V. P. Ustinov, Institute of Experimental Meteorology, submitted for publication 5 September 1978]

Abstract: This paper gives the results of laboratory experiments for determining the dependence of the Q value (spectral characteristic of transmission of radiation in the absorption band 2.06μm CO_2) on the CO_2 concentration. There was found to be a substantial difference between the derived experimental dependence from the computed dependence used for determining the atmospheric CO_2 content. A method is proposed for introducing a correction for the computed dependence on the basis of experimental data.

[Text] Modern data on the background concentration of carbon dioxide and its variations in the atmosphere have been obtained as a result of systematic measurements by the sampling method and by analysis of air samples with the use of optical-acoustic nondispersion IR gas analyzers [7]. The taking of air samples is accomplished at specially selected points with unique geophysical conditions [6]. The choice of sites with geophysical conditions suitable for background measurements of CO_2 content is extremely limited. At the same time, the sampling method makes it possible to measure the CO_2 concentration only locally and it is impossible to exclude an influence on its value from weak local natural and anthropogenic CO_2 sources.

The limitations associated with the choice of a measurement site and the influence of weak CO_2 sources are excluded by measuring the total CO_2 content in a vertical column of the atmosphere by the spectroscopic method.

This method is used extensively for measuring the gas components of the atmosphere, especially those whose concentration varies greatly with time [5].

The principle of the spectroscopic method is the registry, using a spectrometer, of the absorption spectrum of the investigated gas during the passage of solar radiation through the entire thickness of the atmosphere and then the computation of its concentration on the basis of this absorption. Therefore, the principal requirement on the point for measuring the gas content in the atmosphere by the spectroscopic method is an adequate number of sunny days.

A variant of the spectroscopic method, suitable for measuring the mean vertical concentration of CO_2, a gas component of the atmosphere with a concentration slightly varying with time, was proposed in [3]. The following parameter is used as a characteristic depending on the CO_2 concentration in a column of the atmosphere

$$Q = \frac{T_1 + T_3}{2T_2}, \tag{1}$$

where T_2 is mean transmission in the absorption band of CO_2 with its center at 2.06μm; T_1, T_3 are the mean transmissions in specially selected spectral intervals in the wings of this band.

Since the CO_2 absorption band at 206μm under atmospheric conditions overlaps with the absorption lines of water vapor, the width of each of these three intervals was selected in such a way that the influence of water vapor on the Q value is minimum. The dependence of Q on the CO_2 concentration is computed by direct computations on an electronic computer using the parameters of spectral lines in the band 2.06μm and real vertical temperature and pressure profiles published in the literature. The carbon dioxide is assumed to be uniformly mixed in the atmosphere, which when computing the mean transmissions T_i (i = 1, 2, 3) in (1) is broken down vertically into n temperature- and pressure-homogeneous layers with an approximately equal air mass w_n. In this case

$$T_i = \frac{\delta\nu}{\Delta_i} \sum_l \left\{ \prod_n \exp\left[-Cmw_n \sum_j k_n(\nu_l, \nu_j) \right] \right\}, \tag{2}$$

where ν_j is the frequency of the center of the j-th CO_2 line; $k_n(\nu_l, \nu_j)$ is the absorption coefficient at the frequency ν_l, determined by the Lorentz line contour j in the n-th layer of the atmosphere, ν_l is the frequency at which monochromatic transmission is computed, $\delta\nu = \nu_l - \nu_{l-1}$ is the frequency interval with which the monochromatic transmission is computed; Δ_i is the width of the i-th spectral interval; C is the CO_2 (in millionths by volume); m is atmospheric mass.

The value of the mean vertical concentration of carbon dioxide C is then determined from a comparison of the Q_{meas} value, obtained in the measurement, with the calibration dependence Q_{comp} on the product C_m computed from (1) and (2).

The application of this method under field conditions [4] led to reduced (understated) CO_2 contents in the atmosphere in comparison with known data from local measurements in air samples, which can be caused by errors in the employed initial spectroscopic information and the peculiarities of the selected computation procedure.

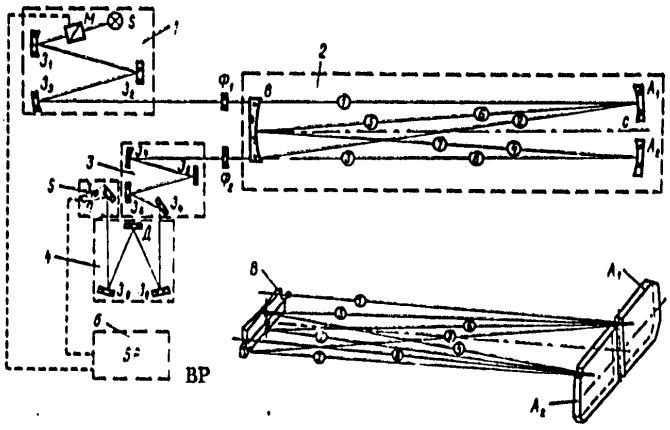

Fig. 1. Optical diagram of laboratory apparatus (S -- radiation source; $З_1$ - $З_7$, $З_{10}$ -- matching mirrors; $Ф_1$, $Ф_2$ — filter windows in cell; A_1, A_2, B -- cell mirrors; $З_9$ — monochromator mirrors; D -- diffraction grating; П -- radiation detector; BP -- registry system, including amplifier with synchronous detector, M is a modulator of radiation and generator of reference voltages for a synchronous detector. The figures 1-8 in the small circles illustrate the successive path of the radiation with eightfold passage.

In this study the dependence of the Q value on the concentration of carbon dioxide was found experimentally. For this purpose under laboratory conditions with a controllable change in the CO_2 concentration we measured the mean transmissions in the discriminated spectral intervals of the 2.06μm band and obtained the Q_{ex} values. [experimental = ex or expl]

An optical diagram of the laboratory apparatus used in the experiments is shown in Fig. 1. The principal elements of this apparatus are an optical multipass cell [1], assembled in a White scheme, and a spectrometer with an average resolution entering into the field spectral complex [2] for measuring the CO_2 content in the atmosphere. As the source of the continuous spectrum we used a KGM-6, 6-200 incandescent lamp with a system of mirrors 1, matching the source with the cell 2. Three equifocus mirrors in the cell,

situated at the double focal length 50 m, make it possible to vary the optical length of the path from 0.2 to 2.0 km. The aperture angles of the cell and monochromator 4 are matched with a system of mirrors 3. The monochromator 4 with a diffraction grating with 300 lines/mm, the radiation detector 5 with a PbS photoresistor and the recording unit 6 constitute a spectrometer with an average resolution. The optical multipass cell is supplied with a vacuum system and is filled with the gases to be investigated.

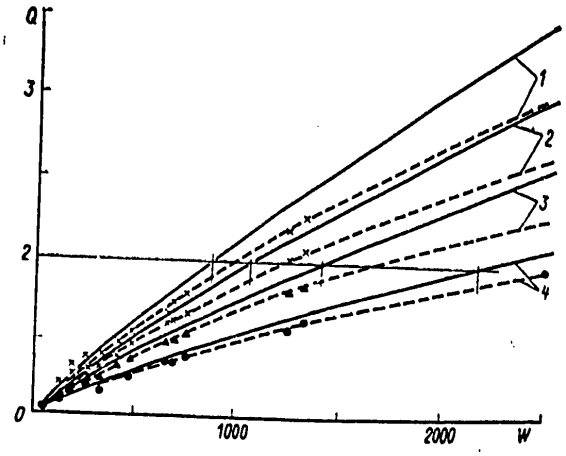

Fig. 2. Dependence of Q value on content of carbon dioxide. 1) P = 1 atm; 2) P = 0.8 atm; 3) P = 0.6 atm; 4) P = 0.4 atm

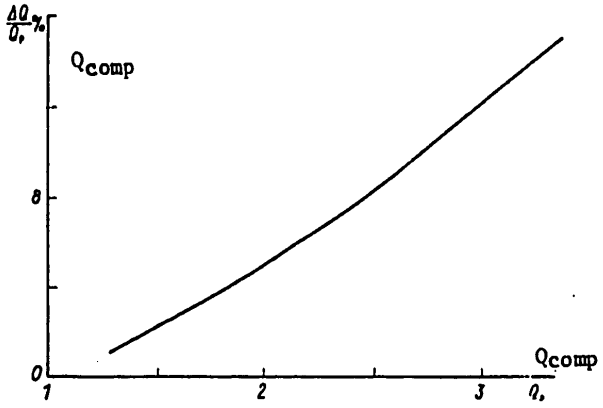

Fig. 3. Dependence $\Delta Q/Q_{comp}$ on Q_{comp}.

The experiments were carried out in the following way. The predried carbon dioxide was fed into a cell in which the residual pressure was 10^{-4} mm Hg. Then dried nitrogen was fed into the cell. The CO_2 concentration was determined from the pressure, measured with an error of ~0.01 mm Hg. The experiments were carried out at a constant temperature of 293°K. The transmission spectrum of CO_2 in the band 2.06μm was measured with P_{CO_2}~0.25, 0.75, 1.04, 1.96, 2.66, 5.54 and 10.20 mm Hg. For each P_{CO_2} value the nitrogen pressure was P = 0.4, 0.6, 0.8 and 1.0 atm successively with lengths of the optical path 0.2, 0.6, 1.0 and 2.0 km. We registered a total of about 600 transmission spectra in the selected CO_2 band 2.06μm with a resolution 3.5 cm^{-1}. The error in determining the Q_{expl} value from these spectra from a unit measurement did not exceed 1.5%. Each of the Q_{expl} values cited thereafter was obtained as the mean of 4-5 spectrograms, registered under one and the same conditions.

In Fig. 2, for one and the same conditions, we compared the experimental (dashed curves) and computed (solid curves) dependences of the Q value on the CO_2 content (w in centimeters at normal pressure). It can be seen that for all the values of broadening pressure and any CO_2 contents Q_{expl} (experimental) is less than Q_{comp} (computed). Since the Q_{comp} values in a homogeneous layer are exaggerated at any general pressure, under field conditions, where when computing Q_{comp} the atmosphere is broken down into n homogeneous layers with different pressures, the measured CO2 concentrations are understated. Therefore, in applying the method in the atmosphere the computed calibration dependences must be refined on the basis of the results of laboratory experiments.

An analysis of the data in Fig. 2 shows that with an error not greater than 1% the value $\Delta Q = Q_{comp} - Q_{expl}$ for a particular Q_{comp} for all values of the broadening pressure can be considered constant. (As an example the noted fact is explained in Fig. 2 for Q = 2). This means that within the limits of the indicated accuracy the ΔQ value is determined only by the Q value, independently of which change in the two physical parameters (quantity of absorbent or broadening pressure) governed this Q value. Accordingly, the dependence $\Delta Q/Q_{comp}$ on Q_{comp}, experimentally found and cited in Fig. 3, can be used for correcting the computed calibration curves under conditions of an inhomogeneous atmosphere. Naturally, the shape of the curve in Fig. 3 is dependent on the procedure of computation of the calibration dependences.

Examples of application of the results of laboratory experiments, especially the curve in Fig. 3, when measuring the CO_2 content in the atmosphere, are given in Table 1, which gives the mean daily values of the mean vertical CO_2 concentration in the atmosphere on the basis of measurements in the summer of 1977 in the Sary-Chelek reservation in the Tien Shan. The first column gives the measurement days. The second column gives the CO_2 concentrations (C_1) obtained with the use only of the computed calibration curve. The third column gives the CO_2 concentrations (C_2) obtained taking into account the correction of the computation curve using data from laboratory experiments.

Table 1

Mean Daily Values of Mean Vertical Concentration of CO_2 in the Atmosphere (ppm)

1 Дата измерения	C_1	C_2
22 июля	280,8	325,1
25 2	274,9	327,7
27	281,2	316,0
30	268,2	322,3
31 3	277,9	332,7
2 августа	269,5	314,3
3	267,3	318,3
7	264,7	322,7
9	291,0	329,3
11	283,7	327,4
13	265,1	323,6
16	264,2	319,8

KEY:
1. Measurement date
2. July
3. August

The data in Table 1 show that the use of the computed calibration dependence with correction on the basis of data from laboratory experiments considerably increases the determined mean vertical CO_2 concentration, bringing it close to 330 ppm -- the typical mean annual volume concentration of CO_2 in the atmosphere, obtained at the present time in local measurements in air samples.

In conclusion we note that the dependence $\Delta Q/Q_{comp}$ on Q_{comp}, used for correcting data from field measurements, can be somewhat refined thereafter by means of taking the influence of humidity and temperature into account.

BIBLIOGRAPHY

1. Aref'yev, V. N., Volkovitskiy, O. A., Goncharov, N. V., Dianov-Klokov, V. I., "Optical Multipass Cell for Investigating Absorption by Artificial Atmospheres," PRIBORY I TEKHNIKA EKSPERIMENTA (Experimental Instruments and Techniques), No 1, 1974.

2. Aref'yev, V. N., Dianov-Klokov, V. I., Malkov, I. P., "Field Spectral Complex for Investigating Atmospheric Content of Contaminating Gases," TRUDY IEM (Transactions of the Institute of Experimental Meteorology), No 8(81), 1978.

3. Brounshteyn, A. M., Paramonova, N. N., Frolov, A. D., Shashkov, A. A., "Optical Method for Determining the Total Content of CO_2 in a Vertical Column of the Atmosphere," TRUDY GGO (Transactions of the Main Geophysical Observatory), No 369, 1976.

4. Brounshteyn, A. M., Faber, Ye. V., Frolov, A. D., Shashkov, A. A., "Experiment in Realizing the Integral Spectroscopic Method for Determining Atmospheric CO_2 Content," TRUDY GGO, No 418, 1978.

5. Kiseleva, M. S., "Modern Data on the Content of Absorbing Gas Components in the Troposphere and Stratosphere," TRUDY IEM, No 8(81), 1978.

6. GEOPHYSICAL MONITORING FOR CLIMATIC CHANGE No 1 (SUMMARY REPORT-1972), edited by J. M. Miller, Environmental Research Laboratories, Boulder, Colo., 1974.

7. Keeling, C. D., Bacastrow, R. W., Bainbridge, A. E., Ekdahl, C. A., Guenther, P. R., Waterman, L. S., Chin, J. F. S., "Atmospheric Carbon Dioxide Variations at Mauna Loa Observatory, Hawaii," TELLUS, Vol 28, No 6, 1976.

UDC 551.515.1

ATMOSPHERIC INSTABILITY

Moscow METEOROLOGIYA I GIDROLOGIYA in Russian No 6, Jun 79 pp 106-112

[Article by Candidate of Physical and Mathematical Sciences N. P. Shakina, USSR Hydrometeorological Scientific Research Center, submitted for publication 3 July 1978]

Abstract: The article gives a classification of the principal types of atmospheric instability in dependence on the forces determining the behavior of disturbances. The author describes the energy sources, conditions for the initial growth of disturbances and the development of nonlinear regimes of stationary waves, vacillations and irregular (turbulent) flow both in the case of static instability (cellular convection) and in the case of hydrodynamic instability. In the latter case the article gives the principal patterns of development of Kelvin-Helmholtz instability, barotropic, baroclinic (including "symmetric" and "geostrophic") and barotropic-baroclinic instability.

[Text] The diversity of manifestations of instability of atmospheric currents and its fundamental importance as a mechanism for the restructuring of the fields of movements and exchange of energy between movements of different scales gives rise to an undiminishing interest of theoreticians and experimenters in the problem of a loss of stability and an enormous number of publications in the scientific literature devoted to different aspects of this problem. We will give only a brief description of the principal types of instability observed in the atmosphere and we will note the most important results obtained by means of a theoretical investigation, numerical modeling or by means of laboratory experiments.

The state of the system is considered unstable if it can substantially change as a result of small effects. In other words, the disturbances introduced in one way or another, whose energy is initially small, in an unstable system

can increase, for this purpose drawing energy from the reserves present within the system. As a result, the energy is redistributed (frequently in this case it passes from one form to another), and a new state is established. The products of instability of different classes of atmospheric movements are cyclones and anticyclones, convective clouds and so-called clear-sky turbulence. At the same time we can mention processes of qualitative transformations of atmospheric fields not associated with the resolution of instability, for example, the appearance of horizontal temperature differences in some layer under the influence of solar heating and transition of this layer to a new, baroclinic state; evidently, there is no manifestation of instability, since this transition occurs under the influence of an influx of considerable energy to the system, and not as a result of the redistribution of energy within the system through the mechanism of an increase in magnitude of initially small disturbances.

The processes of loss of stability and the initial stages of growth of unstable disturbances are usually studied by linear analysis with the following basic assumptions: 1) the disturbances are extremely small ("infinitely small") in amplitude ("infinitesimal"), and all their interactions with one another, and also their influence on the initial main current are negligible; only the effect of the main flow on the disturbances is of importance; 2) the disturbances are represented in the form of a set of harmonic components, and since the interactions are negligible, it is possible to replace an analysis of the behavior of a disturbance of an arbitrary form by an analysis of the behavior of all its wave components, called "elementary waves" or also "normal modes" of disturbances.

If it is found that some of the elementary waves can increase in this main flow, then the most rapidly growing wave is evidently of the greatest interest: it will dominate in the process of development of the disturbances. Accordingly, a linear analysis of stability includes the discrimination of that class of conditions when there can be an increase in disturbances, the finding of the indices of growth of unstable waves and the characteristics of the most unstable wave.

Real disturbances have finite, not "infinitely small" amplitudes; nevertheless, a linear approximation is physically extremely informative. It can be asserted that if this state is unstable according to linear theory, it is also unstable relative to finite changes of the main flow (see [3]). At the same time, it is impossible to consider linear analysis in all cases to be adequate: states stable according to the linear theory can be unstable relative to finite disturbances [25].

When it is impossible to neglect all the interaction effects, in some interval of amplitudes the disturbance can be considered "small, but finite." This concept means physically that the energy of the disturbances remains small in comparison with the energy of the main flow and nonlinear effects only to a small degree distort the form of the wave. The curve of temporal

change in the amplitude of small but finite disturbances differs greatly from the exponential curve given by linear theory: the increase may be slowed, with a tendency to emergence in a regular regime (the case of "soft excitation") or still more rapid ("hard excitation"). When the energy of the disturbances is not small in comparison with the energy of the main flow a theoretical examination is difficult and the main means of investigation are a laboratory experiment, and to a lesser degree -- numerical modeling. There are three principal highly nonlinear regimes [15]: two regular -- a regime of stationary waves and a regime of "vacillations" -- and an irregular (turbulent) regime of unordered mixing (Fig. 1). "Vacillations" or oscillations mean a periodic change in the wave characteristics (amplitudes, forms or even wave number). The choice of the regime is determined by the parameters of the main flow.

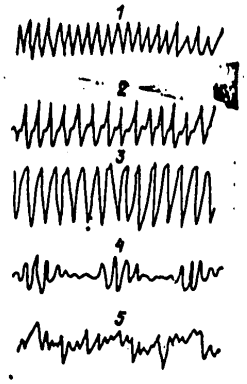

Fig. 1. Characteristic records of fluctuations of temperature at fixed point within a fluid in a rotating annular channel [15] for different types of well-developed nonlinear regimes. 1-3) stationary waves; 4) vacillations of amplitude; 5) irregular flow

Depending on which of the forces acting in the atmosphere determine the behavior of the disturbances, different types of instability can be distinguished. We will characterize them, adhering to Table 1; the greatest attention will be devoted to hydrodynamic instability.

Static or convective instability in pure form, that is, outside the influence of the deflecting force of the earth's rotation and in the absence of the mean wind, in a viscous medium leads to an increase in spatial-periodic movements, drawing energy from the potential energy of the main flow. The equation for the linear problem of ordered (cellular) convection includes the Rayleigh number Ra, which is also the stability parameter. Beginning with the work of Rayleigh (see [19]), in which it was found that in a layer at rest the two- and three-dimensional modes have identical indices

of growth and an identical critical Ca. The efforts of numerous researchers have been directed to the study of cellular convection in the presence of different modifying factors. In the presence of a mean wind with a vertical shear, and also in the field of Coriolis force, the most unstable disturbances are those in the form of "walls," elongated along the wind or along the wind shear [2, 6, 19]. In both the laboratory and under atmospheric conditions one can observe all three nonlinear regimes, developing after the stage of a rapid initial growth of disturbances; in dependence on the current parameters and on the Ra they can also be obtained by the numerical modeling of convective activity in an unstable layer with upper and lower rigid or free boundaries [2, 6, 18, 22].

If there is a stably stratified layer over a statically unstable layer, convective movements can penetrate from the lower into the upper layer. Then, under the influence of penetrating movements of the stationary cell type the following vertical temperature profile is formed: an unstable layer near the earth, then a mixed layer, having the greatest thickness, with a stratification close to neutral, and finally, the upper layer of the inversion [24]. These results are an example of strong nonlinear interaction in a regular regime.

We will mention still another recently forming direction, considering the spiral cloud bands in tropical cyclones and in so-called thermal cyclones of the middle latitudes to be the result of instability of flow in a circular eddy with a superadiabatic stratification [1, 10]. The banded structures obtained in numerical models and having some characteristics of atmospheric fronts no longer represent primarily convective movements, since they also exist when there is a neutral or a slightly stable stratification [41] as a manifestation of barotropic instability.

Hydrodynamic instability, whose cause is the peculiarities of distribution of the velocity of the main flow, outside the additional influences of Coriolis force and buoyancy force, is observed in laboratory apparatus with a thermally homogeneous fluid; in the atmosphere close conditions are possible in the boundary layers for small-scale movements. The energy source for growing disturbances in a hydrodynamically unstable medium is the kinetic energy of the main flow; if it is distributed in such a way that the vorticity changes monotonically across the flow, then the latter is stable (Rayleigh theorem [3]). If the flow is stably stratified ($\gamma<\gamma_a$), the buoyancy force in it is a stabilizing factor; however, a nonuniform velocity distribution can cause an increase of disturbances and the latter, drawing energy from the kinetic energy of the main flow, will expend part of its work against the buoyancy force. A parameter of this type of instability -- Kelvin-Helmholtz instability -- is the Richardson number Ri, measuring the ratio of the buoyancy force to the inertial force. During the last 15-20 years this type of instability has been intensively studied. It has been established that with $Ri < 1/4$ there is instability in a linear approximation for an interval of wavelengths dependent on Ri and the forms of the wind and temperature profiles in the main flow [4, 26]. In the approximation of small but finite amplitudes the numerical solutions indicate the

possibility of stability loss with Ri values greater than 1/4 and dependent on the amplitude of the disturbance [25], and in addition, the possibility of development of both regular and turbulent regimes [4]; laboratory experiments [39] and observations in the atmosphere show that Kelvin-Helmholtz instability virtually always leads to the appearance of turbulence.

Instability of this type is the principal mechanism of the appearance of turbulent layers or moving spots in the free atmosphere; it regulates the sharpness of fronts and the degree of wind shears by the inclusion of turbulent exchange [8].

Barotropic instability, that is, a type of instability in the field of Coriolis force when the energy source of the disturbances is the kinetic energy of the main flow, is examined most conveniently when in the main flow there are no reserves of available potential energy (the potential air temperature does not change vertically or horizontally). In the simplest form barotropic instability is considered as the instability of zonal flow in which velocity is dependent on latitude.

The barotropic stability criterion is given by the [illegible] theorem [3]: if the potential eddy is monotonically dependent on latitude, the flow is stable. In general, the westerly zonal flow in the middle and high latitudes is barotropically stable, that is, the mean annual, seasonal and mean monthly fields of the zonal wind are stable [33]. However, in specific situations or over individual parts of the hemisphere conditions of barotropic instability can arise [23].

Barotropic instability in the tropics, where there is easterly transfer in the troposphere, is studied in connection with disturbances in the Trade Wind zone; in some cases these develop into typhoons. The averaged easterly flow in the tropics is only slightly unstable [32], but in specific cases the instability can be strong; the properties of unstable waves in the easterly flow have a number of differences from the case of westerly transfer.

In the case of baroclinic instability the disturbances draw energy from the available potential energy of the main flow, on which the Coriolis force acts; the reserve of available potential energy of the main flow is determined by its horizontal thermal inhomogeneity. This type of instability has another, less commonly used name -- "sloping convection" [15]; it indicates the physical content of processes transpiring during the resolution of baroclinic instability. The Coriolis force is an obstacle to the development of simple "overturning" movements in the meridional plane which would indirectly even out the meridional temperature differences and causes a special form of movements primarily in the horizontal plane.

Symmetric instability, or "axially symmetric instability," received its name because in laboratory experiments with rotating annular vessels it leads to the development of movements symmetric relative to the axis of rotation.

Table 1

Principal Types of Instability of Atmospheric Movements (γ -- Vertical Temperature Gradient in Main Flow, γ_a -- Dry-Adiabatic Gradient, u -- Velocity of the Main Flow; the x, y Axes are Horizontal, z -- Vertical)

1 Статическая неустойчивость $\gamma_a - \gamma < 0$	2 II. Гидродинамическая неустойчивость $u = u(x, y, z)$				
	3 вращение Земли пренебрежимо		4 вращение Земли существенно		
	собственно 5 гидродинамическая неустойчивость $\gamma_a - \gamma = 0$ $u = u(z)$	6 неустойчивость Кельвина—Гельмгольца $\gamma_a - \gamma > 0$ $u = u(z)$	7 баротропная неустойчивость $u = u(x, y)$	бароклинная неустойчивость («наклонная конвекция») $u = u(z)$ 8	9 баротропно-бароклинная неустойчивость $u = u(x, y, z)$
—				10 симметричная неустойчивость	асимметричная («геострофическая») неустойчивость 11

KEY:

1. Statistical instability
2. Hydrodynamic instability
3. Earth's rotation negligible
4. Earth's rotation significant
5. Strictly hydrodynamic instability
6. Kelvin-Helmholtz instability
7. Barotropic instability
8. Baroclinic instability ("sloping convection")
9. Barotropic-baroclinic instability
10. Symmetric instability
11. Asymmetric ("geostrophic") instability

For example, assume that the outer wall of the annular channel is warmer than the inner wall. In the absence of rotation in the channel ordinary convection will develop (of the breeze circulation type) with a circulation ring in the vertical plane. But in a rotating channel the vertical movements are suppressed; the vertical velocities of the particles are small in comparison with the horizontal velocities and the meridional velocities are small in comparison with the zonal velocities, so that the wind approaches geostropic. Therefore, symmetric disturbances as a heat transfer mechanism are ineffective; they almost do not decrease the available potential energy of the system. Because of this circumstance symmetric instability is frequently characterized as "barotropic" instability in a baroclinic system [37]. An example of symmetric movements on a planetary scale is Hadley circulation, which, as is well known, is discovered in the earth's atmosphere only in climatic mean fields of motion. On some other planets (for example on Jupiter) the symmetric circulations are dominant.

The theoretical problem of the conditions for the predominance of symmetric or asymmetric instability was examined in [37] in the example of the well-known Eady model [11]: the main zonal flow has a linear vertical profile and falls between two horizontal walls. In such a formulation the only parameter of the problem is the Ri number; the Rossby number does not enter explicitly into the equation of the problem and is actually fixed. According to [37], asymmetric baroclinic instability dominates when $Ri > 0.95$, symmetric instability dominates when $1/4 < Ri < 0.95$, and Kelvin-Helmholtz instability dominates when $Ri < 1/4$. The effects of nonhydrostaticity, the earth's sphericity, viscous and nonadiabatic effects were later included [16, 38]. Experimental data (Fig. 2) indicate that with an increase in the velocity of rotation, when the Coriolis force more and more suppresses vertical movements, the symmetric regimes lose stability and are destroyed, being replaced by baroclinic waves.

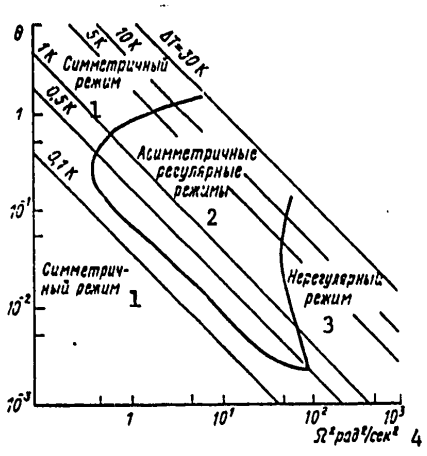

Fig. 2. Regime diagram showing dependence of predominant mode of baroclinically unstable disturbances and types of nonlinear regimes [15] on the square of angular velocity Ω of rotation of annular channel and on the parameter

$$\theta = g\alpha d\,|\rho(T_a) - \rho(T_b)| \Big/ \frac{1}{2}\,|\rho(T_a + T_b)|\,\Omega^2 (b-a)^2,$$

where g is the acceleration of free falling, d is the depth of the fluid, a, b are the internal and external radii of the ring, $\rho = \rho(T)$ is fluid density.

KEY:

1. Symmetric regime
2. Asymmetric regular regimes
3. Irregular regime
4. rad^2/sec^2

In the earth's atmosphere the conditions for symmetric instability are created with inadequately large Ro; this type of instability has been studied recently in connection with mesoscale processes in zones of atmospheric fronts [7, 13, 29]; Langmuir circulations in the ocean are related to it [13]. A linear examination shows that symmetric instability ensures the initial rates of growth of disturbances adequate for the appearance of bands of clouds and precipitation in frontal zones; only the first results have been obtained along the lines of numerical modeling of nonlinear regimes. It was found [7] that the mechanism of symmetric instability of moist-saturated air, in which ascent occurs in accordance with the moist adiabatic law and subsidence occurs in accordance with the dry adiabatic law, is capable in a steady nonlinear regime of forming bands of adequately intensive ascending movements; in a "dry" model [29] the development of symmetric instability is inhibited by nonlinear effects and the resultant stationary circulations remain weak.

Asymmetric or "geostrophic" instability ("instability of baroclinic waves") develops at small Rossby numbers; in this case mixing occurs by waves in the horizontal plane and eddies with vertical axes.

In addition to the widely known study by Eady cited above [11], in which the Coriolis force was considered constant, the linear problem of baroclinic instability was initially investigated by Charny [9] in a β-approximation (the instability criterion was obtained and the shape of the neutral curve was indicated approximately). Then H. L. Kuo [20], in essence in this same formulation, investigated the dependence of the indices of growth and phase velocities of unstable waves on the parameters of the problem and studied the structure of the most unstable wave (with a length of about 3,500 km). Green [14], in addition to the relatively short and growing waves (doubling time of the order of a day) discovered by Charny and Kuo, discovered instability of longer, slowly growing waves. The principal result of the linear examination, which in addition to the mentioned studies, was and is being made by numerous authors in different variants of formulation of the problem (among the recent studies, see [27]), is that almost any main state characteristic for the atmosphere is unstable in a broad range of wavelengths; unstable waves transport heat to the north and transport momentum downward and reveal a number of properties characteristic for atmospheric eddies.

Effects of a finite amplitude in the case of baroclinic instability are being studied by means of numerical modeling and laboratory experiments; recently, in addition, there has been an increase in the importance of studies in which the energy budget of atmospheric movements is computed on the basis of observational data. All three types of well-developed nonlinear regimes have been discovered in baroclinic waves with different parameters of the main flow [15, 35]. Nonlinear exchange leads to the transport of properties (heat, momentum) against the gradients, as a result of which frontal zones and jet streams are formed in baroclinic waves [28, 40]. Nonlinear effects slow or accelerate the growth of unstable waves (as a result, the dimensions of the disturbances dominating in nonlinear regimes can differ from

the most unstable wave according to linear theory [36]) and cause the transfer of energy in the spectrum of atmospheric baroclinic waves -- from some intermediate scale (at which the energy passes from the mean flow to the disturbances) to larger and lesser scales [40]. The role of nonlinear effects is especially great under conditions of regular regimes [15]. This result is interesting from the point of view of the problem of predictability of atmospheric movements, since in its consideration it is usually assumed that with an increase in nonlinearity there is also an increase in irregularity, approaching the turbulence stage.

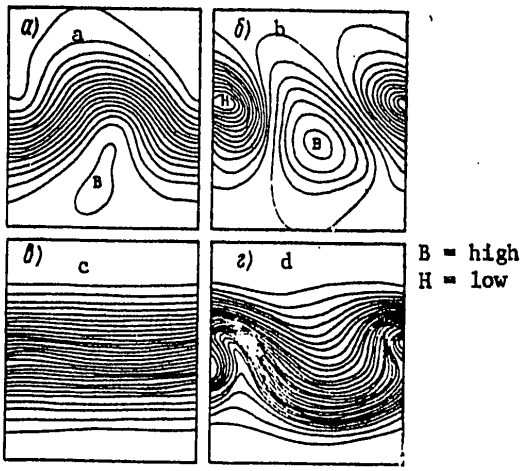

Fig. 3. Results of numerical modeling of growth of baroclinically unstable wave (time of doubling of amplitude 32 hours) in zonal barotropically stable jetlike flow [28]. a, b) field of surface pressure; c, d) buoyancy field $\vartheta'/\overline{\vartheta}$, where ϑ' is the temperature deviation; a, c -- initial field, t = 0; b, d -- solution of total equations at time t = 96 hours.

Regular regimes (stationary waves and vacillations) to a high degree are characteristic for the largest (planetary) scales of atmospheric movements; an irregular regime ("geostrophic turbulence") is more characteristic of movements of a synoptic scale: the elements of "geostrophic turbulence" are middle-latitude cyclones and anticyclones. Their initial growth occurs at the expense of the available potential energy of the main flow, whereas the further development is determined, in addition, by nonlinear interactions [21, 40].

Modern numerical solutions of the problems of nonlinear development of baroclinic waves differ with respect to the complexity of formulation of the problem, taking into account nongeostrophicity [28], release of the heat of condensation [12], horizontal and vertical inhomogeneity [28, 33]. However, the life cycle of cyclones and anticyclones can be traced only

in the stages of growth and deepening, up to the preceding occlusion of the deformation of the warm sector of the cyclone [17, 28]. Recently it has been possible to describe numerically some regular nonlinear regimes [30, 34]

Baroclinic-barotropic instability, that is, the instability of currents with horizontal velocity and temperature gradients, is a more general case in comparison with the two considered above. Specifically this "combined" instability is most characteristic for movements of synoptic scales in the middle latitudes; this is confirmed as well by budget computations [21, 40] and the conclusions of numerical modeling, in particular, the fact that some important characteristics of the structure of atmospheric eddies (for example, fronts in cyclones) can be reproduced only when taking into account both vertical and horizontal inhomogeneity of the wind field (Fig. 3). High-altitude frontal zones in the atmosphere, whose manifestation of instability is large-scale cyclogenesis, and also fronts of the lower half of the troposphere, on which frontal cyclones develop, are precisely characterized simultaneously by a high baroclinicity and great horizontal wind gradients, and with the development of instability in these regions of the atmosphere there is a complex interaction between the baroclinic and barotropic mechanisms of energy transfer. The results of studies of numerical modeling of baroclinic-barotropic instability, in particular those studies in which atmospheric fronts are interpreted as discontinuities, were presented in the review [5]; among the recent publications not included in [5] we note [31].

The cited classification of types of instability makes no pretense at completeness, nor does the presented brief analysis of the status of investigations in individual directions; however, the considered types of instability are nevertheless fundamental for a broad class of atmospheric movements. All the most important atmospheric processes, constituting the subject of dynamic and synoptic meteorology -- cyclogenesis, frontogenesis, life cycle of pressure formations of planetary and synoptic scales, processes of cloud and precipitation formation, genesis and development of jet streams -- are in one way or another related to instability (that is, either directly to the growth of unstable disturbances, or to the processes of their interaction with the environment and one another). The problems in instability of atmospheric processes are now central in meteorology and are attracting the greatest attention. Although there are still many unsolved or inadequately studied problems, the achievements from instability theory during the last 10-20 years undoubtedly are extremely significant and a whole series of results is of fundamental importance both for understanding the mechanisms of atmospheric processes and for the ideology and method of further investigations.

The author expresses appreciation to Ye. M. Dobryshman for useful discussion.

BIBLIOGRAPHY

1. Bugayeva, G. V., Vel'tishev, N. F., "Results of Numerical Modeling of Convective Cloud Eddies," TRUDY GosNITsIPR (Transactions of the State Scientific Research Center for the Study of Natural Resources), No 1, 1976.

2. Vel'tishchev, N. F., Zhelnin, A. A., "Convective Movements in an Air Flow Changing Direction With Altitude," METEOROLOGIYA I GIDROLOGIYA (Meteorology and Hydrology), No 4, 1976.

3. Dikiy, L. A., GIDRODINAMICHESKAYA USTOYCHIVOST' I DINAMIKA ATMOSFERY (Hydrodynamic Stability and Atmospheric Dynamics), Leningrad, Gidrometeoizdat, 1976.

4. Kogan, Z. N., Shakina, N. P., "Waves of Finite Amplitude in a Stratified Jet Stream and Clear Sky Turbulence," IZV. AN SSSR, FIZIKA ATMOSFERY I OKEANA (News of the USSR Academy of Sciences, Physics of the Atmosphere and Ocean), 10, No 4, 1974.

5. Shakina, N. P., "Theoretical Investigation of Atmospheric Fronts and Middle-Latitude Cyclones," METEOROLOGIYA I GIDROLOGIYA, No 7, 1978.

6. Asai, T., Nakasuji, I., "On the Preferred Mode of Cumulus Convection in a Conditionally Unstable Atmosphere," J. METEOROL. SOC. JAPAN, Vol 55, No 2, 1977.

7. Bennets, D. A., Hoskins, B. J., "A Possible Explanation for Rainbands," INT. CONF. OF CLOUD PHYSICS, Boulder, Colo., July 26-30, 1976.

8. Browning, K. A., Harrold, T. W., Starr, J. K., "Richardson Number Limited Shear Zones in the Free Atmosphere," QUART. J. ROY. METEOROL. SOC., Vol 96, No 407, 1970.

9. Charney, J. G., "The Dynamics of Long Waves in Baroclinic Westerly Currents," J. METEOROLOGY, Vol 4, No 5, 1977.

10. Dierks, J., "A Study of Spiral Bands in a Linear Model of a Cyclonic Vortex," J. ATMOS. SCI., Vol 33, No 9, 1976.

11. Eady, E. T., "Long Waves and Cyclone Waves," TELLUS, Vol 1, No 3, 1949.

12. Gall, R., "The Effects of Released Latent Heat in Growing Baroclinic Waves," J. ATMOS. SCI., Vol 33, No 9, 1976.

13. Gammelsrod, T., "Instability of Couette Flow in a Rotating Fluid and Origin of Langmuir Circulation," JGR, Vol 80, No 36, 1975.

14. Green, J. S., "A Problem in Baroclinic Instability," QUART. J. ROY. METEOROL. SOC., Vol 86, No 368, 1960.

15. Hide, R., Mason, P. J., "Sloping Convection in a Rotating Fluid," ADV. PHYSICS, Vol 24, No 1, 1975.

16. Hoskins, B. J., "The Role of Potential Vorticity in Symmetric Stability and Instability," QUART. J. ROY. METEOROL. SOC., Vol 100, No 425, 1974.

17. Hoskins, B. J., "Baroclinic Waves and Frontogenesis. Part I. Introduction and Eady Waves," QUART. J. ROY. METEOROL. SOC., Vol 102, No 431, 1976.

18. Kitade, T., "A Numerical Study of Three-Dimensional Benard Convection. Part III. On the Preferred Roll Diameter," J. METEOROL. SOC. JAPAN, No 1, 1977.

19. Kuettner, J. P., "Cloud Bands in the Earth's Atmosphere: Observations and Theory," TELLUS, Vol 23, No 4-5, 1971.

20. Kuo, H. L., "Three-Dimensional Disturbances in a Baroclinic Zonal Current," J. METEOROL., Vol 9, No 4, 1952.

21. Kung, E. C., "Energy Sources in Middle-Latitude Synoptic Scale Disturbances," J. ATMOS. SCI., Vol 34, No 9, 1977.

22. Lipps, F. B., "Numerical Simulation of Three-Dimensional Benard Convection in Air," J. FLUID MECH., Vol 75, Pt 1, 1976.

23. Lorenz, E. N., "Barotropic Instability of Rossby Wave Motion," J. ATMOS. SCI., Vol 29, No 2, 1972.

24. Manton, M. J., "Penetrative Convection Due to a Field of Thermals," J. ATMOS. SCI., Vol 32, No 12, 1976.

25. Maslowe, S. A., "Weakly Nonlinear Stability Theory of Stratified Shear Flows," QUART. J. ROY. METEOROL. SOC., Vol 103, No 438, 1977.

26. Miles, J. W., "On the Stability of Heterogeneous Shear Flow," J. FLUID MECH., Vol 10, Pt 4, 1961.

27. Min, H. J., Peskin, R. L., "Baroclinic Instabilities of a Deep Fluid," ATMOS. SCI., Vol 33, No 11, 1976.

28. Mudrick, S. E., "A Numerical Study of Frontogenesis," J. ATMOS. SCI., Vol 31, No 4, 1974.

29. Orlanski, J., Ross, B. B., "The Circulation Associated With a Cold Front. Part 1: Dry Case," J. ATMOS. SCI., Vol 34, No 10, 1977.

30. Pedlosky, I., "A Model of Wave Amplitude Vacillation," J. ATMOS. SCI., Vol 34, No 12, 1977.

31. Price, G. V., "A Three-Dimensional Study of Frontogenesis Using a Model Formulated in Stream-Axis Coordinates," J. ATMOS. SCI., Vol 34, No 6, 1977.

32. Philander, S. G. H., "A Note on the Stability of the Tropical Easterlies," J. METEOROL. SOC. JAPAN, Vol 54, No 5, 1976.

33. Simons, T. J., "The Nonlinear Dynamics of Cyclone Waves," J. ATMOS. SCI., Vol 29, No 1, 1972.

34. Smith, R. K., Reilly, J. M., "On a Theory of Amplitude Vacillation in Baroclinic Waves: Some Numerical Solutions," J. ATMOS. SCI., Vol 34, No 8, 1977.

35. Spence, T. W., Fultz, D., "Experiments on Wave Transition Spectra and Vacillation in an Open Rotating Cylinder," J. ATMOS. SCI., Vol 34, No 8, 1977.

36. Staley, D. O., Gall, R. L., "On the Wavelength of Maximum Baroclinic Instability," J. ATMOS. SCI., Vol 34, No 11, 1977.

37. Stone, P. H., "On Nongeostrophic Baroclinic Instability. Part II," J. ATMOS. SCI., Vol 27, No 5, 1970.

38. Stone, P. H., "Baroclinic Stability Under Nonhydrostatic Conditions," J. FLUID MECH., Vol 45, Pt 4, 1971.

39. Thorpe, S. A., "Experiments on Instability and Turbulence in Stratified Shear Flows," J. FLUID MECH., Vol 61, Pt 4, 1973.

40. Tsai, C. Y., Kao, S. K., "Linear and Nonlinear Contributions to the Growth and Decay of the Large-Scale Atmospheric Waves and Jet Stream," TELLUS, Vol 30, No 1, 1978.

41. Willoughby, H. E., "Inertia-Buoyancy Waves in Hurricanes," J. ATMOS. SCI., Vol 34, No 7, 1977.

UDC 551.509(73)

OPERATIONAL SYSTEM FOR NUMERICAL WEATHER ANALYSIS AND FORECASTING AT THE UNITED STATES NATIONAL METEOROLOGICAL CENTER

Moscow METEOROLOGIYA I GIDROLOGIYA in Russian No 6, Jun 79 pp 113-119

[Article by V. A. Antsypovich and Candidate of Physical and Mathematical Sciences S. O. Krichak, USSR Hydrometeorological Scientific Research Center, submitted for publication 3 November 1978]

Abstract: The article examines the principal elements of the operational system for data processing at the United States National Meteorological Center, beginning with the stage of reception of data to the dissemination of prognostic data to users. The rational elements of the discussed system are noted. The authors discuss the peculiarities of organization of routine work at the NMC, the problems involved in the reception and processing of data on electronic computers at the US NMC, assimilation of data in the data processing system, routine numerical prediction of meteorological elements and use of results of numerical forecasts.

[Text] During the period November-December 1977, within the framework of the bilateral exchange of specialists on data processing and the hydrodynamic forecasting of meteorological elements, the authors of this article were sent to the National Meteorological Center (NMC) in the United States. Later, during January-February 1978, the USSR Hydrometeorological Center was visited by specialists from the US NMC J. B. Hovermale and J. G. Sela. In the course of both the assignments there was discussion of different aspects of the problem of preparation and use of meteorological forecasts within the framework of an automated system for the processing of meteorological data. The problems involved in monitoring, objective analysis and hydrodynamic forecasting of meteorological elements under conditions of routine work were considered in particular detail.

Below we describe some of the principal elements of the operational data processing system at the US NMC, beginning with the stage of data reception and through the dissemination of prognostic data to users.

Due to the fact that the problems involved in the organization of work at the NMC and comparison of the quality of forecasts using different models have been repeatedly discussed earlier [2-5], in this article emphasis is on parts of the system not discussed earlier.

I. Reception and Processing of Data on Computers at the US NMC

The computation complex (CC) at the US NMC is structured for the most part on the basis of IBM computers [6]. This complex can logically be broken down into three principal levels:

Level I -- the level of work with communication channels (represented by minicomputers of the type INTERDATA-50 and units operating with terminals of the type IBM 2701, 2702, 2709, 2908);

Level II -- ensuring reception of data, recognizing types of communications and preparation of information for subsequent processing; this level ensures a "man-computer" dialogue; this level is based on a computer of the type IBM 360/40, which with respect to such a characteristic as the memory cycle corresponds to the computers YeS 1040 and IBM 360/30;

Level III -- the principal computer used in decoding information, its storage, checking, objective analysis, prediction and computer processing for supporting scientific research; this level is based on use of an IBM 360/195 electronic computer. In constructing the CC special attention is devoted to the problems of clear discrimination of the work done by the individual computers in the complex, the reliability of functioning and the most complete use of standard mathematical support.

The US NMC, together with other establishments under the authority of NOAA, uses the services of the NOAA computation center. The computation center (CC) is outfitted with three IBM 360/195 computers. (Speed 10-15 million operations per second). According to approximate estimates, the NMC uses 56% of the capacity of the CC processors and 11% of the direct storage memory on magnetic disks.

For the purpose of obtaining and disseminating data the US NMC uses four high- (2,400 bits/sec), 43 medium-(1,050 bits/sec) and low-(100 baud) speed internal channels together with three high- (2,400 bits/sec) and 21 low-(600-100 baud) speed WMO channels. In addition, for the dissemination of graphic information there are 15 facsimile and seven digital channels (duplex, 4.8 KHz-2.50 KHz - 5).

The success of the operational-prognostic operation of the US NMC is ensured to a great extent by use of the "man-computer" operational dialogue (Man-Machine Mix).

The Man-Machine Mix regime can be functionally divided into three levels. In the first level there is revision and correction of the headings of the summaries which have arrived at the NMC with distortions. In the course of

one shift a specialist responsible for the quality of the communication inspects up to 650 headings of summaries not comprehended by the system.

In the second level of the man-machine mix regime there is monitoring and correction of aerological information. In order to detect errors in aerological communications there is an analysis of the arriving aerological communications for syntax, accomplished by the weather analyst from the printout and the drafting of maps by the weathermen using data plotted by means of computer.

At the third level of the man-machine mix regime information is supplied for regions covered by few observations. This supplementation (described in detail below) is accomplished for the earth's surface and for the level 250 mb by means of transfer of the coordinates of isoline points from maps drafted by the weatherman onto punched cards using an automatic device and subsequent input of these data into electronic computers.

At this level the man-machine mix makes it possible to have output of digital information onto the display screen at the weatherman's request. The weatherman has at his disposal data from aerological sounding for the last observation period at any station and for a definite set of stations -- data on the state of the weather during the last few days. Work is also done on the automatic formulation of forecasting texts on the basis of the results of numerical computations.

2. Data Assimilation in the NMC Data Processing System

In routine analysis and forecasting provision is made for the following types of initial information [13]:
-- communications from surface meteorological observations by land stations,
-- communications on meteorological observations from ships,
— radiosonde, pilot balloon and rawin observations from ships and land stations,
-- communications from aircraft,
-- "artificial" data prepared manually in a man-machine mix regime,
-- estimates of wind direction and velocity using photographs of cloud cover from satellites,
-- data from remote sounding of the atmosphere from meteorological satellites.

Information on the number of received communications of different types at different surfaces is accumulated in a special archives and is routinely analyzed for the purpose of clarifying the reasons for loss of information.

Now we will discuss in greater detail the procedures used by the weatherman in preparing additional information for the purposes of objective analysis and forecasting. In this exposition we will emphasize the specific work conditions existing in the preparation of information for analysis and forecasting over a limited territory using data for 1200 hours on 5 December 1977 (GMT), which took place in our presence. Objective analysis for forecasting for a limited territory is accomplished using a scheme based on the successive approximations method [1, 12].

In the course of reception and processing of observational data there is a printout of maps with automatically plotted data arriving by a specific moment of observations. The great rate of representation of data by units of the VARIAN type makes it possible to print out maps with data several times in the course of one data reception session (30-60 sec per map).

The plotting and analysis of these maps is accomplished by the on-duty specialists on transparent film, beneath which, as they appear, are laid new maps with plotted data. In the course of the subjective analysis of pressure maps at sea level and at the AT_{250} surface (where the greatest number of data from aircraft wind observations AEREP, ASDAR, are assigned to the closest standard surface) there is rejection and correction of data present in the electronic computer.

By the end of the data reception session for a regional forecast (0130 hours after the observation time) there is accumulation of a considerable number of communications with the results of meteorological observations. For example, in the course of the described session of 5 December 1977 there was reception of 87 communications with data from remote satellite sounding, 289 communications with data from rawin and radiosonde soundings, 216 communications with data from aircraft and 201 communications with estimates of wind direction and velocity from photographs of cloud cover from satellites.

In addition to the subjective analysis carried out on the basis of newly arriving data, the man-machine mix duty specialists also have prognostic isolines plotted on transparent film with data for the preceding observation period and actual maps for the preceding time.

In accordance with the objective analysis method used at the NMC, the results of the forecast for the current analysis time serve as first-approximation fields in the interpolation of newly arriving data at grid points of intersection. This ensures an increase in the successive character of the results of objective analysis from time to time.

The use of the man-machine mix method makes it possible, in the preparation of data for forecasting purposes, to take into account quite simply those types of information which by virtue of different factors is not used in an automated processing line. At the same time, the man-machine mix regime ensures a decrease in the influence of errors in the first-approximation fields on the analytical results: in those regions where in the opinion of the duty specialist the first-approximation fields at the earth's surface and at the AT_{250} surface differ greatly from the manually analyzed actual maps there will be an input of additional data in the form of communications from fictitious stations. This procedure is carried out by means of the automatic punching of the coordinates of isoline points on punch cards. Depending on the situation and the weatherman's intuition, at one surface there is formation of between 200 and 400 communications from fictitious stations. The preparation of such a quantity of additional data takes only a few minutes.

After carrying out an objective analysis of AT_{1000} and AT_{250} in accordance with the adopted method [12] there is scaling of the first-approximation field for the next surface to be analyzed in order to maintain the static stability of the vertical temperature profile. Upon completion of the analysis at the particular surface the first-approximation field is scaled for the next in the adopted sequence, etc.

In accordance with [12], we will examine the procedure used for the scaling of the first-approximation fields.

Assume that at the grid points we have the results of prediction of AT_{300}, AT_{500} and AT_{1000} and the values obtained after computing the objective analysis, taking into account the additional data H^{A}_{300}, H^{A}_{1000} and it is necessary to determine the first-approximation values H^{A}_{500}.

In accordance with the equation of statics

$$\frac{\partial H}{\partial \Pi} = -C_p \vartheta, \tag{1}$$

where $\Pi = (P/1000)^{2/7}$; the remaining notations are those generally accepted.

We will write the following equation for the predicted values:

$$\frac{H_{500} - H_{300}}{\Pi_{500} - \Pi_{300}} - \frac{H_{1000} - H_{500}}{\Pi_{1000} - \Pi_{500}} = C_p \left(\vartheta^{500}_{1000} - \vartheta^{300}_{500}\right) = S^{300}_{1000}. \tag{2}$$

Here $\Pi_N = \Pi$ when p = N mb, ϑ^{N2}_{N1} is the potential temperature of the N_1-N_2 layer.

The S^{300}_{1000} value characterizes the prognostic stability of the layer 1000-300 mb. Writing a similar equation for the results of the first-approximation computation and using the S^{300}_{1000} value computed earlier on the basis of predicted data, we find that

$$H^{A'}_{500} = 0{,}383\, H^{A}_{1000} + 0{,}617\, H^{A}_{350} + S^{300}_{1000}. \tag{3}$$

In a similar way there is computation of the first-approximation values for the remaining surfaces. (We note that over a long period of time the preparation of additional data was not for the AT_{250} level, but for AT_{300}. The following sequence of computation of analyses was used for different surfaces: 1000, 300, 500, 700, 850, 400, 200, 250, 100, 150 mb).

"Artificial" data are being prepared at the NMC not only for geopotential, but also for the temperature and humidity fields. In the case of the humidity fields particular attention is devoted to the use of data from meteorological observations of cloud cover and photographs of cloud cover from meteorological satellites. Depending on the category of cloud cover in a specific region the values of relative humidity in the troposphere are formed.

Also subject to correction are data from radiosonde observations in the stratosphere. Here the results of temperature and geopotential measurements are corrected for the purpose of eliminating radiation errors at the AT_{100} surface and above. In these computations allowance is made for the type of radiosonde used at each specific station. The importance of carrying out such a correction is also confirmed by work practice in other countries.

The temperature fields of the sea surface are computed using data from remote sounding from satellites [7].

At the NMC great attention is being devoted to the organization of a system for the assimilation of diverse information. In addition to the purely operational requirements the developed system takes into account the need for solving the problems of storage of level-II data in the course of the Global Experiment GARP. By the beginning of the experiment plans call for the following configuration of the data assimilation system [14, 15].

The global prognostic model [23] ensures computation of forecasts using data accumulated with the maximum possible cutoff times (cessation of the collection of data after the observation time). For the observation times 0000 and 1200 hours (here and in the text which follows, GMT) the cutoff time is 11 hours, for the times 0600 and 1800 hours -- 16 hours. All the types of data received in the interval ±3 hours from the observation time are assigned to this time and are used in objective analysis. Thus, the following six-hour data assimilation cycle exists.

1. Objective analysis is carried out using data at 0600 (1800) hours 16 hours after the observation time.

2. A forecast for six hours in advance (to the time 1200 (0000) hours) is computed.

3. Objective analysis is carried out using data at 1200 (0000) hours, 11 hours after the observation time. The first-approximation field here was obtained as a result of satisfaction of point 2.

4. A forecast is computed for 12 hours in advance to the next main observation time 0000 (1200) hours.

The pressure, geopotential, wind, humidity and temperature fields are subjected to objective analysis at the NMC. Plans call for organizing work for the assimilation of data on the basis of the global spectral model developed by J. Sela [17].

At the present time a method based on the interpolation of assimilable data, using a spectral model of global objective analysis, is routinely used at the NMC. A new version of the system is in the testing stage. The optimum interpolation method [1, 14] is used here for computing the values at the grid points of intersection at the computation surfaces in the prognostic model. The grid interval in the interpolation is 5°. Then, using

spectral analysis, the values of the meteorological elements are determined in a grid with an interval of 2.5°.

The use of such an approach easily makes it possible to take into account the different level of errors in measurement data in different observation systems.

The results of global forecasts for 0000 (1200) hours using data at 1200 (0000) are used in objective analysis computations [8] for the NMC routine hemispheric model. The first-approximation fields for objective analysis [12] for a regional model come from the preceding hemispheric forecast.

3. Routine Numerical Forecasting of Meteorological Elements

Adhering to [20], we will briefly examine the principal stages in work for the routine hydrodynamic forecasting of meteorological elements at the NMC. As data are received 1 hour 15 minutes, 1 hour 30 minutes and 4 hours after the observation time, computations begin for a barotropic hemispheric (cutoff time 1 hour 15 minutes, interval 381 km at 60°N) and baroclinic (regional and hemispheric) models. The observation times for stations in the territory of North America, communications from which have not been received at the NMC in the course of 1 hour 30 minutes after the observation time, can be shifted to an earlier time up to one hour. Thus, for such stations the cutoff time is actually 2-2.5 hours.

The NMC regional model [9, 10] (79 x 67 points, grid interval 127 km at 60°N, cutoff time 1 hour 30 minutes), like the hemispheric model [22], is based on solution of the full equations of hydrodynamics in a quasi-static approximation. The use of a σ-system makes it possible to take into account the influence of orography and actual data on pressure in the tropopause. Extremely simple computation methods for taking into account the principal nonadiabatic effects to an adequate degree ensure the energy balance of the system in the forecast. We should mention the special care in using the methods of finite-difference approximation of equations and spatial-temporal filtering.

This model, at the boundaries of the forecasting region, uses the results of computations for a hemispheric model on the basis of data for the preceding time (one-sided interaction of models) [19]. The computation of the forecast is made for a time up to 48 hours.

In those cases when it is necessary to compute a forecast of movement of a tropical cyclone or precipitation associated with a cyclonic formation developing over the United States use is made of a model with a moving grid [11, 16] (cutoff time 7 hours 30 minutes, 50 x 50 points, grid interval 60 km, advance time of forecast 48 hours). This model belongs to the type of regional models with one-sided interaction of grids. Here provision is made for the programmed possibility, in the course of the calculations,

of effecting the movement of the northern hemisphere forecasting region. This possibility is used effectively in predicting the movement of tropical cyclones. The time-variable conditions at the boundary of the forecasting region are determined using the results of prognostic computations using a hemispheric or regional model. During the eight months preceding April 1977 routine computations using this model were carried out 40 times.

Routine forecasts of meteorological elements over the northern hemisphere are made using a hemispheric seven-layer baroclinic model using full equations in a σ-coordinate system [22] (cutoff time 4 hours, 129 x 129 points, grid interval 190.5 km at 60°N. Advance time of forecast up to 84 hours). The model became operational in January 1978. Like the regional model, it is a result of development of the Shuman-Hovermale model [21]. In contrast to the regional model [10], in this case there is no isentropic layer near the upper boundary of the atmospheric model. A condition of the "equator" type is stipulated at the lateral boundaries of the forecasting region. In order to ensure stability in computations, the actual fields near the boundary of the forecasting region are subjected to special processing for the purpose of eliminating the relatively small-scale formations in this region.

Beginning in 1978, three times a week, using the L. Vanderman model [24] (interval 3.75°, cutoff time 10 hours), there has been routine preparation of forecasts up to 16 days with printout, in deviations from the norm, of the results of prediction of temperature and precipitation, averaged for five days, for the third, eighth and thirteenth days.

Also prepared for routine use is a model with two-sided interaction of grids of different resolution, developed by N. A. Phillips, et al. [17]. Here the prediction is made simultaneously in three grids, in each forecasting interval interacting with one another. In the model there are 8-10 layers, the extent of the region is 2,500 x 2,500 km, and the grid interval is 448, 224 and 112 km.

The results of routine forecasts made using hydrodynamic models are transmitted to NMC forecasters and to the network. For example, in the form of plotted maps there is dissemination of data on the predicted geopotential fields at the levels from 1,000 to 100 mb, the fields of wind velocity and temperature at these same levels, dew point temperature at levels from 1,000 to 100 mb, vertical velocity at levels from 1,000 to 400 mb and at 200 mb, pressure and temperature at the tropopause, absolute vorticity at the level 500 mb, stream function field at the level 500 mb, mean (for three layers) relative humidity, relative humidity in the three lower layers of the model, precipitation after 6 and 12 hours, pressure at sea level, temperature, wind and vertical velocity in the three lower layers of the model. In addition, the weatherman has the results of a statistical interpretation of the forecasting results [4].

The data used in the US NMC routine processing system is stored in archives of different categories.

The initial information received through the communication channels is put into sets of data by types of communications, where it is stored in the course of the day.

The working archives (for 36 days for two observation times) on magnetic disks contains the fields of global objective analysis and prognostic fields computed using hemispheric and regional operational models. This archives, each 31 days, is copied on magnetic tapes (62 magnetic tapes with a density of registry 1,600 bytes/inch).

In addition, an archives is organized on magnetic tapes with a storage period of one year. It contains selected fields of the monthly archives and the types of initial information used in routine work.

This archives is on 119 magnetic tapes with a density of 1,600 bytes/inch.

Each year this archives is sent to the US National Climatological Center.

4. Use of Results of Numerical Forecasts of Meteorological Elements

An obligatory stage accompanying the introduction of any element of the system into routine work is the publication of information on the modernization to be carried out and the time it is to be put into operation in a publication of the US Weather Service -- the NOAA TECHNICAL PROCEDURES BULLETIN. Thus, specialists always have the possibility of evaluating the actual effectiveness of each innovation and of participating in the development of the processing system. At the NMC great attention is being devoted to an analysis of the commentaries and recommendations of users. It is noted that such cooperation of service specialists is a powerful means for increasing the effectiveness of the routine processing system.

In the course of routine work there was accumulation of information on the principal characteristics of success of forecasts using NMC models.

For example, source [18] gives the following peculiarities of the models in routine use up to mid-1977 (hemispheric model: interval 381 km at 60°N, six layers; regional model: interval 190.5 km at 60°N, six layers):
Barotropic model
a) The results of the forecasts are quite successful. The new 12-hour forecasts are usually more successful than forecasts computed for 24 hours in advance at the same time.
b) The most successful forecasts are near the latitude of the polar jet stream.
c) The forecasts are more successful than hemispheric models using a baroclinic model for determining the movement of cyclones developing over the southwestern United States and beginning to move in a northerly direction.
d) Usually there is a slowing of the movement of troughs over the southern United States.

Six-layer hemispheric model
a) In the course of interpolation on a σ-surface in some cases there is a loss of up to 30% of eddy kinetic and eddy available potential energy in the initial fields.
b) The development of isolated cyclones over the southwestern United States is successfully predicted.
c) The most successful forecast is for waves with the numbers 7 and 8 (that is, processes of a synoptic-subsynoptic scale).
d) Cyclogenesis at the surface is predicted with systematic delay.
e) Movement of small-scale formations at latitudes where the polar jet stream is located is delayed.
f) A forecast of the amplitude of ridges at the 500-mb level is not always successful.
g) In cases when there is cyclogenesis at the surface and isolation of a cyclone over the southwestern United States with its subsequent movement to the north there is a tendency to a slowing of movement of the center at the 500-mb level. The prediction of pressure at the earth's surface is completely successful.

Six-layer regional model
In comparison with a hemispheric model, forecasts for a region have the following advantages:
a) There is better prediction of the velocity of movement of short waves.
b) Errors of the type (g) for a hemispheric forecast are manifested here to a lesser degree.
c) There is better prediction of all stages of cyclogenesis at the underlying surface.
d) There is better prediction of the movement of cyclones on the underlying surface.

All models are characterized by a lesser success of forecasts over the western United States and Alaska; this is attributable to inadequate data coverage for the Pacific Ocean area.

Such information on the success of forecasts using different models is actively employed by the users of NMC forecasts, who, depending on the situation, trust the results of forecasts based on a specific model to a greater or lesser degree. However, in general, according to unofficial evaluations of NMC specialists, in the compilation of short-range weather forecasting charts the weatherman trusts the numerical forecasting result at the 95% level. In the preparation of forecasts for a time greater than three days the contribution of the weatherman increases to 30-40%. In addition, the study of success and the reasons for success of the forecasts made using the models favors the choice of an optimum strategy in solving the problem of a changeover to routine use of new versions of NMC prognostic models.

In conclusion the authors take the opportunity to thank the NMC staff and in particular Doctor F. G. Shuman, NMC director, for the possibility afforded for the thorough study of the different aspects of operations at the US NMC.

BIBLIOGRAPHY

1. Gandin, L. S., OB"YEKTIVNYY ANALIZ METEOROLOGICHESKIKH POLEY (Objective Analysis of Meteorological Fields), Leningrad, Gidrometeoizdat, 1963.

2. Kontarev, G. R., "Experiment for Comparison of the Numerical Weather Forecasting Schemes of the US National Meteorological Center and the Computation Center Siberian Department USSR Academy of Sciences," METEOROLOGIYA I GIDROLOGIYA (Meteorology and Hydrology), No 12, 1974.

3. Sitnikov, I. G., "Numerical Modeling of the Atmosphere and Automatic Processing of Meteorological Information in the United States," METEOROLOGIYA I GIDROLOGIYA, No 7, 1974.

4. Snitkovskiy, A. I., Sonechkin, D. M., Fuks-Rabinovich, M. S., Shapovalova, N. S., SISTEMA OB"YEKTIVNOGO KRATKOSROCHNOGO PROGNOZA YAVLENIY I ELEMENTOV POGODY V SShA (System for Objective Short-Range Prediction of Weather Phenomena and Elements in the United States), Obninsk, Inf. Tsentr VNIIGMI-MTsD, 1978.

5. Chernova, V. F., "Prediction of the Pressure Field Using the Full Equations of Hydrodynamics US NWC," INFORMATSIONNYY SBORNIK, No 1: REZUL'TATY ISPYTANIYA RAZLICHNYKH SPOSOBOV KRATKOSROCHNOGO PROGNOZA POGODY (Collection of Informative Articles, No 1: Results of Testing of Different Methods for Short-Range Weather Forecasting), Moscow, Gidrometeoizdat, 1969.

6. Bedient, H. A., "The NMC Front End to the NOAA 360/195 System," NOAA, NWS, NMC Office Note, No 115, 1975.

7. Brower, R. L., Gohrband, H. S., Pichel, W. G., Signore, T. L., Waltar, C. C., "Satellite Derived Sea-Surface Temperatures from NOAA Spacecraft," NOAA TECHNICAL MEMORANDUM, NESS 78, 1976.

8. "A Description of the Flattery Global Analysis Method," No 1, TECHNICAL PROCEDURES BULLETIN, NWS, No 105, 1974.

9. Gerrity, J. F., "The LFM Model -- 1976. A Documentation. NOAA Technical Memorandum," NWS, NMC 60, 1978.

10. "High Resolution LFM (LFM-II), NOAA TECHNICAL PROCEDURES BULLETIN, NWS, No 206, 1977.

11. Hovermale, J. B., Livezey, R. E., "Three-Year Performance Characteristics of the NMC Hurricane Model," PROCEEDINGS OF THE HURRICANE TROPICAL CONFERENCE, Miami, 1977.

12. McDonell, J. E., "Notes on Operational Objective Analysis Procedures," ADVANCED PREDICTION TECHNIQUES COURSE FOR NWS FIELD FORECASTERS, 1974.

13. McDonell, J. E., "Preparation of the Data Base for Use in an Operational Environment," THE GARP WORKING GROUP ON NUMERICAL EXPERIMENTATION. PROCEEDINGS OF THE JOC STUDY CONFERENCE ON FOUR-DIMENSIONAL DATA ASSIMILATION, Report No 11, 1976.

14. McPherson, R., Bergman, K. H., Kistler, R., Rasch, G., Gordon, D., "Global Data Assimilation by Local Optimum Interpolation," VOL. CONF. PAPERS. THIRD CONF. ON NUMERICAL WEATHER PREDICTION, BAMS, Omaha, 1977.

15. McPherson, R. D., Kistler, R. E., Rasch, G. E., Bergman, K. H., Gordon, D. S., "Status Report on the NMS Global Data Assimilation System Based on Statistical Interpolation," THE GARP WORKING GROUP ON NUMERICAL EXPERIMENTATION. RESEARCH ACTIVITIES IN ATMOSPHERIC AND OCEANIC MODELLING, Report No 15, 1977.

16. "The Movable Fine Mesh (MFM) -- A New Operational Forecast Model," NOAA TECHNICAL PROCEDURES BULLETIN, NWS, No 160, 1976.

17. NUMERICAL WEATHER PREDICTION. PROGRESS REPORT FOR 1976. World Meteorological Organization.

18. "Performance Characteristics of the Operational Models of the National Meteorological Center (NMC)," NOAA TECHNICAL PROCEDURES BULLETIN, NWS, No 107, 1974.

19. "Reduction of the Pillon Effect in the Output of the Limited-Area Fine Mesh (LFM) Model," NOAA TECHNICAL PROCEDURES BULLETIN, NWS, No 90, 1973.

20. Shuman, F. G., PLANS OF THE NATIONAL METEOROLOGICAL CENTER FOR NUMERICAL WEATHER PREDICTION, NOAA, NWS, NMC, Office Note, No 144, 1977.

21. Shuman, F. G., Hovermale, J. B., "An Operational Six-Layer Primitive Equation Model," J. APPL. METEOROL., Vol 7, No 4, 1968.

22. Stackpole, J. D., "The National Meteorological Center's Operational Seven-Layer Model on the Northern Hemisphere Cartesian 190.5 Grid," NOAA, NMC OFFICE NOTE, No 177, 1978.

23. Stackpole, J. D., "The NMC 9-Layer Global Primitive Equation Model on a Latitude-Longitude Grid," NOAA, NWS, NWC OFFICE NOTE, No 178, 1978.

24. Vanderman, L. W., "Global Three-Layer Forecast Model," THE GARP WORKING GROUP ON NUMERICAL EXPERIMENTATION AND OCEANIC MODELLING, Report No 15, 1977.

REVIEW OF MONOGRAPH 'ATLAS OKEANOV. T. II. ATLANTICHESKIY I INDIYSKIY OKEANY' (ATLAS OF THE OCEANS. VOLUME II. ATLANTIC AND INDIAN OCEANS), Leningrad, Voyenno-Morskoy Flot SSSR, 1977

Moscow METEOROLOGIYA I GIDROLOGIYA in Russian No 6, Jun 79 p 120

[Article by B. L. Yedskiy]

[Text] The USSR Navy has continued publication of the ATLAS OKEANOV (Atlas of the Oceans), a fundamental scientific work reflecting modern knowledge concerning the water medium of the world ocean and the air space over it.

The first volume, TIKHIY OKEAN (Pacific Ocean), was published in 1974. The second volume, ATLANTICHESKIY I INDIYSKIY OKEANY (Atlantic and Indian Oceans) was published in 1977. The maps included in the atlas were compiled on the basis of Soviet and foreign scientific data, collected during the entire history of study of the ocean, including during the IGY (1957-1958), International Year of Geophysical Cooperation and IQSY (1964-1965), accumulated in the USSR.

The first section of the atlas, "History of Investigation of the Oceans," consists of maps of geographic discoveries, maps of the most important oceanographic expeditions working in the Atlantic and Indian Oceans from the beginning of the 19th century to 1975, and also maps of Soviet oceanographic expeditions in 1957-1975, making an outstanding contribution to the investigation of these oceans.

In the section "Ocean Floor," there is a description of bottom relief, morphometric characteristics, earthquakes and volcanoes, tectonics, geomorphology, types of shores, bottom sediments, etc.

The section on "Climate" gives information on the heat, water and circulation regimes of the atmosphere. The section ends with a world map of climatic zones and regions making it possible to judge the principal climatic patterns of the Atlantic and Indian Oceans. As a result of allowance for all the climate-forming factors it was possible to give a map of climatic regionalization.

The section "Hydrology" consists of maps of temperature, salinity and density of waters and the speed of sound at the ocean surface and at different depths, hydrological sections, maps of surface and deep currents, level

fluctuations and waves and is the largest section in the atlas.

In the section "Geochemistry" all the available information on the chemical regime of the waters of the Atlantic and Indian Oceans is presented with adequate completeness. It contains information on the distribution of dissolved oxygen, biogenous elements, concentration of hydrogen ions and alkalinity at the ocean surface and at various depths. Hydrochemical sections and hydrochemical regionalization of the oceans are given.

The section "Biogeography" is of special interest. It contains a lengthy description of the organic life in the ocean -- from the intensity of photosynthetic processes to the distribution of marine mammals. It should be noted that for the first time important information is given on the magnitude of primary production, the biomass of zooplankton and bottom fauna, on bottom trophic regions. There is a detailed discussion of the distribution of fish (herring, garfish, mackerel, sea perch, cod, flounder, croakers, salmon, milkfish, and others), and also the distribution of geographic complexes of commercial fish.

The section "Reference and Navigational-Geographic Maps" contains maps of terrestrial magnetism, astronomy, sea and air communications, medical-geographic conditions and distribution of sea animals dangerous for man. The section ends with navigation-geographic maps at a scale of 1:12,000,000 and also maps of the most important straits, ports and approaches to them.

We should note the diversity of information contained in the atlas, its high scientific level of generalization and exposition, high cartographic mastery of the compilation and publication of maps and the aesthetic merits of the latter. All this makes it possible to call the atlas a real achievement of cartography in the 20th century.

The atlas is intended for scientific workers, officers of the Soviet Army and Navy, captains and navigators of the merchant marine and fishing fleets.

The extensive material concentrated in the atlas is of great informative value, can be used successfully in teaching and without doubt will meet the needs of the most inquiring reader.

REVIEW OF MONOGRAPH BY G. I. SHVETS ENTITLED "MNOGOVEKOVAYA IZMENCHIVOST' STOKA DNEPRA" (VARIABILITY OF RUNOFF OF THE DNEPR OVER THE CENTURIES), LENINGRAD, GIDROMETEOIZDAT, 1978, 84 PAGES

Moscow METEOROLOGIYA I GIDROLOGIYA in Russian No 6, Jun 79 pp 120-121

[Article by Doctor of Technical Sciences P. F. Vishnevskiy]

[Text] The reviewed book by G. I. Shvets is devoted to the timely problem of hydrological investigations — a reconstruction of the annual runoff of the Dnepr during the past centuries. In solving this problem the author has employed an original reconstruction method, as initial data using information on silt deposits in Sakskoye Lake (Crimea). The data used, covering the period from 2249 B.C. up to 1894, were published by B. V. Shostakovich on the basis of analysis of a column of deposits extracted in 1931 from the thickness of lacustrine deposits. Shostakovich's data are highly regarded by many Soviet and foreign specialists. They have been used in an investigation of climatic variations in the basin of the Caspian Sea, on the Russian Plain during the historical period and in other investigations.

The availability of parallel data on deposits in Sakskoye Lake and on the annual runoff of the Dnepr at Lotsmanskaya Kamenka during the period 1818-1894 made it possible to derive a correlation used in reconstructing the annual runoff of the Dnepr during the period from 2149 B.C. through 1817 (Shostakovich's data for the period 2294-2150 B.C. were not used).

As a genetic basis for deriving the correlation it was assumed, on the basis of the conclusions drawn by many researchers, that the formation of river runoff and deposits in lakes occurs under the influence of climatic factors, the most important of which is precipitation. It can be added here that the regime of atmospheric precipitation in the territory of formation of Dnepr runoff and in the basin of Sakskoye Lake is determined by general synoptic conditions.

The derivation of a computed correlation was a complex and extremely important stage in the work. First the author had to evaluate the possibility of using other initial data — dendrological information, data on solar activity

and so forth, carry out a detailed analysis of information on deposits, study the conditions for the formation of deposits in Sakskoye Lake in a historical perspective, carry out graphic and tabular comparisons, etc. in several variants.

The annual runoff of the Dnepr, reconstructed for a long period (3,966 years), is of exceptional interest in many respects, but naturally, the problem arises of its suitability for practical use.

It should be noted that the author has devoted considerable attention to a qualitative evaluation of the reconstructed runoff. In this case limited possibilities dictated the use of a differentiated method for individual periods. For the period 1818-1872 an evaluation was made by a comparison with the "hydrometric" runoff; for the period 945-1817 -- by a comparison with the qualitative characteristics of runoff, determined for individual years (of which there were 318) from different sources in the literature; during the period from 2149 B.C. through 1716 -- by comparison of periods with an abundance and paucity of water with the moistening of European regions as evaluated by different researchers. The author's general positive evaluation of the reconstructed runoff and its suitability for practical use causes no objections.

The reconstructed annual runoff values (for 3,966 years) were combined with the available "hydrometric" runoff for the period 1818-1975 (158 years) and it was possible to compile a continuous multicentury chronological series with a duration of 4,124 years, for which there is no equal in world practice. The author used this series for drawing some practical conclusions.

As a result of analysis of the variability of the annual runoff of the Dnepr over a period of many centuries the author arrived at the following conclusions: the variability of annual runoff occurs cyclically, without a one-sided tendency; the alternation of cycles is a "mottled" pattern and does not fit into a rigorous scheme with a regular change of cycles; the conditions for the formation of runoff in the Dnepr basin developed earlier than the investigated period and during a period of 4,000 years did not experience significant change.

Very interesting conclusions were drawn in an investigation of the computed parameters of annual runoff (norm, variation and asymmetry coefficients). The computations of these parameters in 48 variants gave basis for recommendations in computations using ordinary data series.

The book sets forth considerations on the limiting values of annual runoff of the Dnepr, on the influence of human activity on runoff, considerations on the representativeness of the conclusions drawn by the author.

The text of the book is written concisely, with an effort to validate the postulated positions. It can only be noted that the section on the derivation of the computed correlation for reconstructing runoff should be set

forth more clearly, without omitting technical details. Unfortunately, it must be stated that Figures 6 and 7, showing integral curves, are poorly designed. These are unique curves, in graphic form illustrating the multicentury variability of runoff, and they should be presented on a larger scale. The book has annoying misprints in Tables 7 and 12. However, the mentioned shortcomings do not lessen the overall positive evaluation of the book.

The reviewed book of G. I. Shvets is a result of long-time purposeful work. It is an example of a nonstandard approach to hydrological investigations. Its most valuable part is a unique, multicentury, chronologically continuous series of data on the annual runoff of the Dnepr (4,124 years). This series is a basis for hydrological, climatic and water management investigations and computations, for characterizing the multicentury variability of geographic phenomena, for validating new stochastic computation schemes and prognostic dependences.

This book by G. I. Shvets is a significant contribution to the published hydrological research in our country.

CONFERENCES, MEETINGS AND SEMINARS

Moscow METEOROLOGIYA I GIDROLOGIYA in Russian Jun 79 pp 122-127

[Article by V. N. Zakharov, Yu. G. Slatinskiy, G. N. Danilova, G. V. Rudnev, K. P. Vasil'yev and N. Z. Pinus]

[Text] During the period 12-13 December 1978, at the State Hydrological Institute, there was a session of the Section on Surface and Ground Water Resources and Water Balance of the Scientific Council "Multisided Use and Conservation of Water Resources" of the State Committee on Science and Technology. Those present examined the principal results of work for evaluating the possible changes in hydrological and hydrogeological conditions and also water quality in regions of territorial redistribution of runoff.

In a generalizing report of the Deputy Director I. A. Shiklomanov, entitled "Hydrological Principles of Interzonal Redistribution of Water Resources," the speaker presented the basic directions of research carried out by the State Hydrological Institute in collaboration with other organizations in solving a broad range of problems in hydrological studies of the redistribution of runoff.

The section also heard other reports of the State Hydrological Institute, including the following: N. M. Alyushinskaya, I. B. Vol'ftsun, O. D. Markova, Yu. V. Russ, O. G. Sorochan: "Evaluation of Possible Changes in the Water Balance and Water Regime in the Basin of the Ob' River in Relation to the Territorial Redistribution of Runoff"; S. I. Kharchenko, V. V. Sumarokova and K. V. Tsytsenko, "Change in Inflow into the Aral Sea in Relation to the Development of Irrigated Agriculture and Shifting of the Runoff of Siberian Rivers"; I. B. Vol'ftsun, P. A. Ignat'yev, O. L. Markova and R. A. Nezhikhovskiy, "Change in the Regime of Water Bodies in the Northern Part of the European USSR in Realizing the First Stage in the Project for the Shifting of Runoff"; R. V. Donchenko, "Evaluation of the Possible Changes in the Ice and Thermal Regimes of Rivers Under the Influence of Shifting of Runoff."

A report entitled "Prediction of Changes in the Principal Indices of the Quality of Surface Water Resources in Relation to the Shifting of Some of the Runoff of Northern and Siberian Rivers into the Southern Regions of the

Country" was presented by A. A. Zenin (Hydrochemical Institute).

In addition to the scientists of the State Committee on Hydrometeorology, the session was addressed by T. I. Malinin (Institute of Lake Sciences USSR Academy of Sciences) with a report entitled "Water Balance and Hydrological Regime of Lacha, Vozhe, Kubenskoye Lakes and Possible Changes in Relation to the Shifting of Runoff" and V. D. Grodzenskiy (All-Union Scientific Research Institute of Hydrology and Engineering Geology) gave a report entitled "Evaluation of Changes in Operational Reserves of Ground Water in Regions of Shifting of Runoff." A report was given by specialists of the All-Union Scientific Research Institute of Hydrology and Engineering Geology, B. Ye. Antypko, V. A. Krivenkov and Ye. S. Shevlyakova, entitled "Preliminary Evaluation of Changes in Regional Hydrogeological Conditions Along the Routes of Shifting of Runoff."

In the adopted section resolution it was noted that specialists of the State Hydrological Institute have evaluated changes in the hydrological regime of watercourses along all routes of the initial shifting of runoff, taking into account the influence of economic activity. Computations were made of the discharges and levels of different guaranteed probability, heat and ice regimes, flooding of floodplains along the Ob', Irtysh, Pechora, Sukhona, Severnaya Dvina, Onega and Neva Rivers.

The All-Union Scientific Research Institute of Hydrology and Engineering Geology has prepared a prediction of changes in natural hydrogeological and geological engineering conditions under the influence of shifting of part of the runoff of northern and Siberian rivers into the southern regions.

The Institute of Lake Sciences USSR Academy of Sciences has made an evaluation of the present-day hydrological, hydrochemical and biological regimes of Lacha, Vozhe and Kubenskoye Lakes. Specialists have computed the water balances and prepared a forecast of the anticipated changes in the water balance of lakes, their hydrological regime, hydrochemical and biological indices in relation to the territorial redistribution of runoff.

The Hydrochemical Institute prepares a preliminary prediction of possible changes in the chemical composition of water along the paths of shifting of runoff.

It was established by the investigations made that the volumes and directions of runoff shifting planned in the first stage will not result in large-scale changes in the water regime, but will exert an influence on the regional hydrological, hydrochemical and hydrogeological peculiarities of water bodies affected by the shifting of runoff.

At the same time it was noted that there is a lag in work on the preparation of a forecast of changes in the quality of surface and ground water along the routes of shifting of runoff. In the implementation of this aspect

of the work there is not the necessary contact with institutes of a hydrobiological profile. There are also other shortcomings in the research carried out.

In a resolution attention was given to the need for concentration, in 1979-1980, of the greatest attention to refinement of existing prognostic evaluations of hydrological, hydrochemical, hydrobiological and hydrogeological changes in regions of shifting of waters; development of simulated mathematical models of river basins involved in schemes for the shifting of runoff and individual paths along which such shifting occurs; evaluation of change in the quality of water bodies in regions of paths of shifting of waters on a unified methodological basis with clarification of the hydrobiological aspect of the forecast.

V. N. Zakharov

On 13 December 1978, at Sevastopol', there was a session of the Basin Section of Southern Seas and the Indian Ocean of the Scientific Council on the Problem "Study of the Oceans and Seas and the Use of Their Resources" of the State Committee on Science and Technology. A study was made of the preliminary results of complex investigations of the Mediterranean Sea, the results of studies under the SKOICh-78 program, the draft of a plan for expeditionary investigations in the basin of the Mediterranean Sea and the Indian Ocean for 1979-1980, a plan for the activity of the section for 1979. Reports and communications were presented by I. M. Ovchinnikov (Southern Division Institute of Oceanology USSR Academy of Sciences), S. G. Boguslavskiy (Marine Hydrophysical Institute), Yu. P. Zaytsev (Odessa Division Institute of Biology of the Southern Seas), V. A. Bryantsev (Sea of Azov and Black Sea Scientific Research Institute of Fishing and Oceanography), L. F. Yermakova (Sevastopol' Division State Oceanographic Institute) and others.

It was noted in the reports and communications of participants in the sessions that during recent years the scientific research institutes and establishments represented in the basin section have carried out a number of interesting oceanographic, biological and fishing investigations in the Mediterranean Sea basin. The Southern Division of the Institute of Oceanology USSR Academy of Sciences and the Institute of Biology of the Southern Seas Ukrainian Academy of Sciences are actively carrying out investigations throughout this basin. A great volume of work is also being done by the subdivisions of the State Committee on Hydrometeorology. For example, the Sevastopol' and Odessa Divisions of the State Oceanographic Institute during 1974-1978 carried out five major expeditions in the Aegean Sea aboard the scientific research ships "Mgla" and "Gakkel'." About 600 abyssal stations were occupied, extending over the entire area of the sea. They collected extensive material (about 30,000 measurements) for studying the chemical structure of the waters of the Aegean Sea and the migration of contaminating substances through its waters. Particular attention was devoted to those regions through which pass the busiest ship routes and which can serve as potential centers of formation of the fields of contaminating substances. The results of the observations make it possible to

compute the background concentrations of individual ingredients and the possible ranges of their occurrence.

In 1978 expeditions of the Sevastopol' Division of the State Oceanographic Institute for the first time carried out a survey (13 stations) beyond the limits of the Aegean Sea in the region of the abyssal Rhodes basin, which made it possible to obtain new data on the variability of the hydrological and hydrochemical characteristics in the Eastern Mediterranean Sea.

The participants in the session devoted much attention to the results of work in the Black Sea under the SKOICH-78 program. Interesting observations of the variability of geophysical fields with the use of satellite information were carried out by the Marine Hydrophysical Institute Ukrainian Academy of Sciences aboard the scientific research ship "M. Lomonosov." The Odessa Division of the Institute of Biology of the Southern Seas in 1978 continued its long-term work for studying the structure of the biological associations in the northwestern part of the Black Sea. Interesting data have been obtained on the dynamics of coastal phenomena and fluctuations of biological productivity in individual regions of the sea. An unusual catalogue of fishkill phenomena was compiled. This type of work has been done since 1973. The collected data make it possible to detect centers of occurrence of fishkills and proceed to the development of practical recommendations on contending with this phenomenon.

A great volume of work has also been done by the subdivisions of the State Committee on Hydrometeorology. In 1978 the Sevastopol' Division of the State Oceanographic Institute, in collaboration with the Odessa Division of the State Oceanographic Institute, the Northern Caucasus Administration of the Hydrometeorological Service and the Administration of the Hydrometeorological Service of the Ukrainian SSR carried out 20 expeditions with a total duration of 450 days. More than 3,000 hydrological stations were occupied both in the coastal zone and in the open sea. New data were obtained for evaluating the scales of water and salt exchange between Taganrog Gulf and the Sea of Azov. Thirteen multiday stations were occupied along a line between Dolgaya and Belosarayskaya spits (244 series of observations); 10 automatic buoy stations and bottom units were set out. This made it possible to obtain more than 1,000 horizon-days of observations of currents. Similar work has been done in Kinburnskiy Strait at the point of the projected dam, which should transform the Dnepr-Bug estuary into a gigantic reservoir of fresh water with a volume greater than five cubic kilometers.

The most interesting expedition was carried out in November 1978 aboard the scientific research weather ship "G. Ushakov." Specialists of the scientific research institutes of the State Hydrometeorological Committee and other departments participated in the expedition. Also participating in the expedition was a large group of scientists from the Socialist Economic Bloc countries: East Germany, Poland, Romania and Bulgaria. There was an intercalibration of methods for determining the chemical composition of sea

water, experimental observations of the settling and scattering of finely dispersed fractions of hydrocarbons at the water-atmosphere discontinuity, tests of new equipment for the setting out of automatic buoy stations and containers of the towed measuring complex, a hydrochemical survey of the western half of the Black Sea and other studies.

While noting the indisputable achievements in the development of research in all the basic directions of study of the southern seas, the plenary session of the basin section also noted a number of unsolved problems in the organization of these studies.

Yu. G. Slatinskiy

The first scientific and technical conference devoted to the rational use and conservation of the water resources of Rostovskaya Oblast was held at Rostov-na-Don during the period 15-16 December 1978.

Participating in the work of the scientific and technical conference were more than 200 persons -- representatives of the basin administrations, sanitary-epidemiological stations, scientific research institutes, major industrial enterprises of the oblast, Party and soviet agencies. The conference heard 26 reports, which with respect to the substance of the considered problems can be arbitrarily divided into three groups.

In the first group of reports the authors examined problems relating to the state of water resources in Rostovskaya Oblast in their close relationship to the state of land and forest resources. The need for studying the state of water resources was dictated by the productive activity of human society and therefore a study must be made of the factors leading to their qualitative and quantitative exhaustion. These problems were discussed in reports of specialists at the Oblast Administration of Melioration and Water Management, Northern Caucasus Scientific Center of the Higher School, Yuzhgiprovodkhoz, Novocherkasskiy Engineering-Melioration Institute, Yuzhgiprozem, Sevkavgiprosel'khozstroy.

The conference noted that the principal means for rational complex use of water resources are: saving of water by a decrease in its consumption per unit of production, increase in the efficiency of irrigation systems, use of progressive methods and techniques for the watering of irrigated lands, automation of water distribution, and also introduction of systems for cyclic water supply, repeated use of water in industry and agriculture, redistribution of runoff within the region, use of modern methods for the purification of waste waters and their use for the irrigation of agricultural fields.

A second group of reports gave a thorough analysis of the present state of the quality of surface waters in Rostovskaya Oblast and the tendencies in its changes during a long-term period of observations.

These were primarily the reports of specialists of the Hydrochemical Institute.

A third group of reports, presented by specialists of the Don Basin Administration for Regulating the Use and Conservation of Water Resources, Novocherkasskiy Polytechnic Institute, sanitary-epidemic stations, Volga-Don Affiliate of the All-Union Scientific Research Institute of Surface Active Substances, dealt in detail with the sources of contamination of surface waters in Rostovskaya Oblast.

It was noted at the conference that in cities and populated places, at industrial and agricultural enterprises in the oblast, work is being done on the construction of sewage and purification structures; systems for the cycling of water supply and water-cycled technological processes are being introduced; a rigorous statistical inventory of the used water has been set up; new water supply and interregional water lines are under construction. In addition to the measures ensuring reduction of the discharge of unpurified waste water, work is being done on the sanitizing and certification of purity of small rivers and a plan is being drawn up for carrying out a complex of measures in the water conservation zones of the Don and Severskiy Donets Rivers.

It was noted at the conference that as a result of the organized purification of waste water and the repeated use of waste water there has been a considerable reduction of its annual discharge into the water bodies in the oblast. For example, in 1977 a total of 460 tons of valuable substances were removed from the waste water; this had an economic effect of 6.0 million rubles. At the same time, waste waters of cities, enterprises and agricultural complexes are still being dumped into the water bodies of the oblast without purification or with inadequate purification.

The enterprises of the metallurgical, coal, machine building, light, food and other branches of industry remain the principal contaminants of water bodies in the neighborhood of Taganrog, Rostov, Azov, Sal'sk, Kamensk, Sulin, Chertkovo, and elsewhere.

The conference noted a whole series of important problems and tasks in the further improvement in use of the water resources of Rostovskaya Oblast. These must be dealt with during 1979-1985 and include:

— by the end of 1980, in a number of cities and industrial enterprises, end the construction of all water conservation projects, ensure cessation of the discharge of unpurified waste water, complete meliorative work on the Temernik River and end the cleaning up of eight small rivers contaminated by the wastes of mines and industrial enterprises;

— the carrying out of the construction of water conservation projects at kolkhoz enterprises in the oblast, particularly at livestock complexes and farms; strengthen water conservation zones along small rivers, the Don and the Sev. Donets;

-- the prevention of contamination of water bodies by waste waters from rice irrigation systems by means of restricting the use of poisonous chemicals and herbicides and their replacement by substances harmless for water bodies, and also the introduction of repeated use of water;

-- an increase in the effectiveness of use of state irrigation systems and irrigation based on local runoff, with provision being made for the maximum use of waste waters of cities, livestock complexes and farms and mine waters.

It was noted at the conference that the problem of preserving the environment, including the conservation of water, land and forest resources, is more and more acquiring an extradepartmental character and an ever-greater number of different specialists are being involved in this work.

The conference materials, being of great interest for a broad scientific community, will be published.

G. N. Danilova

During the period 25-27 October, at Moscow, there was an all-union scientific and technical conference with the participation of delegates from the socialist countries of Europe on the theme: "Investigation of the Agroclimatic Resources of a Territory and Experience in the Hydrometeorological Servicing of Agriculture," organized by the Central Administration of the Scientific and Technical Division of Agriculture, the State Committee on Hydrometeorology and the All-Union Exhibition of Achievements in the National Economy USSR. The conference was attended by 180 specialists of institutes of the State Committee on Hydrometeorology, USSR Agriculture Ministry, academic institutes, and the hydrometeorological (meteorological) services of the German Democratic Republic, Hungary, Bulgaria and CzSSR. Twenty-five reports and communications were presented on the role of the Scientific and Technical Society of Agriculture in the hydrometeorological support of agricultural production, methods for evaluating agroclimatic resources and the state of plants, or methods for agrometeorological forecasts.

It was pointed out in a report by the author that during the last decade there has been considerable development of contacts between the Hydrometeorological Service and the Scientific and Technical Society of Agriculture, established through the network hydrometeorological institutes and the agrometeorological sections of peripheral organizations of the Scientific and Technical Society of Agriculture. These contacts are directed to the broad popularization of hydrometeorological materials, which favors an increase in the sophistication of agriculture and the productivity of agricultural work as a whole. The most complete effectiveness of hydrometeorological information will be achieved when agricultural workers are widely informed concerning the content and sources of this information and its use in everyday work. Contacts between agriculture and the hydrometeorological service through the Scientific and Technical Society of Agriculture

must be specially developed with the introduction of automated systems into agricultural production, developing on the basis of interkolkhoz cooperation and agroindustrial integration.

It was demonstrated in a report by V. A. Smirnova that in agriculture, where economic processes are closely intertwined with natural processes and are essentially dependent on the latter, the problem of rational distribution of production cannot be successfully solved without a detailed study of the environment. Calculation and evaluation of natural resources precede an economic analysis. The conclusion is drawn that plans drawn up on the basis of an inventory of natural resources help in a critical analysis of economic feasibility and desirability of the developing distribution of agricultural crops and will help in formulating recommendations for its improvement.

It was demonstrated in a report by A. P. Fedoseyev and V. V. Vol'vach that the essence of the hydrometeorological validation of agrotechnical and meliorative measures to all intents and purposes can be reduced to the development of a scientifically sound scheme for taking hydrometeorological data into account in organizing the technology of sowing of agricultural crops as a unified purposeful system. This system consists of a group of optimized subsystems or special systems for working the soil, sowing (planting), fertilizing, care for plants, irrigation or drainage, protection of plants, etc. It is emphasized that there are considerable reserves for increasing the effectiveness of use of hydrometeorological information for the validation and rational realization of schemes for the cultivation of agricultural crops.

In a report by O. D. Sirotenko, et al. a study was made of a simulation model of the "soil-plant-atmosphere" system, constituting a closed system of differential equations describing the processes of exchange of heat, moisture and carbon dioxide in two contacting media -- the surface air layer and the soil, "sewn together" by plants. The results of these studies make it possible to raise the question of the development and introduction of an automated system for the agrometeorological support of agriculture based on a methodology common for all crops, that of dynamic models, a unified information base, the extensive use of electronic computers and data from remote measurements.

Yu. I. Chirkov reported on the results of joint work on study of the agroclimatic resources of the socialist countries of Europe.

E. V. Khershkovich (Bulgaria) reported on major agroclimatic investigations carried out earlier and being carried out at the present time and used in practical agricultural production in Bulgaria.

A report by Pal Bozou (Hungary) described the results of investigations of agroclimatic resources in Hungary.

Josef Hrbec (CzSSR) reported on agrometeorological problems in the agriculture of the CzSSR.

A number of communications dealt with the results of work on problems involved in evaluating the agroclimatic and microclimatic resources for planning the distribution of agricultural crops, hydrological support of irrigated agriculture and other methodological problems.

It is recommended in an adopted resolution, in particular, that measures be taken for accelerating the creation of a bank of agrometeorological data, and also methods for processing operational and regime agrometeorological information on an electronic computer, disseminating more widely the attainments of agrometeorological science and the leading experience of the agrometeorology sections of the Scientific and Technical Society of Agriculture in agricultural journals and newspapers, and also in the "Hydrometeorological Service" pavilion at the USSR All-Union Exhibition of Attainments in the National Economy.

G. V. Rudnev

During the period 29 January-2 February, at the WMO, there was an unofficial conference on the planning of complex study of the observation system over the ocean.

At the conference those in attendance examined the means for proposed investigations for determining the role of the observation stations in the North Atlantic (OSNA) in the combined observation system for the North Atlantic region, necessary for the satisfaction of both operational and scientific requirements.

Also considered were the results of investigations of the importance of OSNA observational data for hemispheric numerical analyses and medium-range weather forecasts (Great Britain) and prediction of storm-induced level changes (Netherlands). Also discussed was a draft of the work plan for the Commission on Basic Systems (CBS) of the WMO for study of a combined system of ocean observations.

As a result of the discussion recommendations were formulated on the following matters:
-- the significance of the network of OSNA stations for operational, research and climatological purposes;
-- further investigations of the working group of the CBS for study of a combined system of ocean observations;
-- implementation of an additional study of the influence of OSNA data on numerical weather forecasting models with an advance period up to 24 hours for a local region and on the quality of storm warnings;
-- a detailed investigation of structure of an ocean observation system based on data obtained after ending the First Global Experiment program.

K. P. Vasil'yev

The Seventeenth General Assembly of the International Union of Geodesy and Geophysics (IUGG) will be held during the period 3-15 December 1979 at Canberra, Australia; the IUGG includes the International Association of Meteorology and Atmospheric Physics (IAMAP).

An IUGG assembly is held once each four years. Earlier assemblies were held in Europe (Helsinki, 1960; Luzerne-Zurich, 1967; Moscow, 1971; Grenoble, 1975) and in North America (Toronto, 1957; Berkeley, 1963). For the first time, on the invitation of the Australian Academy of Sciences, the IUGG will meet in the southern hemisphere. The site of holding of the assembly, as will be seen from what follows, will find a definite reflection in the scientific program of its work.

At the assembly attention will be given to organizational problems related to the further development and international coordination of work in the field of geodesy and geophysics (including meteorology and physics of the atmosphere). The directorates of the IUGG, its associations and the international commissions of the associations will be elected.

In accordance with established tradition, at the assembly there will be organization of interassociation scientific symposia and symposia of individual associations. A series of papers will be presented on modern and timely problems, in particular on the problems "Climates of the Earth" and "Weather Forecasting."

The Interassociation symposia in which there will be participation by the International Association of Meteorology and Physics of the Atmosphere, the International Association of Physical Sciences of the Ocean (IAPSO), the International Association of Hydrological Sciences (IAHN) and other associations will be devoted to the following important geophysical problems:
1. Geochemical evolution of the atmosphere, oceans and the crust.
2. Sea level, ice sheets and climatic variations.
3. Problems of coastal and mouth zones (including breezes).
4. Origin and structure of the Antarctic Ocean.
5. Interaction between changes in the earth's rotation and geophysical phenomena.
6. Volcanism and climates.
7. Oceanic and atmospheric boundary layers.
8. Mean atmosphere.
9. Tidal interactions.
10. Contribution of geodesy to oceanography.

A special symposium under the direction of the IUGG board will be devoted to the problem "New Technology of Geophysical Equipment."

The IAMPA has planned a major program. It is organizing the following symposia at the assembly:

1. "Numerical Weather Forecasting for Intermediate and Long Periods." This symposium will devote its particular attention to long-range weather forecasting, evaluation of the behavior of numerical prognostic models in integration from several days to several weeks, evaluation of the resolution of the modeled physical processes and stipulation of the initial and boundary conditions, evaluation of the theoretical and attainable limits of predictability.

2. "Role of Atmospheric Electricity in Solar-Terrestrial Relationships." Plans call for devoting particular attention at this symposium to electric phenomena at all levels, galactic cosmic radiation, solar radiation, interplanetary medium, magnetosphere, upper atmosphere and troposphere, statistical data processing and evaluation of the significance of solar-terrestrial relationships.

3. A large symposium will be devoted to modern attainments in the field of meteorology of Antarctica and the Subantarctic, at which plans call for examining problems related to synoptic meteorology and data transmission, heat and moisture transfer, planetary boundary layer, energy budget of the underlying surface, influence of the Antarctic atmosphere on global climate, remote sounding of the atmosphere and the underlying surface.

4. "Climatic variations." It is proposed that this symposium be devoted to theoretical and experimental investigations of climate with a period of 100,000 years, climatic variations during the course of the last century on the basis of observations of fluctuations of temperature and circulation in the atmosphere and ocean, detection of real variations against a background of effects associated with the observation method and their possible reasons.

5. "Composition of the Atmosphere and Climate." The symposium will examine the results of investigation of the composition of the atmosphere in the southern hemisphere and problems relating to the potential effect on weather and climate. In particular, plans call for discussing problems relating to the general and regional composition of the atmosphere in the tropical, temperate and polar latitudes, historical data on atmospheric composition obtained from tree rings, the ice caps, sedimentary rocks in the ocean and other sources, the influence of exchange between the hemispheres on the composition of the atmosphere in the southern hemisphere, influence of southern hemisphere oceans on composition of the atmosphere, investigation of composition of the stratosphere, and global models of the stratosphere.

6. "Meteorology of the Upper Atmosphere." A major symposium will be devoted to this subject. There will be a discussion of problems relating to the agreement between theoretical models and observational data, the results of investigation, on the basis of empirical data, of the spatial-temporal variability of parameters in the stratosphere and mesosphere, large-scale circulation, ozone distribution, dynamics, diffusion and turbulence, planetary and gravitational waves, interaction of waves, energy transfer, new

data on the properties of waves, hypotheses of solar-terrestrial relationships, which could be included in numerical prognostic models.

7. One symposium will be devoted to radiation processes in the atmosphere. It is proposed that these processes be examined in the light of general problems in meteorology, especially in the southern hemisphere.

8. "Remote Measurements of Cloud Parameters." Those in attendance will examine the use of remote methods for sounding for measuring atmospheric parameters important for the formation of clouds and precipitation, present status of satellite, airborne and surface measuring systems and the results of their practical application.

As we see, the subject matter of the symposia will give some idea concerning the directions and possibilities of international cooperation and coordination of scientific investigations in the field of meteorology and physics of the atmosphere.

At the Inderdepartmental Geophysical Committee of the Presidium USSR Academy of Sciences, with the participation of the USSR State Committee on Hydrometeorology and Monitoring of the Environment, Ministries of Higher and Intermediate Special Education and other departments, active preparations are being made for the participation of Soviet scientists in the impending international forum of geophysicists.

NEWS FROM ABROAD

Moscow METEOROLOGIYA I GIDROLOGIYA in Russian No 6, Jun 79 pp 127-128

[Article by B. I. Silkin]

[Text] In recognition of the outstanding successes of Soviet science in the field of atmospheric studies, Corresponding Member USSR Academy of Sciences Mikhail Ivanovich Budyko has been elected an Honorary Member of the American Meteorological Society.

***

As reported in SCIENCE NEWS, Vol 114, No 4, p 55, 1978, the Consultative Commission on Weather Modification (United States), established in 1976, consisting of 17 outstanding American meteorologists, has formulated its recommendations for the next two decades.

In these recommendations it is pointed out, in particular, that there is a real possibility, by the 1980s, by artificial modification, for increasing by 10-30% the snow cover in the mountains and precipitation in the form of rain in the plains region situated directly to the east of the Rocky Mountains and in the Middle West. In addition, by the 1990's it will be possible to decrease the intensity of hurricanes by 10-20% and bring about a 50% decrease in the frequency of recurrence of hailfalls over the territory of the entire country.

In organizational respects it is recommended that the US Commission on Use of Meteorological Resources be combined with NOAA.

In the opinion of the Consultative Commission, the development and improvement of the cloud "seeding" method for the modification of precipitation requires an increase in appropriations up to 37 million dollars in 1980 and up to 90 million dollars in 1985. There is also need for a deeper study of the social and economic aspects of weather under the influence of man's purposeful actions.

***

As reported in EDIS: ENVIRONMENTAL DATA AND INFORMATION SERVICE, September 1978, p 16, in June 1978 a new scientific institute was established in the United States -- an information center for the shores of the Great Lakes -- in Ann Arbor, Michigan. The center has the responsibility for supplying local official agencies, industrial institutes, and organizations involved in preservation of the environment with information on the state of the waters and shores of this region, places of storage of detailed information, existing local peculiarities of the rules and laws for land and water use.

Similar centers already exist in the northwestern and northeastern Pacific Ocean coastal zones of the United States. A distinguishing characteristic of the new center is that specialists not only of the United States, but also Canada, to which the northern shores of the Great Lakes belong, will participate in its work.

The new center is subsidized by NOAA, which has allocated $50,000, and the University of Michigan, which has assigned the center $25,000.

OBITUARY OF VASILIY VLADIMIROVICH SHULEYKIN (1895-1979)

Moscow METEOROLOGIYA I GIDROLOGIYA in Russian No 6, Jun 79 p 128

[Article by members of the Board of the USSR State Committee on Hydrometeorology and Environmental Monitoring]

[Text] Soviet science has experienced a heavy loss. On 25 April death took from the ranks of Soviet science an outstanding researcher and teacher, the founder of marine physics, Academician Vasiliy Vladimirovich Shuleykin.

All our present-day marine researchers have been trained using the studies of Vasiliy Vladimirovich and very many received the basic sum of their knowledge of the sea at his brilliant lectures at the Moscow Hydrometeorological Institute and at the Moscow State University imeni M. V. Lomonosov, at which he headed the departments which he organized there.

An entire epoch in geographic research, the formation of an independent branch of this science, physics of the sea, is associated with the name V. V. Shuleykin.

Energy, purposefulness and exceptionally high work capacity were characteristic of Vasiliy Vladimirovich. He wrote his first study in the field of electrical engineering in 1916. In 1929 he organized the Black Sea Hydrophysical Station at Katsiveli. That same year he was elected a Corresponding Member USSR Academy of Sciences.

At the beginning of the 1930's V. V. Shuleykin ended his main work -- the two-volume monograph FIZIKA MORYA (Marine Physics).

MARINE PHYSICS is not simply a direction in geophysical research. It is an entire branch of science which as component parts includes not only the already known marine dynamics, but new directions as well: "marine acoustics," "molecular marine physics," "marine biophysics," and "marine technical physics."

At the beginning of the Great Fatherland War, already being recognized as an authoritative scientist, Corresponding Member USSR Academy of Sciences V. V. Shuleykin called on the Deputy People's Commissar of the US Navy, Admiral I. S. Isakov, with a request that he be put on active military duty.

In Leningrad as a Military Engineer (First-Rank) he did important work for calculating the supporting capacity of the ice on the famed ice road across Lake Ladoga. Then, stationed in Arkhangel'sk, he continued these studies applicable to sea ice.

Immediately after the freeing of the Crimea in 1944, V. V. Shuleykin began to organize the Marine Hydrophysical Laboratory USSR Academy of Sciences at the site of the destroyed Black Sea Hydrophysical Station.

The scientific services of V. V. Shuleykin were recognized by his election, in 1946, as a full member of the USSR Academy of Sciences.

In 1947 Vasiliy Vladimirovich was designated chief of the Main Administration of the Hydrometeorological Service of the USSR Council of Ministers. At the same time he carried out scientific direction of the Hydrophysical Laboratory, on the basis of which the Marine Hydrophysical Institute USSR Academy of Sciences was organized in 1948.

Academician V. V. Shuleykin carried out fundamental investigations of the theory of interaction of the ocean, atmosphere and continents, the theory of sea currents, the theory of wind waves and tropical hurricanes. His monograph FIZIKA MORYA, which has already become a classic, has been republished several times and each successive edition has been greatly revised and supplemented. The fourth edition, which appeared in 1968, is a work which seamen will use for many years.

Vasiliy Vladimirovich was awarded two Orders of Lenin, the Order of the October Revolution and three other orders.

The memory of Vasiliy Vladimirovich Shuleykin will always be kept by all who knew him.

[9-5303]

-END-